



William de Souza Barbosa

**Development, construction, analysis and
control of upper limb orthosis using bio-signals**

Tese de Doutorado

Thesis presented to the Programa de Pós-graduação em Engenharia Elétrica, do Departamento de Engenharia Elétrica da PUC-RIO in partial fulfillment of the requirements for the degree of Doutor em Engenharia Elétrica.

Advisor : Prof. Guilherme Penello Temporão

Co-advisor: Prof. Marco Antônio Meggiolaro

Rio de Janeiro
September 2022



William de Souza Barbosa

**Development, construction, analysis and
control of upper limb orthosis using bio-signals**

Thesis presented to the Programa de Pós-graduação em Engenharia Elétrica da PUC-RIO in partial fulfillment of the requirements for the degree of Doutor em Engenharia Elétrica. Approved by the Examination Committee:

Prof. Guilherme Penello Temporão

Advisor

Departamento de Engenharia Elétrica – PUC-RIO

Prof. Marco Antônio Meggiolaro

Co-advisor

Departamento de Engenharia Mecânica – PUC-RIO

Prof. João Roberto de Toledo Quadros

CEFET/RJ

Prof. Mauro Speranza Neto

Pesquisador Autônomo

Dr. Saul Eliahú Mizrahi

INT

Prof. Vivian Suzano Medeiros

Pontifícia Universidade Católica do Rio de Janeiro – PUC-RIO

Rio de Janeiro, September the 26th, 2022

All rights reserved.

William de Souza Barbosa

Holds master's degree in Electronics Engineering (2014) from UERJ, a bachelor's degree in Control and Automation Engineering (2011) from the Pontifical Catholic University of Rio de Janeiro (PUC-Rio) and Technician in Mechanics (2001) from CEFET/RJ. He is currently a researcher at Tecgraf Institute (PUC-Rio), Researcher at Instituto Nacional de Pesquisas Hidroviárias (INPH) and an assistant professor of Control and servomechanisms in the Electrical Engineering Department of PUC-Rio. He has experience in the area of Engineering Educational Resources, Industrial Electronics, Control Systems and Rigid Body Dynamics, Signal Processing, Manufacturing Processes and Digital manufacturing. He currently works in research in the field of Non-Linear Control Theory, Embedded Systems and Control, Mobile Robots for Marine and agricultural purposes and bio-prosthesis and bio-orthosis.

Bibliographic data

Barbosa, William de Souza

Development, construction, analysis and control of upper limb orthosis using bio-signals / William de Souza Barbosa; advisor: Guilherme Penello Temporão; co-advisor: Marco Antônio Meggiolaro. – 2022.

112 f: il. color. ; 30 cm

Tese (doutorado) - Pontifícia Universidade Católica do Rio de Janeiro, Departamento de Engenharia Elétrica, 2022.

Inclui bibliografia

1. Engenharia Elétrica – Teses. 2. Órtese. 3. Controle Não Linear. 4. Indústria 4.0. 5. Processos de Fabricação Digital. 6. Otimização Multi lattice. I. Temporão, Guilherme Penello. II. Meggiolaro, Marco Antônio. III. Pontifícia Universidade Católica do Rio de Janeiro. Departamento de Engenharia Elétrica. IV. Título.

CDD: 621.3

To God, for illuminating my paths all the time.
To my parents, brothers and wife for their support
and encouragement.

Acknowledgments

First I would like to thank my family, for helping me and giving me the necessary emotional support and all my friends for trusting and believing in my potential.

To my advisor Guilherme Temporão and my co-advisor Marco Antônio Meggiolaro for dedication, guidance and continuous support on the development of this thesis. My sincere thanks also goes to professor Ana Maria Beltran Pavani for encouragement in moments of doubt.

To the professors and employees of the Mechanical Engineering Department and the Electrical Engineering Department of PUC-Rio and the team of Digital Fabrication Laboratory of Tecgraf Institute (PUC-Rio), for the quality of teaching and excellent infrastructure, essential for the development of this work.

Finally, to the Coordenação de Aperfeiçoamento de Pessoal de Nível Superior (CAPES) and to Conselho Nacional de Desenvolvimento Científico e Tecnológico (CNPq) for the scholarship and financial support to this research.

This study was financed in part by the Coordenação de Aperfeiçoamento de Pessoal de Nível Superior - Brasil (CAPES) - Finance Code 001.

Abstract

Barbosa, William de Souza ; Temporão, Guilherme Penello (Advisor); Meggiolaro, Marco Antônio (Co-Advisor). **Development, construction, analysis and control of upper limb orthosis using bio-signals**. Rio de Janeiro, 2022. 112p. Tese de Doutorado – Departamento de Engenharia Elétrica, Pontifícia Universidade Católica do Rio de Janeiro.

Developing and building a prosthesis or orthosis with easy adaptation for the user is still a major challenge in the engineering area in general. In addition, the use of electromechanical elements inserts autonomy and portability as factors of difficulty in construction. Another point is that variations in human factors, such as spasticity, muscle tone or changes resulting from diseases such as cerebral palsy or nerve damage, interfere with the construction of the device.

Therefore, the construction of an orthosis is a challenging and multidisciplinary job, which involves a deep and detailed analysis from the application to the actual construction. The use of Industry 4.0 techniques to make the orthosis comfortable, lightweight, and easy to use is fundamental to this, as is the analysis and processing of biosignals and control, making sure that each step is connected and adjusted so that it functions correctly.

This aims to evaluate the theoretical and experimental methods of construction and dynamic evaluation of a bio-orthosis of upper limbs using the concept of industry 4.0, digital manufacturing processes, multi-structural optimization, bio-signal processes and non-linear control techniques. This study was motivated by the advancement of the use of digital manufacturing in the field of bio-medicine, by the great challenge from the point of view of control, by the variability that these processes can have in the construction of orthoses in improving the quality of life of people with disabilities.

Keywords

Orthosis; Nonlinear Control; Industry 4.0; Digital Manufacturing Processes; Multi lattice Optimizatio.

Resumo

Barbosa, William de Souza ; Temporão, Guilherme Penello; Meggiolaro, Marco Antônio. **Desenvolvimento, construção, análise e controle de órtese de membros superiores utilizando biosinais**. Rio de Janeiro, 2022. 112p. Tese de Doutorado – Departamento de Engenharia Elétrica, Pontifícia Universidade Católica do Rio de Janeiro.

Desenvolver e construir uma prótese ou órtese com fácil adaptação para o usuário ainda é um grande desafio na área de engenharia em geral. Além disso, o uso de elementos eletromecânicos insere a autonomia e a portabilidade como fatores de dificuldade na construção. Outro ponto é que variações de fatores humanos, como espasticidade, tônus muscular ou alterações decorrentes de doenças como paralisia cerebral ou lesão nervosa, interferem na construção do aparelho.

Deste modo, a construção de uma órtese é um trabalho desafiador e multidisciplinar, que envolve uma análise profunda e detalhada desde a aplicação até a construção propriamente dita. O uso de técnicas de indústria 4.0 para tornar a órtese confortável, leve e de fácil uso é fundamental para isso, assim como a análise e processamento de biosinais e o controle, fazendo com que cada etapa esteja ligada e ajustada para que o funcionamento esteja correto.

Esta tese tem como objetivo avaliar os métodos teóricos e experimentais de construção e avaliação dinâmica de uma bio-órtese de membros superiores utilizando o conceito de indústria 4.0, processos de manufatura digital, otimização multiestrutural, processamentos de biosinais e técnicas de controle não linear. Este estudo foi motivado pelo avanço do uso da manufatura digital no campo da biomedicina, pelo grande desafio sob o ponto de vista de controle, pela variabilidade que esses processos podem ter na construção de órteses na melhoria da qualidade de vida das pessoas com deficiência.

Palavras-chave

Órtese; Controle Não Linear; Indústria 4.0; Processos de Fabricação Digital; Otimização Multi lattice.

Table of contents

1	Introduction	16
1.1	Related Works and Background	17
1.1.1	Construction of Prosthesis and Orthosis by Using Digital Manufacturing	17
1.1.2	Multi lattice Optimization	19
1.1.3	Control Theory and Design for Rehabilitation	20
1.1.4	EEG,EMG and ECG Signal Processing	23
1.1.5	Control Theory and Design for Orthosis Activation	24
1.2	Objectives	26
1.3	Research innovations and boundary	27
1.4	Thesis Organization	28
2	Study of the physiology of the Upper-Limb Movements	29
2.1	Nature of the Upper-limb Movements and the Brachial Plexus	29
2.2	Stroke and its Consequences	31
2.3	Brachial Lesion and its Consequences	33
3	Digital Manufacturing in the construction of the orthosis	35
3.1	Industry 4.0 Concepts and Definitions	35
3.2	Digital Manufacturing and Construction of Upper-limb Orthosis	38
3.2.1	Virtualization of the model	38
3.2.2	Computer simulation of the orthosis	40
3.2.3	Process customization	41
3.2.4	Manufacturing on demand using hybrid manufacturing	41
4	Multi lattice optimization applied to FDM processes	44
4.1	Lattice structures	45
4.2	Multi lattice optimization	47
4.3	Mechanical tests	49
5	Fusion and Processing of EEG, ECG and EMG signals	54
5.1	Signal Characterization	54
5.2	Acquisition Procedures	59
5.3	Database Creation	63
5.4	Filtering Procedures	64
5.4.1	Types of Filters	66
5.4.2	Filters by each bio signals	68
5.5	Data Analysis	69
6	Robust and Adaptive Control Techniques Applied to the Orthosis	72
6.1	Types of Controllers	72
6.1.1	Classic Control Techniques	72
6.1.2	Intelligent Control Techniques	73

6.1.3	Modern and Robust Control Techniques	73
6.1.4	High-Order Sliding Mode Controller	75
6.2	Mathematical Modelling	78
6.3	Control Requirements, Parameters and Objectives	82
6.3.1	Stability Proof	84
6.3.2	Real Parameters	85
6.3.3	Embedded Electronics	85
6.3.4	Simulations and Real-Time Actuation	86
7	Conclusions	90
7.1	Advances and Outcomes	90
7.2	Future Works	92
	Bibliography	93

List of figures

Figure 1.1	First prosthesis design by Paré (extracted from [8])	16
Figure 1.2	modified wheelchair (extracted from [18])	18
Figure 1.3	3D printed orthosis (extracted from [24])	18
Figure 1.4	example of multi lattice structure (extracted from [34])	19
Figure 1.5	Examples of Electro stimulators	20
Figure 1.6	BCI Scheme (extracted from [67])	23
Figure 1.7	(A) 3D model of exoskeleton robot of article [76] (B)3D model and prototype of exoskeleton robot of article [77]	25
Figure 1.8	Prototype of exoskeleton robot of article [80]	25
Figure 1.9	Elbow Bending movement	27
Figure 2.1	Illustrative scheme of brachial plexus (adapted from [83])	29
Figure 2.2	Muscle groups of the brachial plexus(extracted from [85])	30
Figure 2.3	Illustrative scheme of a stroke (adapted from [90])	32
Figure 2.4	Example of temporary orthosis (X-cat Rom Endurance) (adapted from [93])	33
Figure 2.5	Illustrative scheme of brachial lesion caused by falling and stretching (adapted from [95])	33
Figure 2.6	Illustrative scheme of brachial lesion caused at birth (extracted from [97])	34
Figure 3.1	Illustrative scheme of a Industry 4.0 (adapted from [110])	36
Figure 3.2	Scheme of 3D printing technologies (adapted from [110])	37
Figure 3.3	<i>X sens</i> [®] motion capture	39
Figure 3.4	virtual 3D model	39
Figure 3.5	virtual 3D models of orthoses	41
Figure 3.6	test of the orthosis	42
Figure 3.7	prototype of the orthosis	43
Figure 4.1	Types of lattice structures	45
Figure 4.2	Types of standard FDM infill structures (extracted from [131])	46
Figure 4.3	Variation of lattice structures	49
Figure 4.4	3D print simulation	50
Figure 4.5	Traction force vs. elongation curves (non-optimized specimen)	50
Figure 4.6	Traction force vs. elongation curves (optimized specimen)	51
Figure 4.7	Compression force vs. elongation curves (non-optimized specimen)	51
Figure 4.8	Compression force vs. elongation curves (optimized specimen)	51
Figure 4.9	Fixing of the specimens in the machine	52
Figure 5.1	Scheme sectors of the brain (adapted from [52])	55
Figure 5.2	Scheme of Muscular activation (adapted from [52])	55

Figure 5.3	Scheme and parts of a neuron (adapted from [133])	56
Figure 5.4	Example of EEG waves (adapted from [136])	57
Figure 5.5	Example of ECG waves (adapted from [141])	57
Figure 5.6	example of EMG waves	58
Figure 5.7	Apparatus	59
Figure 5.8	Elbow Bending movement and <i>Labview</i> [®] interface	60
Figure 5.9	Position of ECG probes (adapted from [100])	60
Figure 5.10	Position of EEG probes	61
Figure 5.11	Position of EMG probes	61
Figure 5.12	Multiparameter medical equipment	62
Figure 5.13	<i>Matlab</i> [®] Toolbox <i>EegLab</i> [®] window	65
Figure 5.14	Scheme of system acquisition	65
Figure 5.15	Examples of Butterworth filter response (extracted from [147])	66
Figure 5.16	Scheme of EEG signal filtering	68
Figure 5.17	Scheme of ECG signal filtering	69
Figure 5.18	Scheme of EMG signal filtering	69
Figure 5.19	Scheme of acquisition and actuation system	70
Figure 6.1	Basic scheme of a PID controller.	72
Figure 6.2	Examples of Intelligent Controls.	73
Figure 6.3	Classic ESC Scheme (adapted of [176]).	74
Figure 6.4	Generic SMC Scheme (adapted of [192]).	75
Figure 6.5	(A) Common Convergence (B) SMC Convergence.	76
Figure 6.6	Figure showing the dynamics of muscular contraction [47].	78
Figure 6.7	Schematic diagram of an arm movement, adapted from [73].	79
Figure 6.8	Behavior of some switching functions.	83
Figure 6.9	Behavior of the controllers for step inputs.	87
Figure 6.10	Behavior of the controllers for sinusoidal inputs.	87
Figure 6.11	Angular error of the controllers for sinusoidal inputs.	88
Figure 6.12	Real-time example 1.	88
Figure 6.13	Real-time example 2.	89

List of tables

Table 1.1	List of Recent Articles	22
Table 1.2	Classification of Disabilities	26
Table 2.1	Muscles and Movements	30
Table 4.1	Types and characteristics of lattice structures	46
Table 4.2	Analysis of the simulations (BCC infill)	48
Table 4.3	Analysis of the simulation (hex pattern or honeycomb 70% infill)	48
Table 5.1	Frequency Bands of the EEG Signal	56
Table 5.2	Duration of the ECG waves (adapted from [142] and [143])	58
Table 6.1	Ergonomic Measurements(extracted by[65])	85
Table 6.2	Servomotor Parameters	85

List of Abbreviations

ABRAFIN – Associação Brasileira de Fisioterapia Neurofuncional

ANVISA – Agência Nacional de Vigilância Sanitária

BP – Brachial Plexus

BCI – Brain Computer Interface

CNC – Computer Numeric Controller

DMLS – Direct Metal Laser Sintering

DOD – Binder jetting

DoF – Degrees of Freedom

DFT – Discrete Fourier Transform

EEG – Electroencephalogram

EMG – Electromyography

ECG – Electrocardiogram

ESC – Extremum Seeking Control

ERD – Event-related desynchronization

ERS – Event-related synchronization

FDM – Fused Deposition Modeling

FES – Functional Electrical Stimulation

FFT – Fast Fourier Transform

HMI – Human Machine Interface

HOSM – High Order Sliding Mode

IMU – Inertial Measurement Unit

LPH – Human Performance Laboratory

MRAC – Model Reference Adaptive Control

NMES – NeuroMuscular Electrical Stimulation

OBPL – Obstetric Brachial Plexus Lesion

PCM – Pulse Code Modulation

PID – Proportional Integral Derivative

PLA – Polylactic Acid

SISO – Single Input Single Output

SLS – Selective Laser Sintering

SLA – Stereolithography

SMC – Sliding Mode Controller

*Education is the most powerful weapon which
you can use to change the world.*

Nelson Mandela.

1 Introduction

Since ancient times orthosis and prosthesis have been used by human beings. According to [1] and [2], the first known principles of an orthosis were created by Archytas from Tarentum in 350 BC and consisted of a system of flying bird powered by steam, as shown in [3]. Furthermore, the first known human orthosis was created by Ambroise Paré [4] [5] [6] [7], that developed several mechanisms (Figure 1.1).



Figure 1.1: First prosthesis design by Paré (extracted from [8])

It is very common to confuse the use of the term orthosis with the use of the term prosthesis. While the first is used for some mechanism that supports or aids movement (e.g. splint, glasses, exoskeletons), the second is used when the equipment replaces the limb or body part (e.g. mechanical leg, mechanical arm, mechanical finger).

The use of robotic orthoses or prostheses are spreading in last years [2] with the popularization of micro controllers, such as Arduino[®] and Raspberry Pi[®]. Furthermore, the increase of power processing of these components and their easy programming language become complex applications in simple solutions.

From the website [9]: *"According to Amputee Coalition, in the United States alone, there are nearly two million people living with limb loss. Approximately 185,000 amputations occur in the US each year due to causes varying from vascular disease to trauma. What's more, prosthetics can cost anywhere from US\$ 5,000 to upwards of US\$50,000"*.

However, the user's difficulty in adapting to the prosthesis or orthosis is one of the main causes of withdrawal from use [10] [11]. Furthermore, the construction of an orthosis or prosthesis that adapts to the user's needs is extremely difficult, since several factors such as type of injury [12], physical changes due to surgery [13] or congenital factors [14] modify the structure and performance of the prosthesis or orthosis.

1.1 Related Works and Background

In this section, several advances and recent works in four different fields will be described: Digital manufacturing processes, structural optimization, control theory and signal processing, all applied, in some way, to the construction of prostheses and orthoses.

1.1.1 Construction of Prosthesis and Orthosis by Using Digital Manufacturing

In the article "Additive or subtractive manufacturing: Analysis and comparison of automotive spare-parts" [15] the authors defines subtractive, additive and digital manufacturing. According this work, digital or hybrid manufacturing is a combination of several conventional techniques with additive manufacturing and use of robotic arms [16] with the aim to construct some pieces.

Furthermore, digital or hybrid manufacturing gains evidence every day, with the concepts of Industry 4.0, term given to the fourth revolution and that extends to various sectors, including the medical field, being called "Medicine 4.0" or "Health 4.0".

Due to the advance and popularization of 3D printers and scanners in the last 10 years, several initiatives for the construction of prosthesis and orthosis have been proposed, as shown at "www.amputee-coalition.org" in this article

[17] and through the "e-nable" initiative. Furthermore, several techniques and applications of Industry 4.0 have been inserted in the manufacture of prostheses and orthoses as made in the Bio engineering Laboratory at Hospital das Clinicas, University of São Paulo, Brazil [18] in which several prostheses and orthoses are developed by using scanners and CNC milling machines (Figure 1.2).



Figure 1.2: modified wheelchair (extracted from [18])

Other projects using digital manufacturing have been described in [19] and [20], which review the latest techniques and implementations of upper limb prostheses. Furthermore, the case study [21] shows a successful implementation of a prosthesis using a 3D printer in an 8-year-old patient.

An interesting way to implement is also the use of active prostheses using sensors and electronic devices such as Arduino[®] and Raspberry Pi[®], as shown in [22] and [23].

In “MyOrthotics: Digital Manufacturing in the Development of a DIY Interactive Rehabilitation Orthosis” [24] the authors built a hand prosthesis using additive manufacturing (Figure 1.3) and simple electronic components based on microcontrollers and driven by electrical signals using as reference the electromyographic (EMG) signals captured from the forearm region.



Figure 1.3: 3D printed orthosis (extracted from [24])

1.1.2 Multi lattice Optimization

The manufacturing processes and optimization of castings have been debated in [25], [26], [27], whether using parameters that are purely mathematical, as described in [28], either in the construction of the molds ([29]) or by optimizing the construction of the part ([30]). However, when it comes to additive manufacturing, there are two sets of parameters that guide this optimization: structural optimization, in terms of part filling (or topological) [31] [32] and morphological optimization, under the macro-constructive aspect of the piece.

The union of these two parameters is called multi-scale topological optimization or "multi lattice optimization", which has been largely used and evaluated in sintering processes and 3D printing in general, as described in [33], [34] and [35]. Usually, this concept is linked to the optimization of the part filling during sintering, forming microstructures organized for different purposes, such as normalizing internal stresses, increasing structural rigidity [36], reducing the weight of the part and others.

An interesting work in this aspect was the one proposed by [34], which had the purpose of the construction of microstructures aiming at high resistance and decreased weight of sintered parts (Figure 1.4).

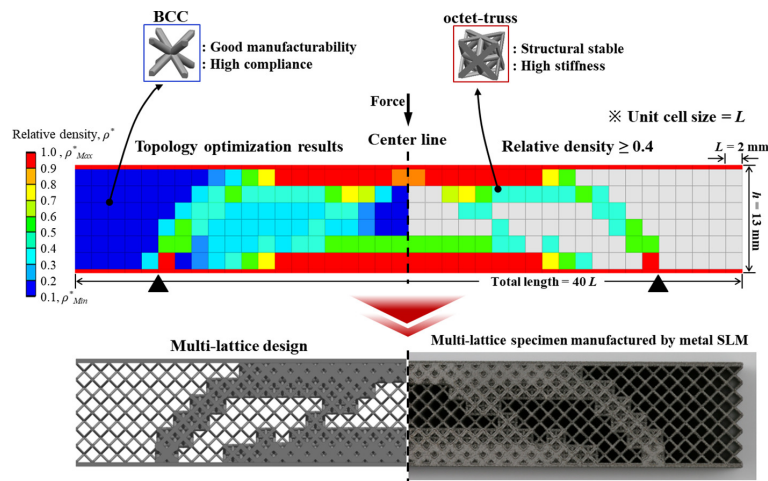


Figure 1.4: example of multi lattice structure (extracted from [34])

Another job, still with multi lattice structures, was discussed in [37], in which the microstructure is optimized to absorb impact energy in polymeric composites. Still under the aspect of optimization of mechanical properties, there are techniques that combine finite elements [38] or predictive models [39] and even evolutionary algorithms [40].

Another point of view for lattice structures is their mixture with different materials, guaranteeing stiffness or flexibility in different places of the structure, in order to guarantee the properties according to the request, or using materials of different characteristics in different positions [41].

1.1.3 Control Theory and Design for Rehabilitation

Electrotherapy has been used for the treatment of paralysis, contractions and other nervous disorders ([42]), much like the use of torpedo fish, eels and bottles of Leiden (precursors of current capacitors). Over the years, and with advances in electronics and computing, medical equipment for such purposes has become specialized and portable. They open a range of options for this type of treatment as well as for Functional Electrical Stimulation (FES)(Figure 1.5).



Figure 1.5: Examples of Electro stimulators

The concept behind electrotherapy is called Functional Electrical Stimulation (FES), which is the electrical simulation of neuromotor muscle groupings ([43]).

The neurologically affected areas are reactivated, or else seek new neural groupings to replace those affected by the injury. This approach can be applied to another disease, like brachioradial lesions ([44] [45]), which occur when the nerve is broken due to an accident or at birth. Another application is on patients with cerebral palsy ([46]), in which the natural neuromuscular stimulus is noisy, by using the electrical stimulation to force the movement of the limb.

However, the Functional Electrical Stimulation (FES) is not only used to stimulate these nerve clusters. Its primary purpose is to, in fact, move the affected limb or assist it in performing an action ([47] [48]) (e.g. grabbing a glass of water and bringing it to the mouth, or bringing silverware to the mouth).

Such an idea is very important, since the human organism has the so-called "muscle memory" ([49] [50]), so that the brain already knows what action to do and the muscles "remember" the movement. However, the "control system" formed by the nerve channels has been affected, so movement sometimes becomes erratic and inaccurate. Electrically stimulating other groups (or the same) forces the patient to perform the function correctly ([51]), making the "control system" adapt to the current situation and seek a new solution ([52]), hence the importance of movement intent in treatment ([53]).

Another objective of this work is to study the behavior of several control techniques to make the patient reach a desired target angle ([55]), maintaining it for a certain amount of time through an electrical stimulus. Table 1.1 shows eleven recent articles of great importance for the areas of control and rehabilitation, as described below, sorted by date.

The first four papers aim to control a functional electrostimulation system through nonlinear or intelligent controllers combined with classical controllers, in order to reduce the recovery time of patients with temporary injuries. In all of them, although the contribution in the medical field is strong, the biggest contribution is in the application of control theory to FES.

The fifth and sixth articles in the table focus on the medical field and the impacts of FES on patients' lives and rehabilitation. The seventh, eighth, and ninth papers are concerned with nonlinear control techniques based on switching or cost functions for controlling FES systems.

The tenth paper aims at a junction of switching and cost function based techniques coupled with a probability function in order to improve the performance of the FES system. Finally, the eleventh paper uses a classical controller (PID) tuned by genetic algorithms in comparison to a non-linear adaptive controller, in order to verify the performance of the two techniques and to prove a simplified mathematical model for this type of system. All these articles are further described in the article [54], which is a survey of various control techniques applied to FES.

Table 1.1: List of Recent Articles

Title	Field	Year
Adaptive fuzzy control of electrically stimulated muscles for arm movements ([56])	Control and Medical	1999
A Nonlinear Approach to Modeling of Electrically Stimulated Skeletal Muscle ([57])	Control and Medical	2001
Development of the FES System with Neural Network +PID Controller for the Stroke ([58])	Control and Medical	2005
Closed-loop control for FES: Past work and future directions ([59])	Control and Medical	2005
Histoire de l'electrostimulation en medecine et em reeducation ([42])	Medical	2008
A critical review of the most popular types of neuro control ([60])	Medical	2012
Nonlinear model predictive control of functional electrical stimulation ([61])	Control and Medical	2017
Time-scaling based sliding mode control for Neuromuscular Electrical Stimulation under uncertain relative degrees ([62])	Control and Medical	2017
Extremum Seeking-based Adaptive PID Control applied to Neuromuscular Electrical Stimulation ([63])	Control and Medical	2019
Model-Free Neuromuscular Electrical Stimulation by Stochastic Extremum Seeking ([64])	Control and Medical	2019
Human Arm Stabilization and Rehabilitation using Intelligent Control Techniques ([65])	Control and Medical	2020

1.1.4 EEG,EMG and ECG Signal Processing

Several studies in recent years have been using electromyographic (EMG) and electroencephalographic (EEG) signals to classify levels of consciousness, communication and intention to move. Furthermore, some studies on the subject will be presented and inserted into the context of the present work.

The article [66] explains a study on the fusion of EEG and EMG signals to detect the level of consciousness from waking up to sleeping. The article explains the use of Neural networks to classify and infer the state of consciousness of 30 individuals.

According to [67]: *"Electro-biological signals have become the focus of several research institutes, probably stimulated by the recent findings in the areas of cardiology, muscle physiology and neuroscience, by the availability of more efficient and cheaper computational resources, and by the increasing knowledge and comprehension about motor dysfunctions"*

The aim of the above study was to create and evaluate HMIs triggered by EEG and EMG signals to move a mobile robot or robotic arm. In addition, a very interesting schematic representation of a brain machine interface (BCI) was shown (Figure 1.6):

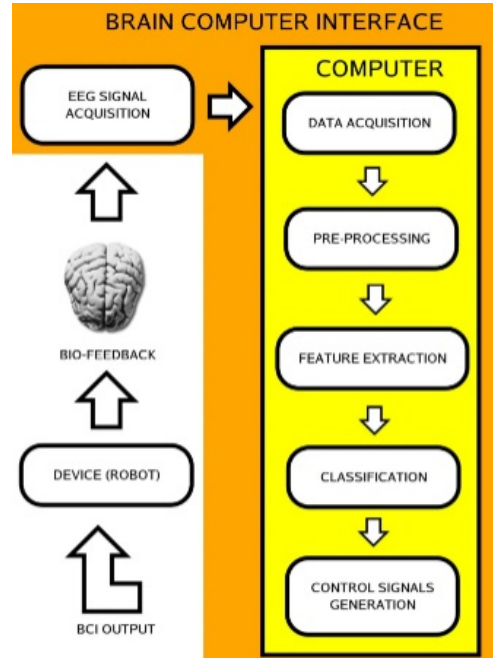


Figure 1.6: BCI Scheme (extracted from [67])

However, the BCI using EMG signals in the study, instead of capturing the signal of biceps or triceps neuromotor muscle, captured the signals through the blink of an eye. The BCI using EEG captured the alpha frequency-band

with the aim to detect activity of the occipital part of the brain (responsible for processing visual information). Both BCI from the study were focused on capturing signals from the visual, rather than the motor, to infer the intention of movement.

In [68], the authors use the EEG and EMG signals to infer the intention of movement to control wearable robots, however the signals was acquired directly from the muscles instead from the visual stimulus. The same was done in [69], where the authors prioritize EEG signals for the movement of an exoskeleton for upper limbs.

Another focus for the application of EEG, ECG and EMG signals is shown in article [70], which assesses the performance and alteration of these signals and compares them with the natural process of muscular and mental fatigue when performing some physical activity. Furthermore, [71] and [72] evaluate the intention of movement of the foot and fingers, respectively.

1.1.5 Control Theory and Design for Orthosis Activation

However, the common way to activate and control a orthosis or prosthesis is using biological signals, such as electromyographic (EMG) and electroencephalographic (EEG). In this way, some articles in the control field uses those signals with the aim to control an upper-limb orthosis. In the PhD thesis "Interface cérebro-máquina baseada em biotelemetria e eléctrodos secos" [74], the author set out to create a human machine interface for motion inference. In it, EEG signals were decoded and filtered using a wavelet transform.

In the master thesis "Proposta de um sistema baseado em redes neurais e wavelets para caracterização de movimentos do segmento mão-braço" [75], the author creates a system with the aim to characterize the executed movements of the muscles of the hand-arm segment, by using EMG signals.

In the article "Sliding mode control of an exoskeleton robot for use in upper-limb rehabilitation"[76], the authors uses a shoulder/arm/forearm exoskeleton robot to assist the rehabilitation (Figure 1.7 (A)). The Conventional Sliding Mode Controller was used and adjusted by Genetic Algorithms with the aim to execute a given trajectory. Another article [77] developed a similar project with the same goal (Figure 1.7 (B)), but without using genetic algorithms for tuning the Conventional Sliding Mode Controller.

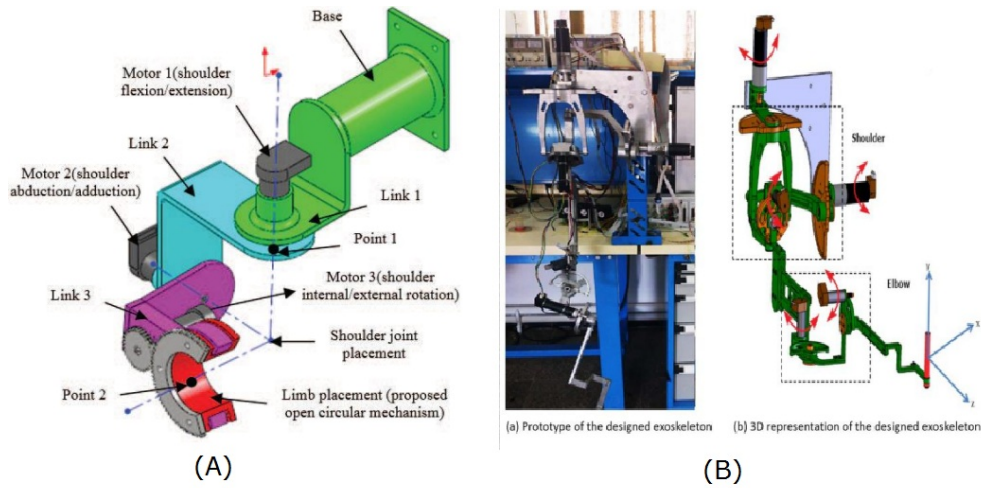


Figure 1.7: (A) 3D model of exoskeleton robot of article [76] (B) 3D model and prototype of exoskeleton robot of article [77]

In [78], the authors used a Sliding Mode Observer to move a leg orthosis using a defined trajectory. Another article [79] developed a similar project with the same goal, but using an Adaptive High Order Sliding Mode Controller.

Finally, in [80], the authors construct and simulates the control of an upper limb orthosis (Figure 1.8) by using High Order Sliding Mode Controller.

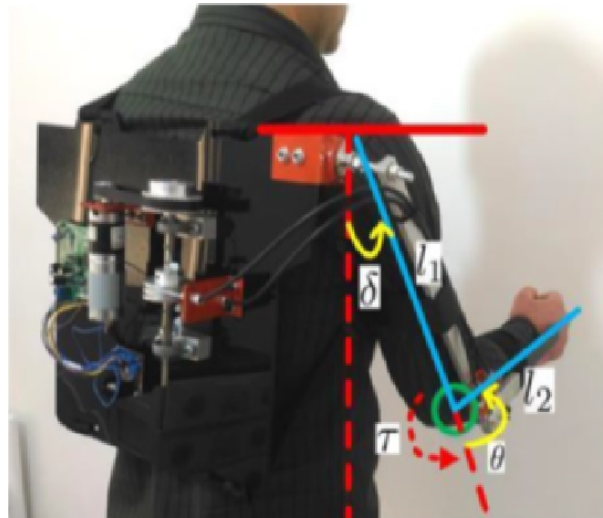


Figure 1.8: Prototype of exoskeleton robot of article [80]

1.2 Objectives

Analysing the literature review, it can be seen that most of the recent work uses robust or intelligent control. In addition, there are no recent studies that use all three types of signals together to infer motion, and there are not many recent studies that construct prosthesis or orthosis using digital manufacturing techniques.

Another interesting point is that none of the researched studies differentiate signals of only planned movements from signals of planned and executed movements, or even associative tasks (e.g. drinking water, bringing the hand to the mouth).

In this way, the main objective of this work is the creation of a human-machine interface using digital manufacturing techniques and the concepts of Industry 4.0 [16] for the manufacture and control of an orthosis of upper limbs that is adjustable, easy to adapt and ergonomic, in order to minimize the time of adaptation of the user to the orthosis.

The challenges to be overcome are important for improving the quality of life of people with disabilities. The first challenge is to assess the deficiencies, their origin and their impact on the construction of the orthosis. In this respect, disabilities were classified into two major branches: Disability due to an accident or medical error and disability due to degenerative or adverse diseases. The (Table 1.2) below presents this classification:

Table 1.2: Classification of Disabilities

Disease	Origin
Stroke Parkinson Alzheimer	Disease
brachioradial injury Cerebral palsy	accident or medical error
Malformation	Congenital diseases

The second challenge is the creation of a resistant, durable and low-cost orthosis. This is because orthoses and active prostheses are still very expensive and out of touch with many people in the world. Furthermore, the manufacturing of orthoses and prostheses must be fast, in order to prevent the disabled person from waiting for the equipment for a long time.

The third challenge is the use of control theory for mathematical modelling the neuromusculoskeletal system to be able to apply control techniques

that can be robust to parametric variations that would represent human being diversity.

The fourth and last challenge is to capture and use biological signals so that movement intentions to trigger the orthosis or prosthesis can be decoded and inferred.

1.3

Research innovations and boundary

As discussed in Section 1.2, there are several types of origins for loss of movement of the upper limbs. Thus, for the most significant approach, only brachial plexus injuries and post-stroke patients will be studied. This choice was made based on the following quote from [81]: *"From 2008 to 2013, the number of hospitalizations due to land transport accidents increased by 72.4%. In 2013, SUS registered 170,805 hospitalizations for traffic accidents and R\$ 231 million was spent on assisting victims. This figure does not include costs with rehabilitation, medication and the impact on other areas of health."*

According to [82]: *"Brachial Plexus Injury is most commonly caused by stretching, such as after a motorcycle accident and also, during some births. Plexus injury at the time of delivery bears the name of obstetric brachial palsy and may cause, in addition to loss of movement, loss of sensation and stretch or damage the upper nerve roots causing nerve damage."*

This type of injury affects the elbow bending movements and often the opening and closing of the hands. Thus, this specific movement was chosen to be analyzed and reproduced, see Figure 1.9.



Figure 1.9: Elbow Bending movement

Evaluating current research in the fields of optimization, control, signal processing and manufacturing processes, the present work has several innovations and establishes scientific contributions, described below.

Regarding structural optimization, the present work contributes to the application of multi-lattice structures in FDM 3D manufacturing processes with the aim to minimize the spent material and maximize the stiffness and strength of the constructed pieces. Furthermore, the use of digital manufacturing to assist the construction of orthoses is something increasingly new and has

as principles the combination of design and ergonomics concepts with technical concepts such as meta materials and a mixture of different types of materials.

Regarding control theory and design, as seen in [55], the human neuro-motor system is time varying, non linear and with parametric variation. Thus, nonlinear or robust control techniques are extremely important to control this type of system. The contribution of this work in control theory is the application of robust control techniques, such as super twisting, or higher order sliding mode observers.

Regarding signal processing, filtering of the EEG, EMG, and ECG signals will be used in order to infer the intention of the elbow bending movement and correct the movement using control techniques. In addition, a database of the collected signals will be assembled in order to allow other researchers to reproduce or use for various other related purposes.

Thus, this work fills several gaps left by previous research, since it intends to use three types of bio-signals, combined with robust and nonlinear control techniques, besides using lattice structures to reduce the use of material to make the orthosis, which impacts on a decrease in the weight of the device, while maintaining the mechanical characteristics necessary for proper functioning and execution of the desired movements.

1.4

Thesis Organization

Chapter 2 presents a description of the problem, showing the physiological analysis and how the signs and movement can be affected depending on the injury or disease.

Chapter 3 presents the study of the construction of the orthosis, having as evaluation the manufacturing process, the weight and the adaptation of one or more users to the orthosis.

Chapter 4 presents the study of structural optimization of the orthosis to make the manufacturing process more viable and cheaper.

In Chapter 5, the signals from the database set up in Chapter 2 are evaluated to assess the nature of the signals and find a way to process them.

Chapter 6 presents a review on dynamic models for human upper limbs and a review on the general formulation for the problem, along with the advantages and disadvantages of the existing techniques, and the integration of simulation techniques with control and electronics in real time to execute a set of established movements.

Finally, Chapter 7 brings suggestions for future work and the conclusions of this thesis.

2

Study of the physiology of the Upper-Limb Movements

2.1

Nature of the Upper-limb Movements and the Brachial Plexus

Upper limb movements can be divided into shoulder movements (horizontal rotation, abduction and flexion), scapular movements (lateral rotation, arm extension, abduction and adduction), axillary movements (medial rotation, arm extension and flexion), arm movements (elbow flexion, supine, adduct and extend the forearm) and hand movements. The responsible for this set of movements is the brachial plexus.

According to [83]:

"The brachial plexus (BP) is a network (plexus) of nerves (formed by the anterior rami of the lower four cervical nerves and first thoracic nerve (C5, C6, C7, C8, and T1). This plexus extends from the spinal cord, through the cervicoaxillary canal in the neck, over the first rib, and into the armpit. It supplies afferent and efferent nerve fibers to the chest, shoulder, arm, forearm, and hand." The Figure 2.1 below shows a simple scheme of brachial plexus.

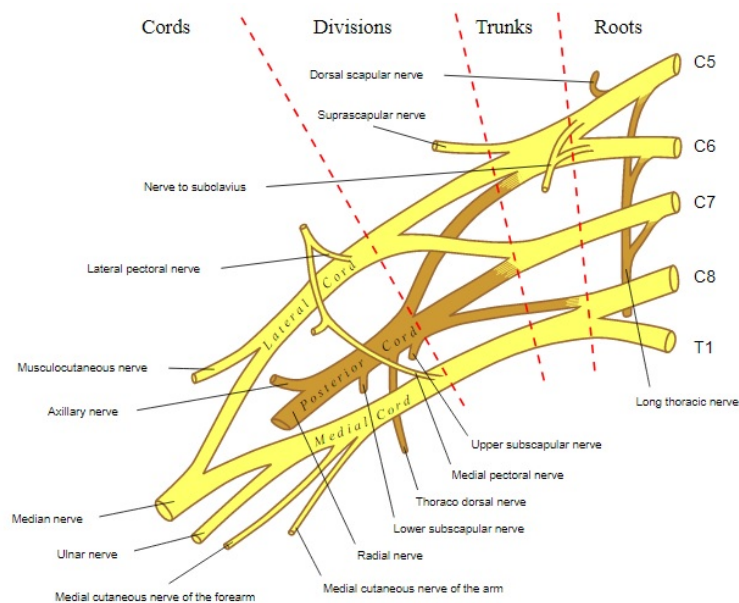


Figure 2.1: Illustrative scheme of brachial plexus (adapted from [83])

The brachial plexus region has the function of sending and receiving stimuli for different movements [84], associated with the contraction and extension of different muscle groups. However, as described in Section 1.3, the elbow bending movement was chosen to be analyzed. Table 2.1 associates the muscle and its importance for the respective movement, while Figure 2.2 shows all muscle groups that are activated by the brachial plexus.

Table 2.1: Muscles and Movements

Muscle	Movement
Biceps Brachii	Flex the forearm at the elbow joint and forearm supinator, accessory arm flexor at shoulder joint
Coracobrachial	Flex the arm at the shoulder joint and adduct the arm
Brachial	Flex the forearm at the elbow joint
Brachial Triceps	Forearm extension at the elbow joint. The long head can also extend and adduct the arm to the shoulder joint
Brachioradial	flex the forearm
Anechoic	extend the forearm

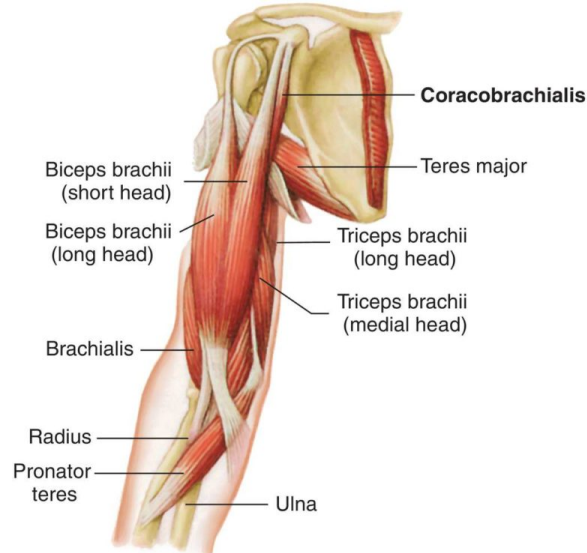


Figure 2.2: Muscle groups of the brachial plexus(extracted from [85])

An important observation about upper limb kinematics is that it has seven degrees of freedom in total (excluding hand movements): three for the shoulders (shoulder pitch, shoulder roll, arm yaw), one for the elbow (elbow pitch), and three for the wrist (wrist pitch, wrist roll and wrist yaw).

An injury or loss of control or communication with the brachial plexus can cause the loss of part of the flexion, adduction and abduction movements of the upper limb [86] and, depending on the extension, the total loss of the ability to move the upper limb. The present study was limited to two types of causes of loss of elbow bending capacity: brachial plexus injury and stroke.

2.2

Stroke and its Consequences

Before assessing the consequences of a stroke, it is interesting to know how it happens and the causes. A stroke can be caused by the clogging of the arteries that carry oxygen to the brain (ischemic stroke) or by the rupture of some artery in the brain (hemorrhagic stroke). Basically, clots and ruptures in the arteries and microvessels of the brain are caused commonly by an unhealthy lifestyle that can alter cholesterol levels in the blood, generating fatty plaques that can clog arteries.

According to the ANVISA and the Brazilian Cardiology Society, 40% of Brazilians have high cholesterol levels. Cholesterol is a fat produced by the body, divided into two types: LDL and HDL. LDL, called "bad cholesterol", in excess can generate the accumulation of fatty plaques in the arteries, preventing or hindering the passage of blood. Furthermore, other factors that can cause a stroke are diabetes Mellitus, atrial fibrillation, and excess of alcohol. Figure 2.3 shows a simple scheme of ischemic stroke caused by atrial fibrillation.

Stroke has different consequences depending on which part of the brain is affected. It can cause loss of speech, vision, affect memory and more [87], however the most common is loss of coordination and motor control, especially on one side of the body. This condition of paralysis is called hemiplegia. Furthermore, strokes may cause cerebrovascular diseases [88], such as depression, anxiety disorder and mania.

Since the present study will only address the elbow bending movement, as discussed in Section 1.3, the only consequence to be analyzed here in depth will be hemiplegia. According to [89], *"Post-stroke hemiplegia is associated with significant impairments of motor function that are believed to compromise the activity of daily life performance and lead to loss of independence. However, a direct causal relationship between strength or weakness and motor function has*

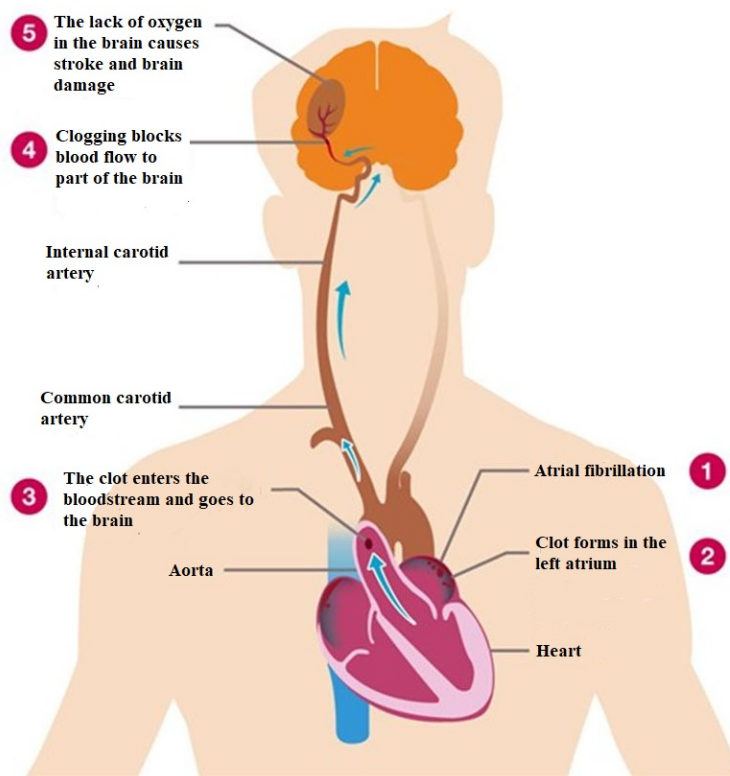


Figure 2.3: Illustrative scheme of a stroke (adapted from [90])

not been established. Traditionally, a strong bias has existed against quantifying strength in hemiplegic persons".

In this regard, hemiplegia post stroke is the loss of motor control, caused by not sending the electrostimuli to the neuroreceptors that activate the muscles. In other words, the muscles and the nerve trunk are perfect, but "the command" is not sent to them due to brain damage [91]. In order to recover "the path" made problematic by a stroke, several treatments like FES have been performed [92], as specified in Section 1.1.3. However, in some cases the loss of control and strength due to spasticity makes the patient need to use orthoses for a significant period of time (called temporary orthosis)(Figure 2.4).



Figure 2.4: Example of temporary orthosis (X-cat Rom Endurance) (adapted from [93])

2.3

Brachial Lesion and its Consequences

Brachial lesion commonly occurs due to three traumas: stretching, falling or at birth. According the website "<https://abraco.numec.prp.usp.br/>" *"The main causes of traumatic brachial plexus injury are traumas related to traffic accidents involving cars, motorcycles, public transport, bicycles and pedestrians - more than 80% of injuries are due to motorcycle accidents. Accidents at work, home, sports and injuries in the neck and shoulder can also cause an injury"*. In [94], a study was presented that resulted in 62% of supraclavicular injuries, with 60% injuries by traction mechanism. Figure 2.5 shows a simple scheme of brachial lesion caused by falling and stretching.

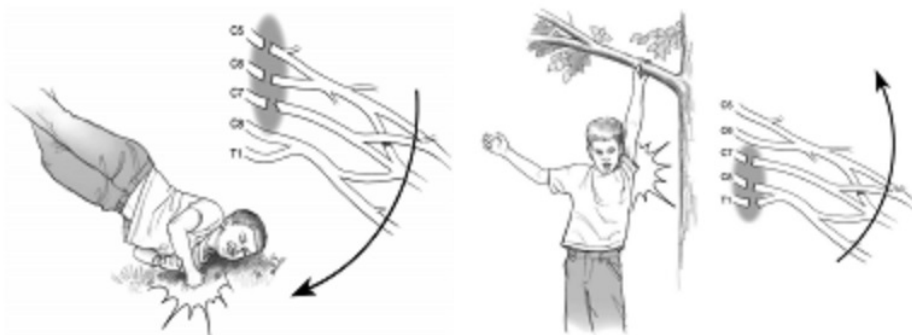


Figure 2.5: Illustrative scheme of brachial lesion caused by falling and stretching (adapted from [95])

However, this type of injury can also occur at birth (Figure 2.6), called obstetric brachial plexus lesion (OBPL). According to [96] *"Obstetric brachial plexus lesions (OBPLs) are caused by traction to the brachial plexus during labor. Typically, in these lesions, the nerves are usually not completely ruptured but form a "neuroma-in-continuity." Even in the most severe OBPL lesions, at least some axons will pass through this neuroma-in-continuity and reach the tubes distal to the lesion site. These axons may be particularly prone to abnormal branching and misrouting, which may explain the typical feature of co-contraction"*.

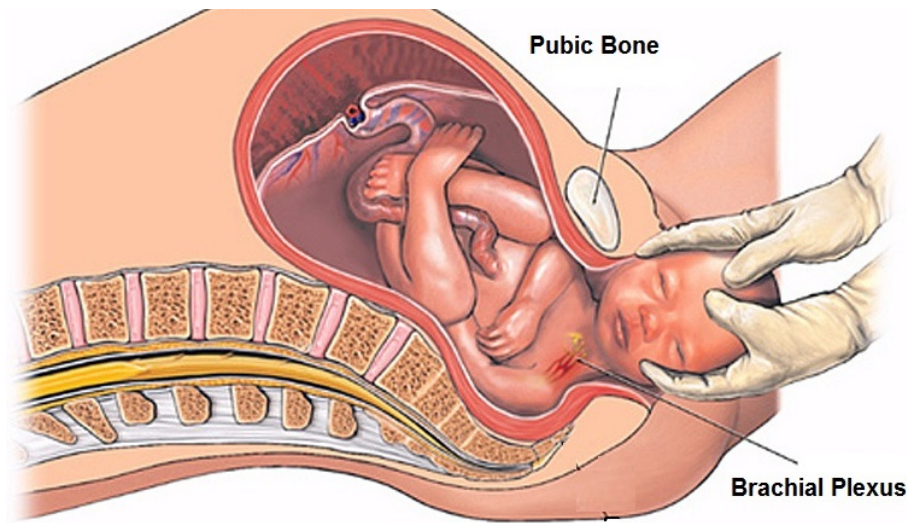


Figure 2.6: Illustrative scheme of brachial lesion caused at birth (extracted from [97])

Mainly due to muscle weakness, joint stiffness and eventually pain, several day-to-day activities may be compromised in brachial plexus injury, such as: drinking water, eating, bathing, dressing, writing, playing sports. This can affect the quality of life of individuals with brachial plexus injuries, and may even limit leisure activities or restrict their performance at work, generating emotional, social and economical consequences.

In this regard, brachial lesion is the loss of motor control, caused by the damage of the brachial plexus that activate the muscles. Simplifying, the muscles and brain are perfect, but "the command" is not sent to them due to nerve damage. In order to recover "the path" damaged by brachial lesion, several treatments with physiotherapy is recommended. However, in some cases the loss of control and strength due to spasticity makes the patient need to use orthoses.

3

Digital Manufacturing in the construction of the orthosis

As presented in the previous sections, digital manufacturing, which is the set of manufacturing processes that start from a virtual model or the virtualization of a piece made by hand, has been growing every day, mainly with the advent of the Industry 4.0 movement. According to [98]:

"Additive manufacturing is a fabrication technology that is rapidly revolutionizing the manufacturing and construction sectors."

In addition, several current works have been showing the evolution of digital or hybrid manufacturing in various branches, such as in the automotive industry [15], oil and gas industry [99], in the prototype manufacturing process [16] and in medicine in general [100] [101].

In this aspect, before addressing the impact of digital manufacturing on the manufacture of orthoses and prostheses, it is necessary to conceptualize the Industry 4.0 movement.

3.1

Industry 4.0 Concepts and Definitions

The Industry 4.0 movement originated around 2008 and consists of a set of manufacturing practices and processes based on breaking constructive paradigms [16]. Furthermore, several authors have been debating the evolution and implementation of this new set of production processes, as seen in [102], [103] and [104]. Industry 4.0 or the fourth industrial revolution changed constructive paradigms, as it implemented the model virtualization process. This aspect was already initiated at the end of the third industrial revolution with the construction of CNC machines (Computer Numeric Control), but it was expanded with the popularization and evolution of 3D printers.

In addition, Industry 4.0 is a set of processes (including additive manufacturing) that generates a complex production model. Therefore, Industry 4.0 processes must have at least one of the following aspects [110]:

- Virtualization of the model or process;
- Computer simulation of the process;
- Process customization;

- Manufacturing on demand using hybrid or additive manufacturing (AM).

According to [110]:

"Based on these aspects, the application of Industry 4.0 techniques in the medical field is extremely beneficial, as it is a multitasking tool. Thus, Industry 4.0 applied to medicine can be called "Medicine 4.0" or "Health 4.0" ([105]), as is already called in design (Design 4.0 [106]) and architecture (Architecture 4.0 [107]), in which elements of IoT (Internet of Things [108]) and BIM (Building Information Modeling [109]) are inserted for the elaboration and development of construction processes" (Figure 3.1).

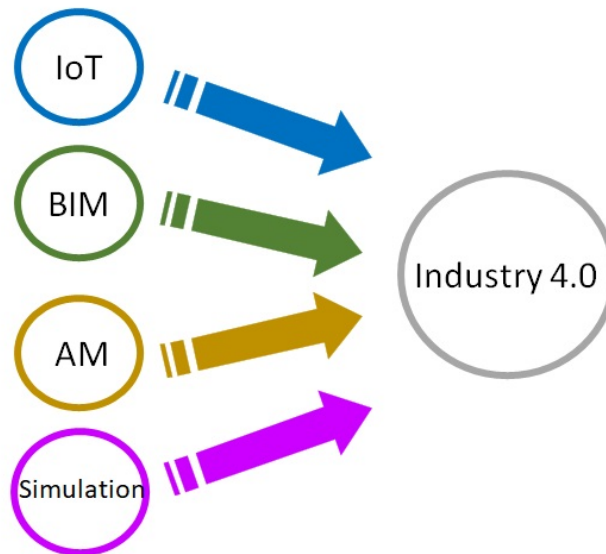


Figure 3.1: Illustrative scheme of a Industry 4.0 (adapted from [110])

Health 4.0 includes elements such as virtualization of prototypes, simulation of surgical processes, use of wearable devices [101], remote monitoring of vital signs [100], and standardization of diagnostic procedures, which support the work of health professionals.

According to [15], the manufacturing processes can be divided into three great areas: subtractive manufacturing, additive manufacturing and digital manufacturing. The subtractive manufacturing corresponds to a set of processes such that the raw block material is modified by material removing. The common processes of subtractive manufacturing are milling, lathe and grinding. The additive manufacturing corresponds to a set of processes where the work-piece is constructed layer-by-layer through material deposition.

There are five types of additive manufacturing technologies, performed layer-by-layer to build the real model:

- FDM (Fused Deposition Modeling), which consists of the deposition of a fused plastic;

- SLS (Selective Laser Sintering), which consists of the laser sintering of a plastic material in powder;
- SLA (stereolithography), which consists of curing a resin material using a UV lamp;
- DOD (binder jetting), which consists of blasting a binding material into a powder (e.g. sand, plaster, plastic);
- DMLS (Direct Metal Laser Sintering), which consists of the laser sintering of a metallic material in powder .

Figure 3.2 summarizes the existing additive manufacturing technologies.

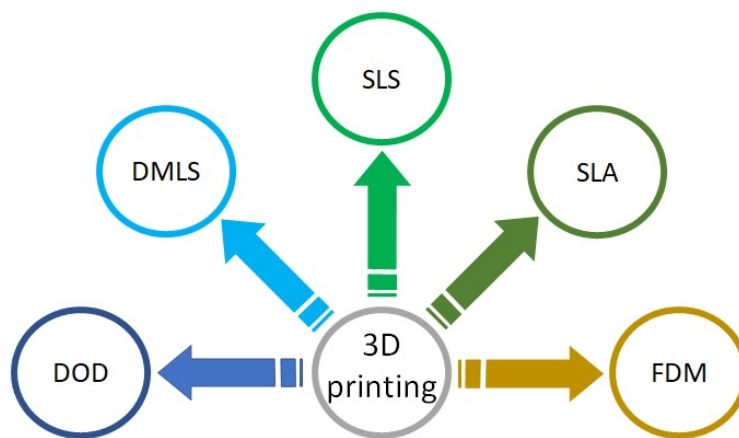


Figure 3.2: Scheme of 3D printing technologies (adapted from [110])

Digital manufacturing is also called hybrid manufacturing. It is the set of manufacturing processes in which a virtual model is transformed into a real model. This set of processes can be subtractive, additive, or a combination of both, with so-called hybrid machines, in which processes of either additive or subtractive manufacturing are carried out.

The movement of Industry 4.0 has been gaining strength in manufacturing in general, because its concepts make manufacturing faster and more competitive. This happens because, using scanning equipment, it is possible to build more reliable digital models, faster than conventional manufacturing processes. Furthermore, using Industry 4.0 concepts allows for greater customization of the manufacturing process, albeit at a low cost.

3.2

Digital Manufacturing and Construction of Upper-limb Orthosis

The manufacture of an orthosis for upper limbs has very unique characteristics. This happens because each individual has a specificity, whether in relation to the acquired disability or due to anthropometric differences. Thus, the manufacturing process of an orthosis is difficult to be standardized and transformed into a large-scale production. However, using Industry 4.0 concepts, production through digital manufacturing becomes viable, as the entire process chain helps in the production of complex and variable format parts. This way, the chain of processes can be divided into the four aspects described before.

3.2.1

Virtualization of the model

The first step in the construction of the orthosis, in addition to assessing the patient's illness, is the biomechanical assessment. This assessment is commonly performed by a medical team consisting of an orthopedist, neurologist and physiotherapist. These professionals will check the results of several exams to find out the extent of the injury and what to do to improve aspects such as posture, locomotion, and understand the limitations, even if temporary.

Using the virtualization aspect inherent to Industry 4.0, two additional steps have been added to the evaluation: the evaluation of efforts and movements through a digital movement capture system, and the patient's digitalization through a 3D scanner. The capture of movements and efforts can be done in different ways. The first would be using a system similar to those for capturing ship movements [111] [112]. The second is through a IMU (Inertial Measurement Unit) [113].

In the present study, both forms of measurement are used, in order to assess which of them has the best performance, using the *Qualisys*[®] 3D tracking system. Composed of 10 high-precision cameras, this system needs a special subroutine to demarcate the simulation space (camera calibration) and also markers with infrared sensors glued to the volunteer's joints to detect movement.

Furthermore, a set of IMUs from *X sens*[®] is placed at certain points on the body of the volunteer, aiming to capture its movement. This system only needs the fixation of the IMUs, not requiring cameras, environment definition or markers. Both systems capture the volunteer's movements, in order to verify the change in movement dynamics due to the patient's injury (OBPL).

In addition, the test is also performed with a volunteer without any disability, in order to have a pattern of movement behavior as a way of comparison, even with individuals having different physical complexion. Figure 3.3 shows the *X sens*[®] IMU interface.

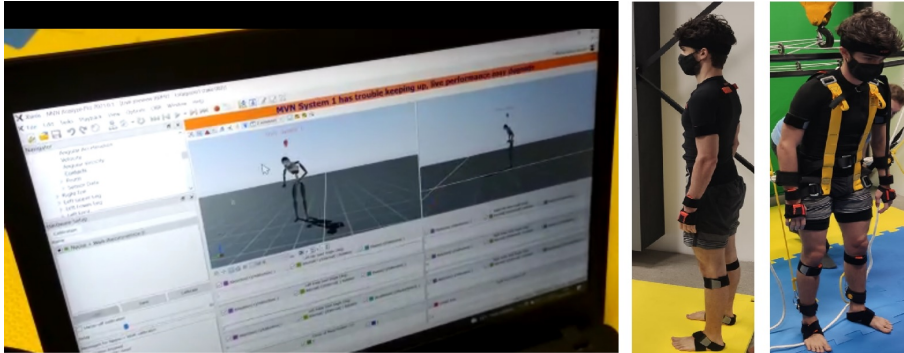


Figure 3.3: *X sens*[®] motion capture

The second stage of this analysis and virtualization is the digitization of the volunteer's body, in order to create a high-precision triangular mesh. This mesh allows an evaluation of measurements and efforts, in addition to ensuring that the virtual modeling of the orthosis is ergonomically pleasing to the future user. The individual has the body digitized using the *Artec Spider*[®] scanner, and a virtual 3D model is generated (Figure 3.4).

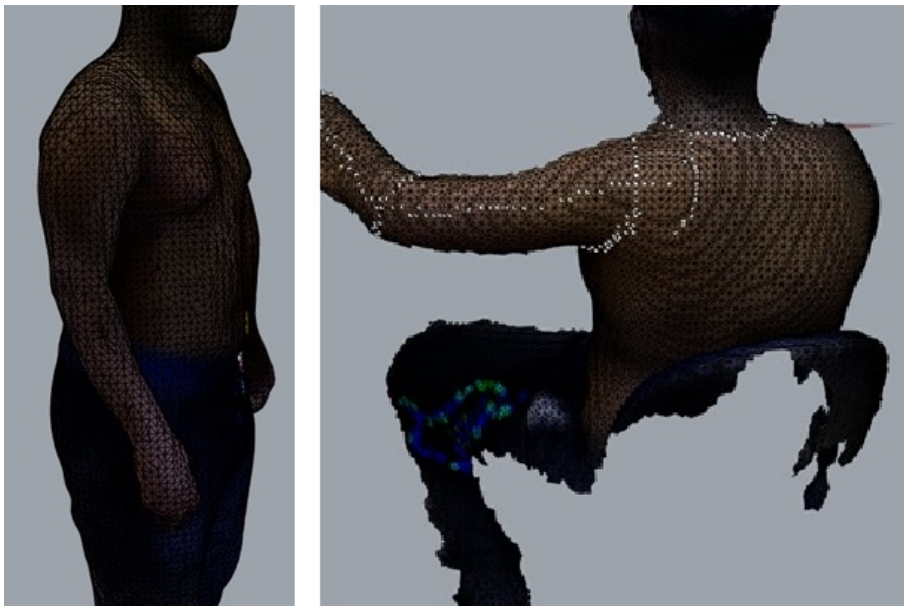


Figure 3.4: virtual 3D model

3.2.2

Computer simulation of the orthosis

As previously described, one of the main causes of rejection of prostheses and orthoses is the difficulty in adapting [10] [11]. This can happen due to several causes, but the main one is the lack of ergonomics of low-cost prostheses and orthoses. This type of prosthesis is not made entirely for the user, but in a generic way and with small adaptations to avoid contact injuries. Another problem that can lead to rejection is the orthosis being heavier or lighter, causing the user to have an ergonomic imbalance when moving around or using it.

In order to delimit the boundaries of the present study, the orthosis here developed is an arm and forearm orthosis, with the purpose of performing elbow bending movements. This orthosis is aimed at both people with low or total mobility in the execution of this type of movement. Thus, the orthosis must be light, resistant and capable of supporting the user's forearm in movements such as drinking water, eating, taking the hand to the head and other similar movements. With this, the weight parameter to be supported was set to 50 kg, and only one planar rotation movement was allowed (rotation in more than one plane is performed by the user's natural shoulder rotation).

The digitization is carried out using the *Artec*[®] Spider scanner, using *Rhinoceros*[®] to join the triangular meshes. For the simulations of the efforts in the constructed orthosis, the inertial measurement system of the company *sens*[®] software is used.

Using the computational simulation aspect of Industry 4.0, two important simulation tools are used. The first is checking the user's weight balance and movements compared to movements without the orthosis, as well as simulations of ergonomic adaptation of the orthosis to improve the patient's comfort with the equipment. This first simulation tool is the *X sens*[®] platform.

These tests are aimed to verify the wearer's efforts, movements and posture with and without the orthosis, evaluating the resulting changes. These simulations define the joint locations of the virtual orthosis, as well as the maximum weight allowed for the equipment. Having defined parameters such as maximum effort and maximum weight, the next step is to use a tool to design the orthosis so that it meets the simulated requirements

Several 3D models are developed using the *SolidWorks*[®] software. After their design, the models are evaluated through simulations using the defined effort parameters. Each evaluated model receives improvements, until two model versions have been considered for a prototype, see Figure 3.5.

The first version, on the left in the figure, was designed to be made

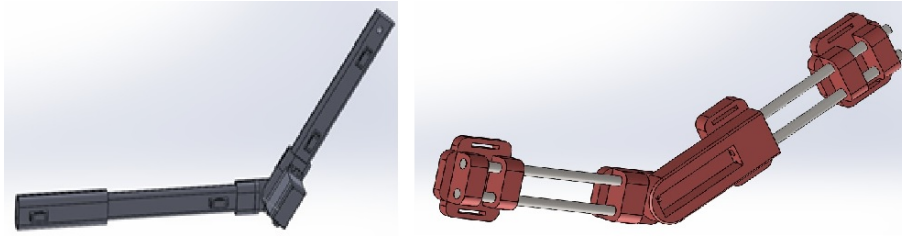


Figure 3.5: virtual 3D models of orthoses

entirely of PLA (Polylactic Acid), being very light. However, this version had some problems regarding stiffness as well as in the upper limb anchoring. The second version proved to be more resistant, despite being heavier than the first. Also, instead of being just made of PLA, it had aluminum parts.

3.2.3

Process customization

The printing process is evaluated to improve the performance of the orthosis in relation to time and manufacturing processes. Here, multi-lattice optimization is used, which will be better explained in the next chapter. Another customization implemented is the possibility of adjusting the orthosis to the user's arm length, which allows for better adaptation and lifetime of the equipment. This adjustment is made by sliding between two pieces, with the fixation on the user's wrist. Furthermore, the pieces can be printed in several available colors, encouraging the user to wear the orthosis as a fashion item.

3.2.4

Manufacturing on demand using hybrid manufacturing

The last major aspect of Industry 4.0 to be described is bracing fabrication. This aspect is the key to the evolution of the process, since orthoses made by conventional manufacturing processes can take months to be completed.

The orthosis models defined to be manufactured have been carefully analyzed in the manufacturing processes. The first model is built entirely through additive manufacturing, using FDM technology with PLA material. The second model underwent a more detailed analysis, and two processes are tested. For the plastic parts, additive manufacturing is used through SLS and FDM technologies, in order to compare the performance of each process. For the metal parts, additive manufacturing is tested using DMLS technology, using a stainless steel alloy similar to ANSI302 and ANSI5052. Alternatively, aluminum bars were also purchased with the design diameter.

Both models described above have been built. One user wears the equipment and undergoes a new evaluation using the set of IMUs from the X

sens[®] platform, in order to check whether the simulated model corresponded to the real printed model. The second version of the orthosis was closest to the objective.

It is important to note that neither of the two models was tested with electronics and on-board motorization, as the purpose of the tests was not to assess the performance of the electronics, but rather an ergonomic and postural assessment of the individual and the impact of inserting the orthosis in relation to their posture and general movements, such as walking, running and jumping. These movements, despite not being made by the orthosis, are impacted by it and can destabilize the mechanical and postural behavior of the volunteer, which makes this analysis of paramount importance .

An incidental point (although not the main scope of the study) is the participation and interaction in the construction and use of the orthosis by the user. The interactive method occurred from the beginning of the manufacturing process, as the user was digitized so that simulations could be performed with the virtual models (Figure 3.6).

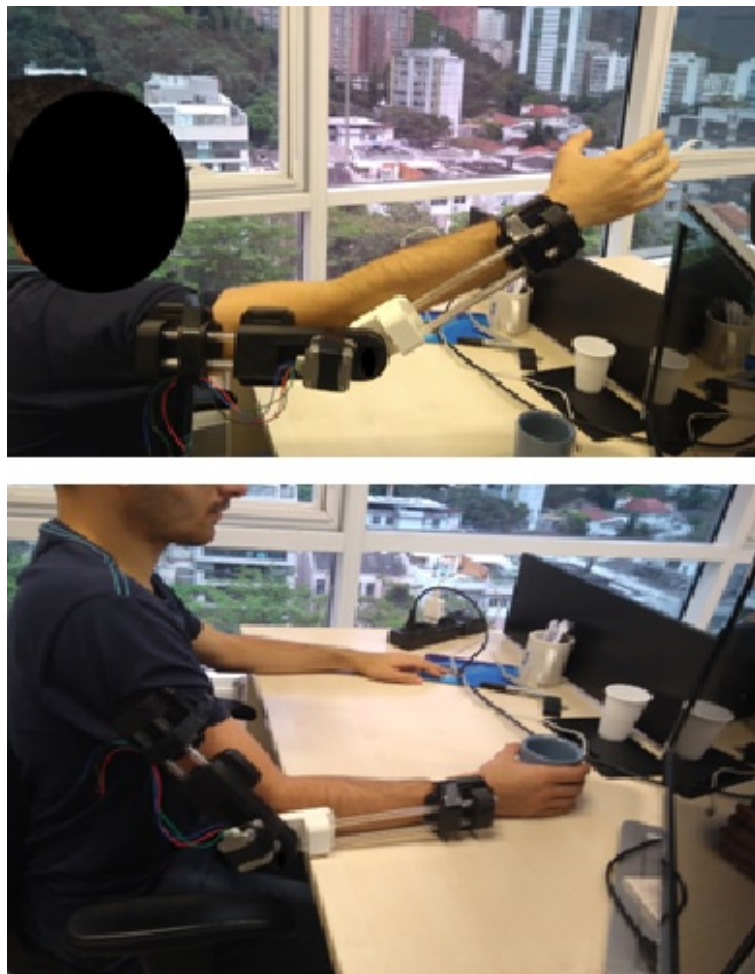


Figure 3.6: test of the orthosis

In addition, after construction, the user wore the orthosis and was fully instrumented through the *X sens*[®] platform, which allowed a full biomechanical evaluation of the user using the orthosis. In other words, the process of virtualization and the interaction between the prosthesis and the patient is very important. Once the orthosis is adjustable to the patient, the parts of the prosthesis can be fixed comfortably so that the movement performed is improved (Figure 3.7).

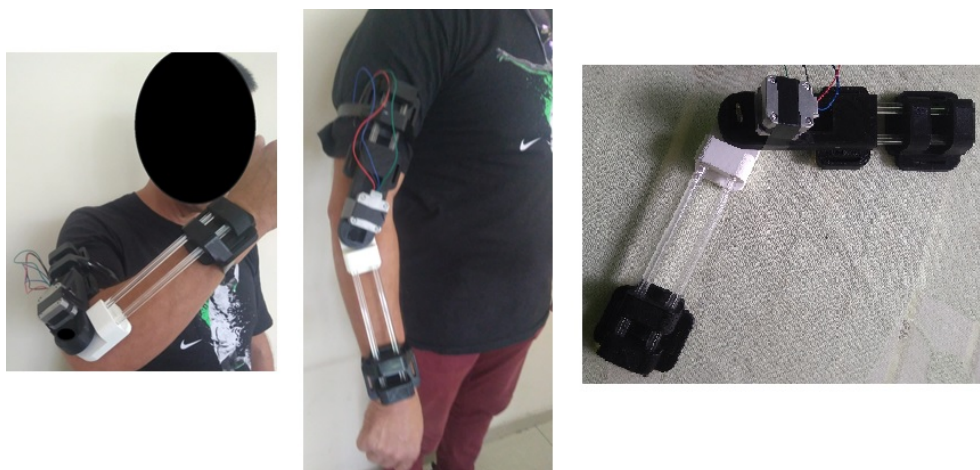


Figure 3.7: prototype of the orthosis

Once the simulation and modeling of the orthosis are finished, the next step will be to optimize the construction using multi-lattice structures, with the aim of saving material, making the orthosis lighter for the user and cheaper to manufacture, as addressed in the next chapter.

4

Multi lattice optimization applied to FDM processes

As described in the previous chapters, the optimization of digital manufacturing processes is one of the premises of the Industry 4.0 movement. Thus, a faster, less costly manufacturing process that maintains the mechanical properties of the product is essential, especially when it comes to a set of customized and special manufacturing processes, such as those used in the construction of orthoses.

All processes performed in this work were made in accordance with ASTM D792 Standard. This standard defines each tensile and compression test process from how to fix on machines to the shape and dimensions of specimens. Regarding the specimens parameters, it was defined that the printing direction would be the one with the greatest mechanical efforts, that is, the construction of the layers would be in the direction of the tensile forces.

This research used the standard PLA filament with 3mm diameter as the base material for printing and the *Sigma^x*® from the company BCN3D as a printer. For the tests, an *INSTRON*® traction/compression testing machine was used.

All simulation analyzes were performed using the *SolidWorks*® software plugin for mechanical properties and the CAD drawings were performed using the *Rhinoceros*® software allied to *SolidWorks*®.

Another interesting point of the research was to define the percentage of filling of the 3D-printed specimen, since this parameter is closely linked to mechanical resistance. This way, different fillings were simulated using the *SolidWorks*® software. The threshold parameter to define the minimum filling was the load of 490N, defined by the maximum load that the orthosis could withstand (parameter defined according to the future electric motor of the orthosis and according to the load to be raised by the individual).

There are several types of optimization, all of which undergo a characterization of specific parameters, such as production time, reduced material use and improved mechanical properties. The present study, as described above, focused on optimizing the use of material in the manufacture of the orthosis based on the modification of the internal structure of its layers. The conventional FDM manufacturing process has several internal filling patterns,

all of which are constructed using regular polygons (e.g. triangles, rectangles, hexagons) perpendicular to the printing axis.

The purpose of this chapter is to create micro structures that replace the standard filling formats in order to reduce the use of material while maintaining the mechanical properties of the structures. For this, several mechanical tests were performed with standard specimens. In the course of this chapter, each test and the results will be described.

4.1

Lattice structures

Lattice structures are based on the crystal structures of metals. According to the type of lattice, the material achieves different mechanical loads. According to [114]: "*Cellular structure solid is a network of truss including struts or plates interconnected each other*". In the article [115], the authors review the impact of the use of lattice structures in additive manufacturing, however they only used SLA type prints (stereolithography).

Another use for lattice structures is demonstrated in [116], which performs mechanical tests on various types of lattice structures printed by DMLS (Direct Metal Laser Sintering) technology.

This work focuses on printing with FDM technology, representing an innovation in this aspect, as this is the cheapest among the existing 3D printing technologies today. In the first part of this study, the different lattice forms were analyzed, as shown in Figure 4.1.

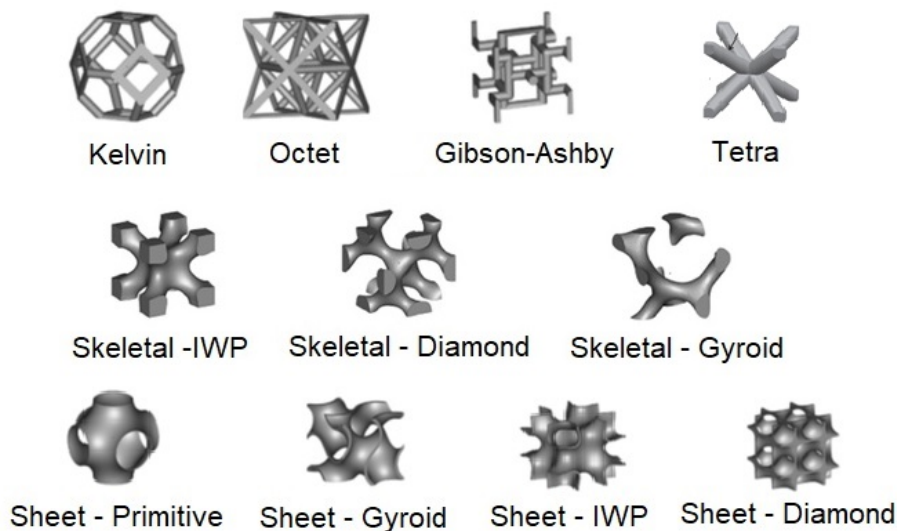


Figure 4.1: Types of lattice structures

Studies from the last six years have evaluated different forms of construction, mainly using DMLS technology [117] [118] [119]. After evaluating

the various structures present in the literature, some of the micro structures were chosen, which are detailed in Table 4.1.

Table 4.1: Types and characteristics of lattice structures

Structure	Characteristic	Reference Study
All Faced-Centered Cubic (AFCC)	XYZ symmetry Suitable for energy absorption	[120]
Body-Centered Cubic (BCC)	Eight struts linked at center Isotropic Unit Cell	[121] [122] [123] [124]
Face-Centered Cubic (FCC)	XYZ symmetry Isotropic Unit Cell	[125] [126]
Two Face-Centered Cubic with BCC combined (F2BCC)	Boolean combination of 2 FCC and 1 BCC cells Suitable for energy absorption	[127] [128] [129]

However, no recent study indicates the use of these types of structures through FDM technology applied to orthoses. After running simulations using the *SolidWorks*[®] software, it was observed that the Tetra-type structure, also called the BCC (Body-Centered Cubic) structure, has the lowest density and manages to have a performance in relation to load distribution similar to others simulated. Moreover, this structure was chosen to be evaluated due to its simplicity and construction similarity to the standard FDM pattern filling structure (Figure 4.2). In the article [130], the authors evaluate the influence of different infill geometry on mechanical properties.

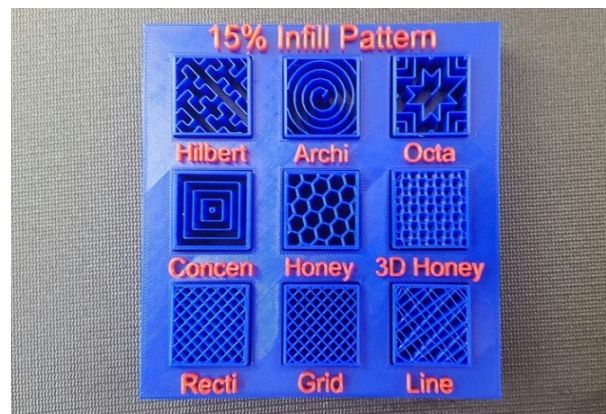


Figure 4.2: Types of standard FDM infill structures (extracted from [131])

The objective of all studies carried out in this chapter was to minimize the use of printed material in order to maintain or improve mechanical strength, replacing the standard honeycomb print filling with BCC lattice structures uniformly disposed in the pieces.

4.2

Multi lattice optimization

There are several ways to optimize a lattice structure. Optimization can be through:

- change in thickness of lattice structure: increasing or decreasing the thickness in regions of greater or lesser effort, the structure can become lighter without losing the desired mechanical characteristic. This type of technique falls under the group of "gradient techniques";
- change in size of structure: it works in a similar way to the change in thickness, as increasing or decreasing the size of the cell in regions of greater or lesser effort, the structure can be lighter without losing the desired mechanical characteristic. This type of technique also falls under the group of "gradient techniques";
- change in type of lattice structures: as described in the previous section, each structure has a particularity, so that their mixture allows combining favorable aspects of each structure depending on the effort to be supported in each region of the part. This type of technique falls under the group of "variation techniques";
- change in position of lattice structures: this type of optimization consists of inserting the lattice structures in strategic positions on the piece in order to ensure improved mechanical properties. This type of technique also falls under the group of "variation techniques".

Also in terms of optimization, the techniques described above can be combined with other types of algorithms, such as finite element modeling, genetic algorithms and deep learning. In the present study, only the optimization through change in size of structure was used, adopting a uniform distribution inside the studied parts and specimens.

Ten cylindrical specimens were built following the ASTM D792 standard, with BCC structures of different diameters, starting with a diameter of 5 millimeters going up to 0.5 millimeters. After that, using the *SolidWorks*[®] software, the density and the maximum efforts of each structure were evaluated. As a result, the one with the best density vs. effort ratio was the specimen with internal structures of 1 millimeter in diameter (Table 4.2).

Table 4.2: Analysis of the simulations (BCC infill)

Test	Specimen	Mass	Maximum Force	Tensile strength
Tensile	BCC+5mm	27.84 g	2000 N	4MPa
	BCC+4mm	23.38 g	1800 N	3.5 MPa
	BCC+3mm	18.39 g	1700 N	2.8 MPa
	BCC+2mm	13.67 g	1650 N	2.5 MPa
	BCC+1mm	10.16 g	1500 N	2.2 MPa
	BCC+0.5mm	9.14 g	750 N	1.2 MPa
Compression	BCC+5mm	27.84 g	7000 N	12 MPa
	BCC+4mm	23.38 g	6500 N	11.5 MPa
	BCC+3mm	18.39 g	6250 N	10.25 MPa
	BCC+2mm	13.67 g	5750 N	9.75 MPa
	BCC+1mm	10.16 g	5000 N	9 MPa
	BCC+0.5mm	9.14 g	3200 N	7 MPa

To choose the best configuration, a honeycomb pattern with 70% infill was used as a comparison (Table 4.3).

Table 4.3: Analysis of the simulation (hex pattern or honeycomb 70% infill)

Test	Mass	Maximum Force	Tensile strength
Tensile	36.12 g	900 N	1.8 MPa
Compression	36.12 g	2900 N	6 MPa

In this way, the best frame configuration (BCC + 1 mm), compared to the default print fill configuration (hex pattern or honeycomb), achieved a 30% weight reduction .

However, when a lattice structure was applied inside the specimen, the simulations showed that there was an increase in the mechanical properties, even with a weight reduction. This happens because the BCC structure, as described in Table 4.1, has an Isotropic Unit Cell, which means a uniform distribution of loads in all directions, which does not happen with the common infill (honeycomb).

The Figure 4.3 presents the variation of the diameter of the inner structures.

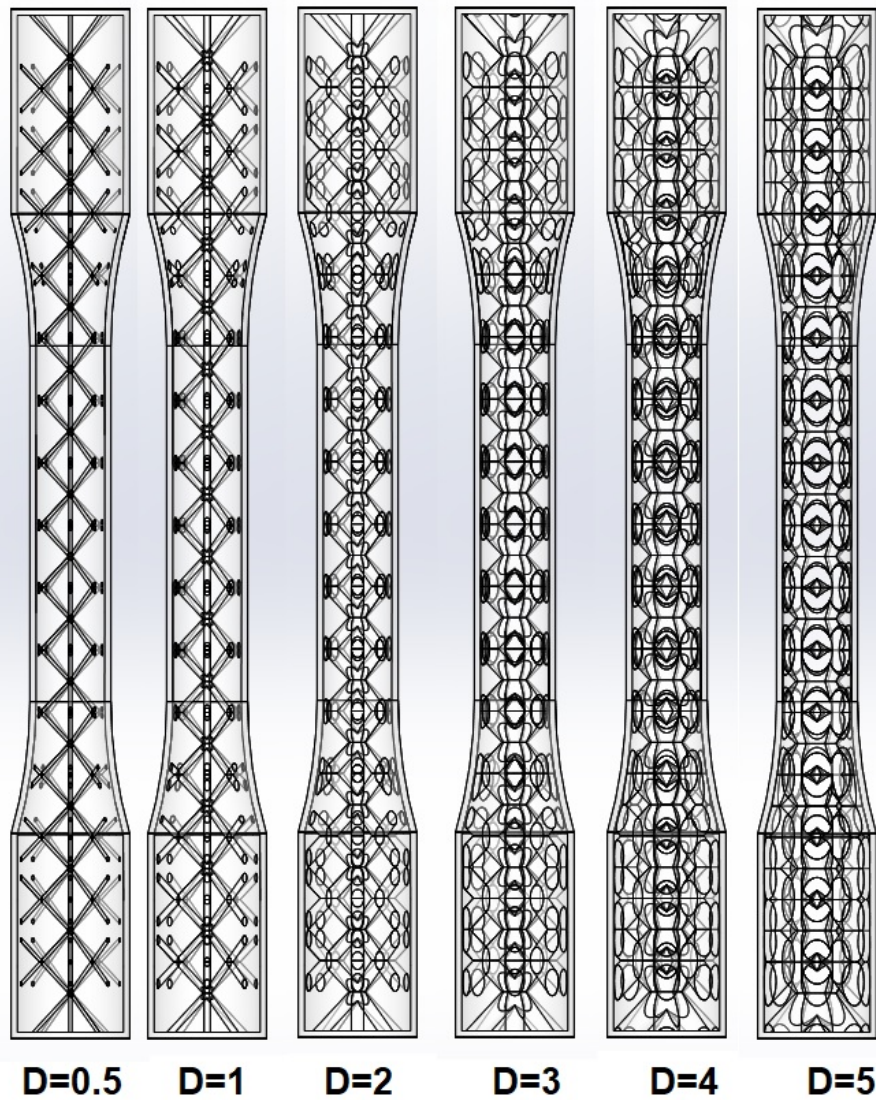


Figure 4.3: Variation of lattice structures

4.3

Mechanical tests

It was shown that, to minimize the use of printed material, it is desirable to replace the standard print filling with lattice structures uniformly assembled in the pieces (Figure 4.3). Due to the good performance of the BCC-type structure found in the simulations via software, this option was chosen to carry out the actual mechanical tests, in order to validate the simulations (Figure 4.4).

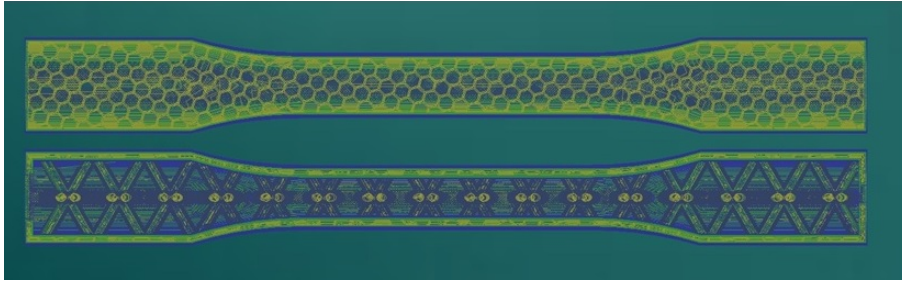


Figure 4.4: 3D print simulation

Two specimens of each type were printed in PLA using FDM technology, to perform tensile and compression tests. All tests were recorded by a computer, generating a series of data composed of force and elongation, which makes it possible to generate a set of traction force vs. elongation curves.

As mentioned before, the tests were performed according to the ASTM D792 standard and the entire research used the standard PLA filament with 3m.m. of diameter as the base material for printing and the Sigmax[®] from the company BCN3D as a printer. For the tests, an INSTRON[®] traction/compression testing machine was used. The sensor for all the tests was the *EX251* that is a strain gauge in double configuration with maximum strain 2.5 mm and base length (50/100 /150) mm.

After performing the tests, traction force vs. elongation curves were obtained for the non-optimized specimen, see Figure 4.5.

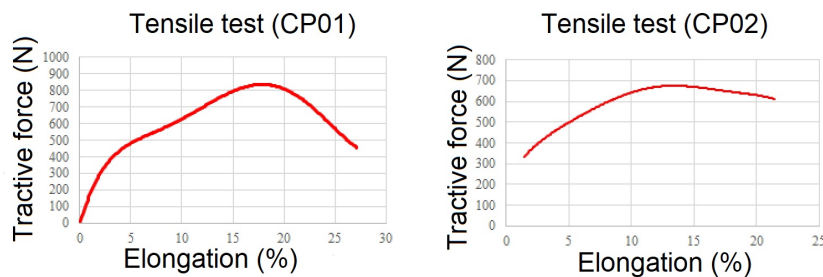


Figure 4.5: Traction force vs. elongation curves (non-optimized specimen)

With this test, an average maximum force of 819N and a maximum tensile stress of 1.54MPa were obtained, results that agree with the software simulations. After that, traction force vs. elongation curves were obtained for the optimized specimen (instead of the non-optimized), see Figure 4.6.

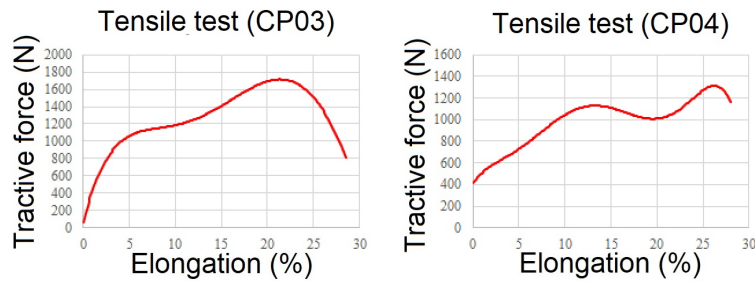


Figure 4.6: Traction force vs. elongation curves (optimized specimen)

With this test, an average maximum force of 1340.5 N and a maximum tensile stress of 2.52MPa were obtained, results that corresponded to the software simulations. Likewise, compression tests were performed on two other non-optimized specimens, obtaining the graphs from Figure 4.7.

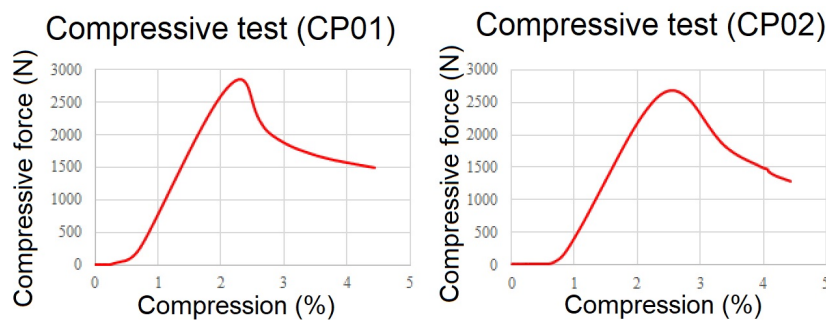


Figure 4.7: Compression force vs. elongation curves (non-optimized specimen)

With this test, an average maximum force of 2766N and a maximum compressive stress of 5.21MPa were obtained, which also agree with the simulations carried out in the *SolidWorks*[®] software. After that, compression force vs. elongation (compression) curves were obtained for the optimized specimen, see Figure 4.8.

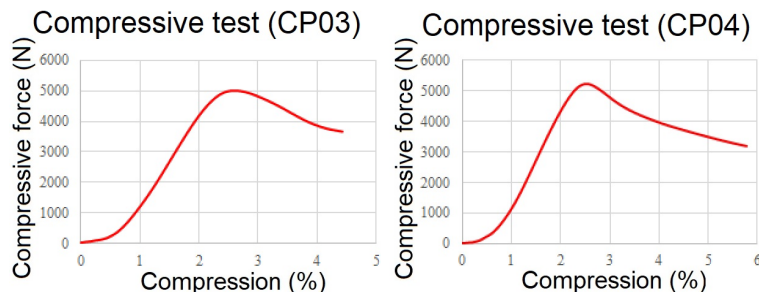


Figure 4.8: Compression force vs. elongation curves (optimized specimen)

With this test, an average maximum load of 5121.5N and a maximum compressive stress of 9.64MPa were obtained, results that corresponded to the software simulations. Figure 4.9 shows the fixing of the specimens in the machine and the position of the instrumentation.

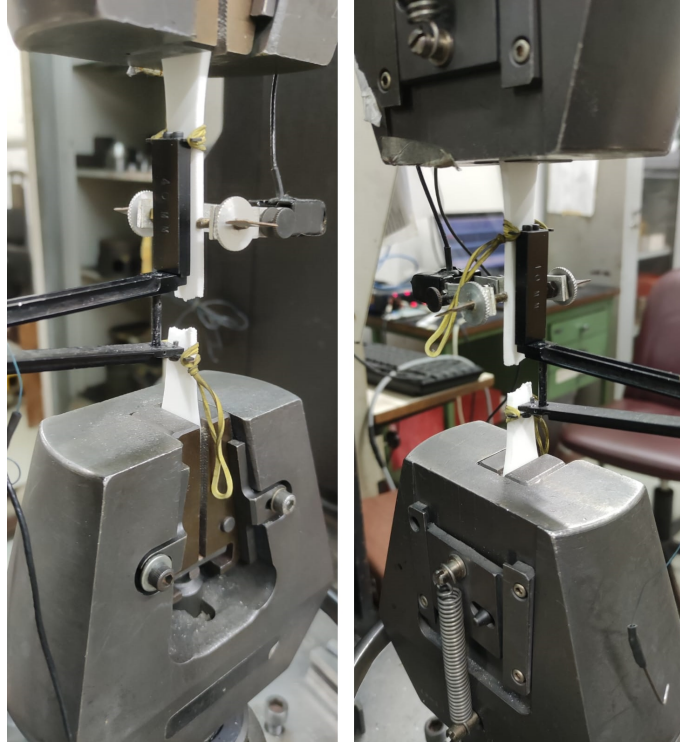


Figure 4.9: Fixing of the specimens in the machine

Observing both simulations and experiments, a considerable increase in the mechanical properties of the optimized specimens has been obtained with the optimization process, with a 30% reduction of the material used (and thus the cost per piece), as well as a 63.4% increase in the tensile and 85% in the compressive strength.

After this evaluation, the orthosis pieces were printed without and with multi lattice optimization, resulting in a 40% decrease in the total weight for the latter. In addition, the orthosis parts were tested under tension and compressions until rupture, confirming the improvements in strength for the optimized case.

It is important to note that the orthosis pieces' strength was not the same as the one for the specimens, due to their different geometry: depending on the direction of formation of the printing layers, weak points can be generated at the joints. However, the printing direction was chosen with the aim to minimize this effect. Notice that no torsion tests were performed on the pieces, as the movements performed by the orthosis do not have significant efforts of this nature in the developed design.

Once the evaluation of the orthosis construction is finished and the weight has been optimized to facilitate its use, the next step involves the characterization of the biological signals, in order to drive a servomotor so that the user can move the arm as desired, as discussed in the next chapter.

5

Fusion and Processing of EEG, ECG and EMG signals

Several studies use EEG and EMG signals to decode movement intention. This chapter will present all the procedures and classifications of biological signals used in the thesis to improve the inference of movement and to correctly trigger an upper-limb orthosis. The signals to be studied will be presented and the ones to be used will be defined. In addition, all the devices built or used in the study will be presented.

Before choosing the signals that will be used, it is first necessary to understand the operation and nature of each signal, to better filter and analyze them.

5.1 Signal Characterization

Although all the functions of our body are controlled by the brain, its complexity means that each element has a basis of control, such as the motor system and the somatosensory system.

The somatosensory system is responsible for the sensations of touch, temperature, and pain. In addition, it is also responsible for the sensation of body positioning, the so-called proprioception [52]. In addition to this system, there is the motor system, which is composed of a collection of neurons and all the muscles in the body. It can be divided into the command and control of the spinal cord over the coordinated contraction, and the command and control of the brain over the motor programs in the spinal cord [52].

For the purpose of this thesis, only the somatic motor system will be studied, i.e. the joints, skeletal muscles, motor neurons and interneurons and how they communicate with each other, mainly the upper limbs. Each part of the brain is responsible for one activity or region of the body, as shown in Figure 5.1.

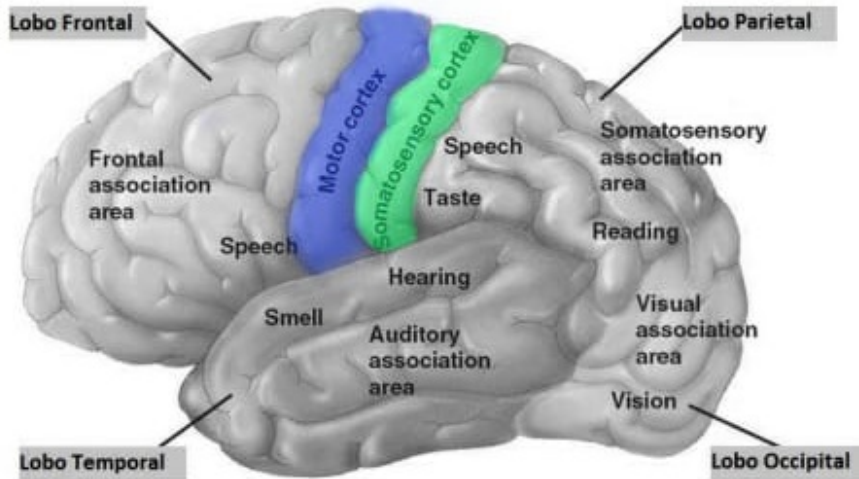


Figure 5.1: Scheme sectors of the brain (adapted from [52])

There are basically two types of muscle, smooth and striated. Smooth muscle is found in the walls of the intestines and arteries, and striated muscle, which is divided into cardiac and skeletal muscle, is found in the heart walls and around the bones. The cardiac striated muscles have the function of contracting and extending the heart, while the skeletal striated muscles perform the motor functions of the body. They have a layer of connective tissue that forms the tendons at their ends, as well as hundreds of fibers, each one innervated by a single axon branch of the central nervous system. Figure 5.2 shows a schematic of skeletal muscle activation.

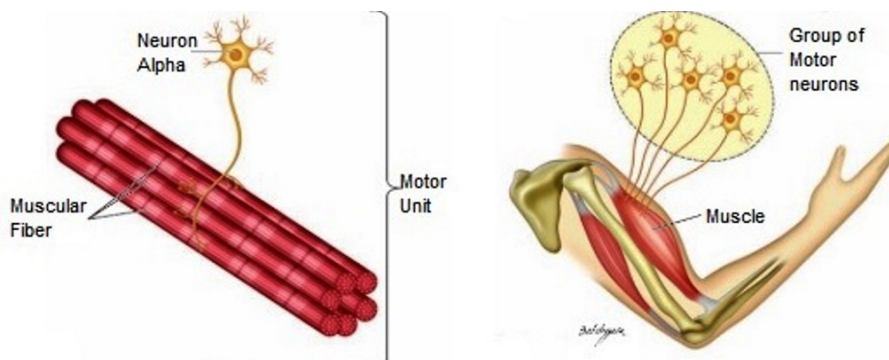


Figure 5.2: Scheme of Muscular activation (adapted from [52])

The activation of these groups of fibers is through motor neurons (Figure 5.3), which are divided into alpha and gamma. Alpha neurons are responsible for the generation of force in muscles, while gamma neurons are responsible for the activation of lower fibers. This study evaluates three natures of signals for motion inference, from an EEG, an ECG and an EMG.

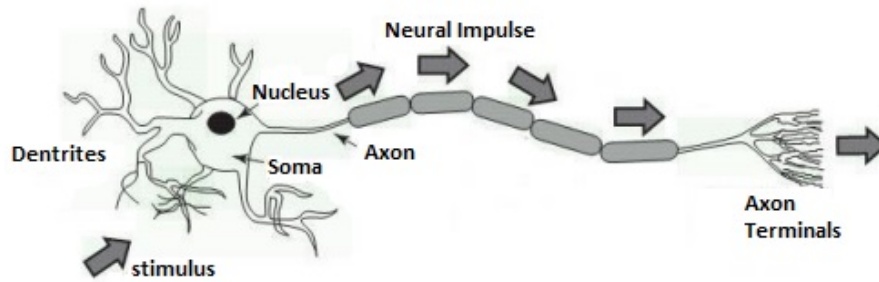


Figure 5.3: Scheme and parts of a neuron (adapted from [133])

The work [132] describes that: *"The Electroencephalogram (EEG) is the recording of brain electrical activities. These signals are generated by the synchronous cooperation of neuronal cells, which generate extracellular electrical potentials during the individual's mental, motor, and sensory activities."* This work also presents the use of the *Matlab*[®] Toolbox called *EegLab*[®], which is also used in this thesis.

The phenomena of Event-related desynchronization (ERD) and Event-related synchronization (ERS) [134] are also investigated in this thesis. They have to do with whether or not the signals are synchronized with the voluntary accomplishment of a movement, e.g. whether the person just thinks about moving the arm or else thinks and actually moves the arm.

EEG signals have significant differences according to mental states [135], so it is possible to relate the discrepancies in the signals to movement or movement intention. These waves or frequencies are divided into five bands, as shown in Table 5.1.

Table 5.1: Frequency Bands of the EEG Signal

Frequency (Hz)	Name
0-4	Delta (δ)
4-8	Theta (θ)
8-12	Alpha (α)
12-25	Beta (β)
25-80	Gamma (γ)

These frequency bands are easily distinguishable when an EEG is evaluated. An example of the waveforms are presented in Figure 5.4.

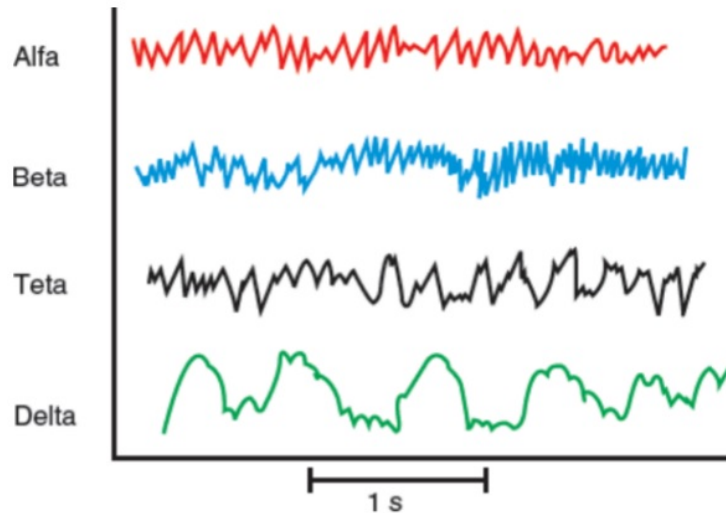


Figure 5.4: Example of EEG waves (adapted from [136])

Several recent studies use EEG signals to create a brain-machine interface [140], so its characterization is still being widely discussed [138] [139].

After characterizing the EEG signals, the next signal to be studied is the ECG. According to [137]: *"The ECG is the recording of the variation in the bioelectric activity of the heart, which represents the contractions and cyclical relaxations of the human cardiac muscle. It provides important information about the functional aspects of the heart and the cardiovascular system."*

The waves from the ECG signal represent the contraction/extension cycle of the cardiac muscles. Figure 5.5 presents the common subsets of the ECG wave.

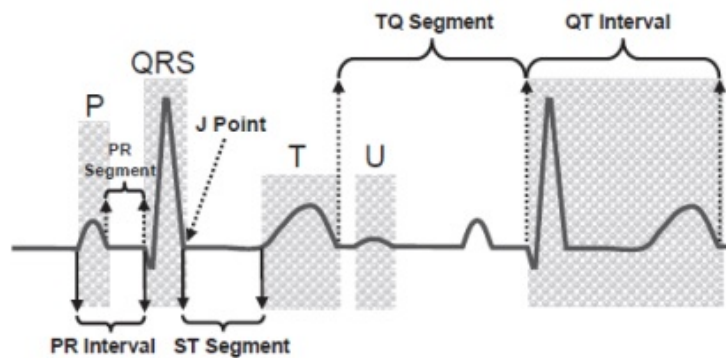


Figure 5.5: Example of ECG waves (adapted from [141])

According to [142] and [143], the duration of all the intervals can be described as shown in Table 5.2.

Table 5.2: Duration of the ECG waves (adapted from [142] and [143])

Interval	Duration (ms)
P wave	60-80
T wave	120-160
QRS	80-120
PR Segment	50-120
ST Segment	80-120
PR Interval	120-200
QT Interval	300-420
RR Interval	400-1200

Each wave or interval corresponds to a part of the cardiac cycle. In addition, they are indicative of factors such as arrhythmias and other coronary diseases. For the case of motion inference the ECG is important because, according to [144]: *"In the case of a shoulder disarticulation patient, an effective site for a nerve transfer involves the pectoralis muscles, as these perform little useful function with a missing limb. Consequently, the myoelectric signals measured from the reinnervated muscles may be corrupted by a large amount of ECG interference"*. Furthermore, the heart rate and RR interval are powerful tools to infer the emotional state of the volunteer, as can be seen in [145].

The last of the signals to be characterized is the signal coming from the EMG. This type of signal is the most common for motion detection, since it is directly linked to the firing of neuromotor groups while muscles are activated. The EMG signals are quite characteristic and comprise a pulse or peak at the moment of initiating and while maintaining muscle contraction. Figure 5.6 presents the common subsets of the EMG wave.

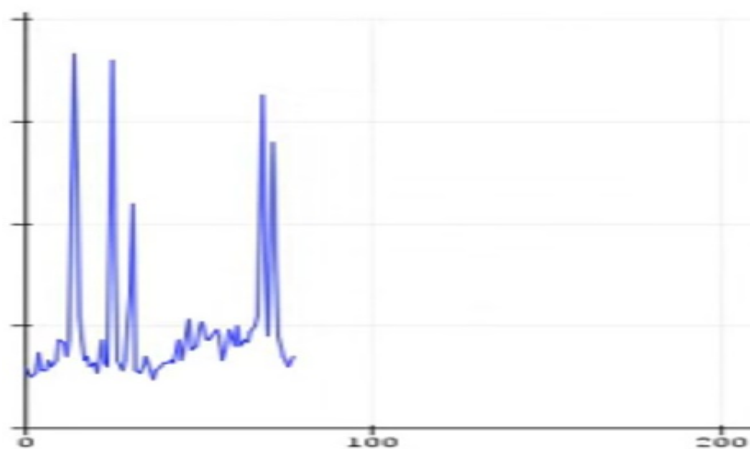


Figure 5.6: example of EMG waves

After all the signals have been characterized, the next step is to create a procedure to standardize the movements to be performed, the placement of the electrodes, and the measurement of the signals.

5.2 Acquisition Procedures

The first step to ensure accurate measurements is the repeatability of the action. In the case of the present study, the defined movement, as described in the previous sections, is the elbow bend. Thus, to ensure that the movements would always be the same and would move the same muscle grouping, an apparatus was created to restrict the movement to the planar movement of the elbow bend, as shown in Figure 5.7.

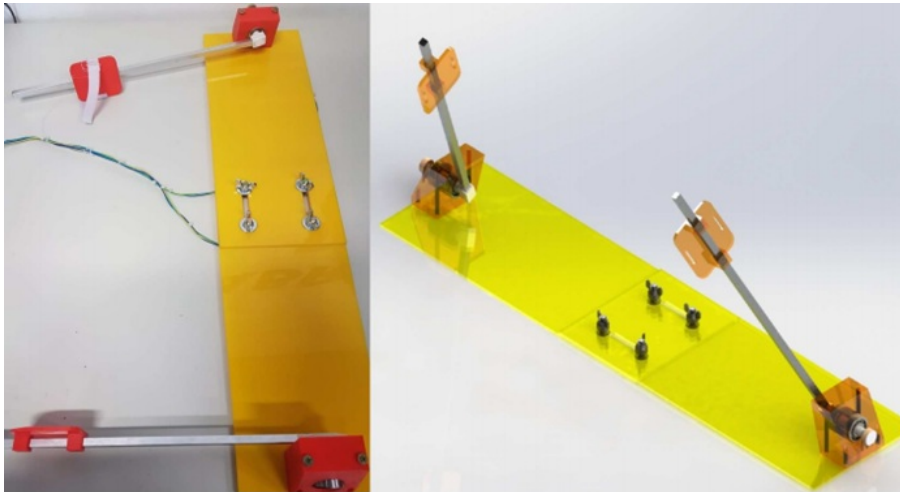


Figure 5.7: Apparatus

Following the concepts of Industry 4.0 explained in the previous sections, the apparatus is composed of laser-cut acrylic parts, two 10mm square aluminum rods, 2 thrust bearings at the base, and parts printed in PLA using FDM technology. Potentiometers were placed at the base of the rods for the purpose of angle measurement.

The representation of the fixation of this apparatus was presented in the Figure 1.9 of that thesis and represented again in Figure 5.8. Furthermore, a visual reference of the angle was implemented by using the *Labview*[®], together with the *Arduino*[®]

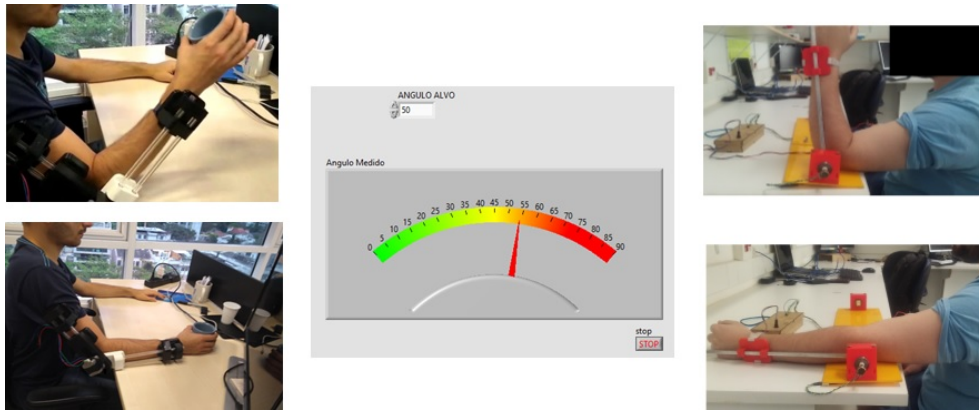


Figure 5.8: Elbow Bending movement and *Labview*[®] interface

The second step in ensuring the quality of the acquired signals is to create a set of procedures for electrode placement. As presented in [100], the positioning of sensors for ECG measurement is standardized (Figure 5.9). It is important to note that before the electrodes were placed for measurement, all volunteers had their chests shaved and sanitized with alcohol for better adhesion of the probes.

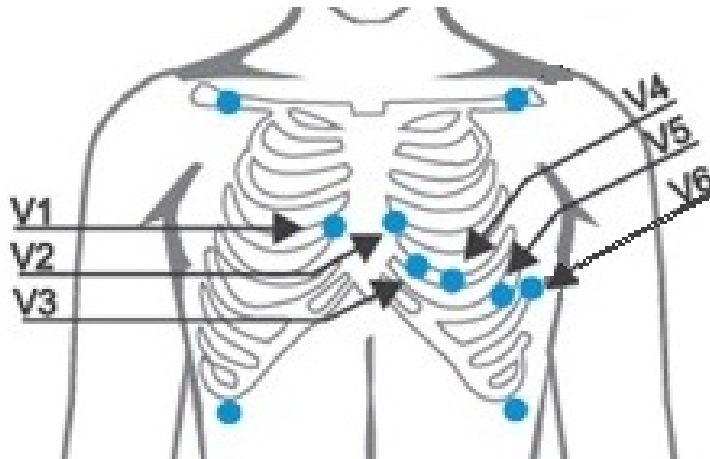


Figure 5.9: Position of ECG probes (adapted from [100])

The EEG signals also have predefined points, so the standard 10-20 system of electrode placement was used. This placement can be done using a standard cap or just by placing the electrodes at the positions. The objective of this work is only to capture or infer movements. As a result, only seven electrodes were placed in the regions of the motor cortex, as shown in Figure 5.10.

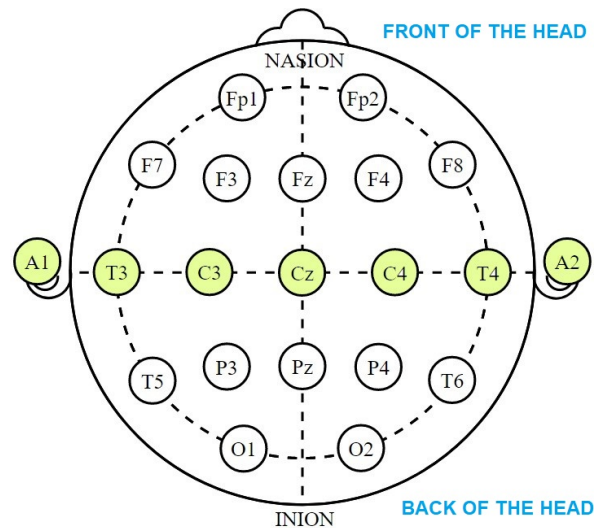


Figure 5.10: Position of EEG probes

The EMG signals do not have a defined point, but there is the possibility of finding a "motor optimum point." This point is easily found through electrostimulation pens widely used in acupuncture therapies. Therefore, a procedure was created in which the volunteer is lightly electrostimulated until these points are found, and then an electrode is placed in position. Furthermore, the electrode placement process goes through the same procedure as the ECG (scraping and cleaning with alcohol). Figure 5.11 presents the procedure of the insertion of the EMG probes.

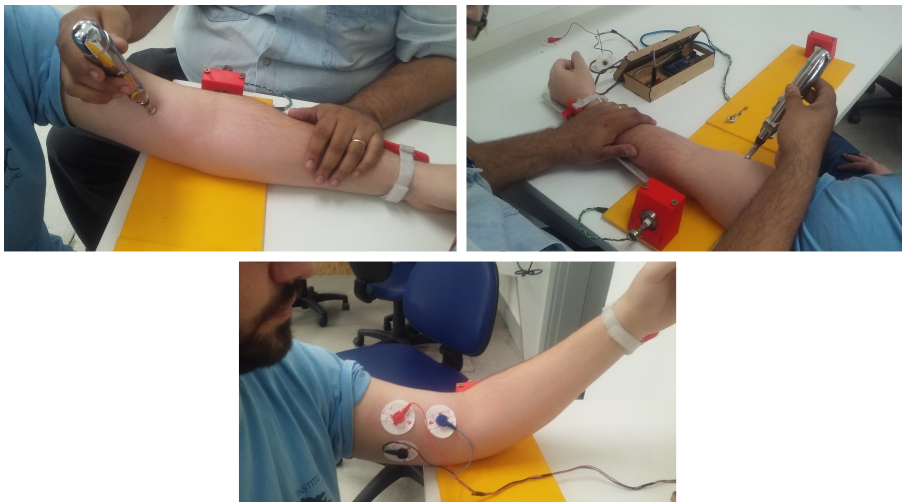


Figure 5.11: Position of EMG probes

For the complete acquisition of the signals, a multiparameter (Figure 5.12) medical equipment was used, containing 20 channels, of which five were for the ECG, seven for the EEG, and three for the EMG.

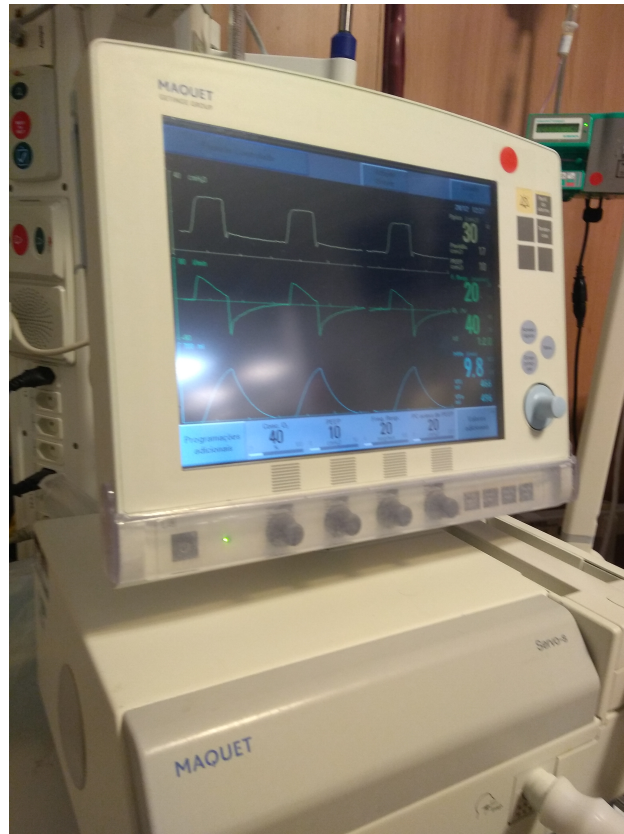


Figure 5.12: Multiparameter medical equipment

For all volunteers, a series of tasks were set in order to observe the acquired signals and create a database for later analysis:

- Test 1: The volunteers were all instrumented and asked to move both arms by performing contralateral movements at 30°, 60° and 45°;
- Test 2: The volunteers were all instrumented and asked to move one arm by performing movements at 30°, 60° and 45°;
- Test 3: The volunteers were all instrumented and asked to think they were moving one of their arms, performing movements at 30°, 60° and 45°;
- Test 4: The volunteers were all instrumented and asked not to think about anything or move anything.

All tasks were repeated 3 times for each volunteer, with a 15-minute spacing between trials to avoid contamination of the results due to muscle fatigue. These tasks are important because they evaluate, in addition to muscle fatigue and the signals themselves, the already described phenomena of Event-related desynchronization (ERD) and Event-related synchronization (ERS).

For the data acquisition procedures, we first used the apparatus shown in Figure 5.8, which has a multi-turn potentiometer responsible for measuring the bending angle performed by the volunteers. The signals from the potentiometers are sent to the *Arduino*[®] and presented in the *Labview*[®] graphical interface, so that the volunteers can see the angle of bend of the elbow. In this stage, the tasks were only monitored, with no control actions involved, having the only purpose of collecting the EEG, EMG and ECG signals and assembling a database for the following stages.

This first stage of testing was interesting, because it was detected that the ECG signals in general were not good for inferring movements, but were of great value for inferring stress, fatigue, and frustration of the volunteers during the tests.

In the second stage of testing, a servomotor was put in place of the potentiometer in order to check whether the volunteer's arm would be bent to the requested angle (performing movements at 30°, 60° and 45°).

In this step, the EEG and EMG signals served as inputs to the actuation system, and the encoder of the servomotor placed in the apparatus was used to check the elbow bending angle. The volunteers performed only tasks 3 and 4 of the test battery, so that all movement intention was detected by the EEG signals, activating the servomotor and having the EMG signal as a parameter to evaluate the effort. Moreover, as the ECG signal showed efficiency in inferring stress and frustration, it was defined as a pause parameter for the volunteer not to get tired during the test.

The third and last step consisted of placing the orthosis on the volunteer's arm, who was asked to perform the same activity as in the second step (performing movements at 30°, 60° and 45°). In this step, all signals were evaluated, with the EEG being considered as the command signal, the EMG as the verification signal, and the ECG as a parameter of frustration or stress for the volunteer. Just as it was done in the second step.

Once the signals and procedures have been defined, the next step is to create a database of all the signals for later analysis.

5.3

Database Creation

Due to the pandemic of COVID-19, the process of attracting volunteers for the trials was very difficult. In addition, the pandemic caused a shortage of electronic equipment in the country, making it difficult to purchase portable measuring equipment.

To circumvent this situation, the facilities of two medical laboratories

that have projects in partnership with the University were used. One of them is the Hospital das Clínicas de Niterói and the other is the LPH (Human Performance Laboratory). All volunteers were accompanied by a responsible physician and a physiotherapist, to ensure that all procedures were being carried out correctly.

During the entire study, forty-five volunteers were tested. Thirty were men between the ages of 35 and 45, without any known congenital disease and working as professional divers. Three were men between 50 and 60 years of age, all with hypertension, and were working as private drivers. Four were men between 40 and 50 years old, with no known congenital disease, and were working as engineers. Eight were women between the ages of 35 and 60, with no known congenital disease, of whom four were retired, three were lawyers, and one was a business administrator.

An important observation is that, in addition to these volunteers, three people were tested, one with obstetric brachial plexus injury (OBPL) (30 years old) and two with brachial injury caused by a fall (37 and 39 years old), both with an injury on the left side of the body. Another observation is that the volunteer with OBPL had no movement of the injured limb, so the electromyographic signals were either nonexistent or inconsistent. All data were acquired and saved in .xls file extension files for future analysis, creating a database of 4,032 samples divided between each task, trial and volunteer (84 samples per volunteer). At the end of all the trials, one of the three injured individuals was chosen to use the orthosis and test it in the laboratory environment.

5.4 Filtering Procedures

After acquiring all the data, the next step is to filter the signals in order to assess what the effective point of the movement was and what this impacted on the saved signals, in order to assess whether there were changes in the waves and to observe the limits and discrepancies between subjects. For this, we used the *Matlab*[®] Toolbox called *EegLab*[®], which already has established tools for decoding and evaluating the signals (Figure 5.13).

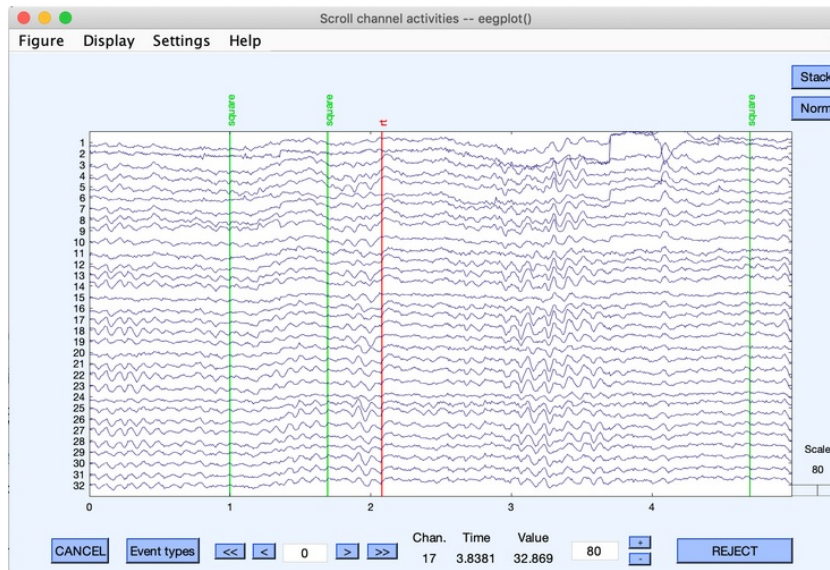


Figure 5.13: Matlab® Toolbox EegLab® window

The use of this toolbox was only for filtering and evaluating the acquired signals, not being used for the real-time application, for which the *Labview*® was used, together with the *Arduino*® toolbox to acquire and act on the orthosis. For the application without the orthosis, only the apparatus to restrict movement and the multi-parameter measuring device were used, while for the use of the orthosis, the data acquired in the apparatus were sent to a notebook connected to an *Arduino*® to command the motor to perform the bending movement (Figure 5.14).

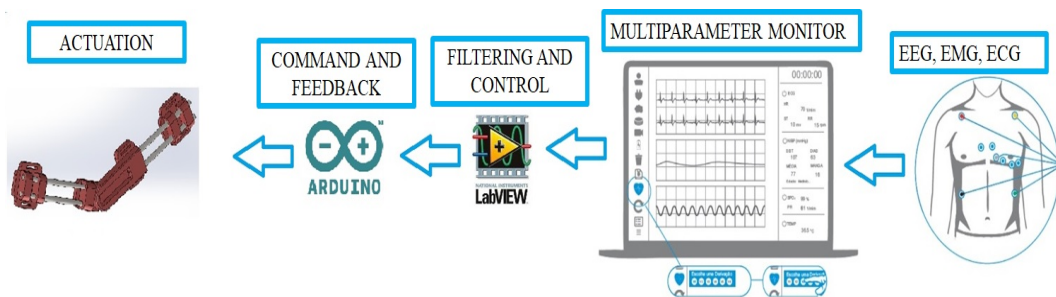


Figure 5.14: Scheme of system acquisition

For each of the signals, a type of filtering and denoising treatment was used. All the filters were implemented using digital processing. The next subsection will describe all the filtering techniques used in this research.

5.4.1 Types of Filters

The first type of filter used in the work was the low-pass filter. This type of filter is often used when the goal is to allow the passage of low frequencies and attenuate the amplitude of frequencies higher than the cutoff frequency. besides the common low-pass filter, one of the classes of low-pass filters used was the Butterworth filter.

According to [146]: "*The Butterworth filter is a type of signal processing filter designed to have a frequency response that is as flat as possible in the pass-band. It is also referred to as a maximally flat magnitude filter.*"

Figure 5.15 presents examples of a Butterworth filter response for different orders.

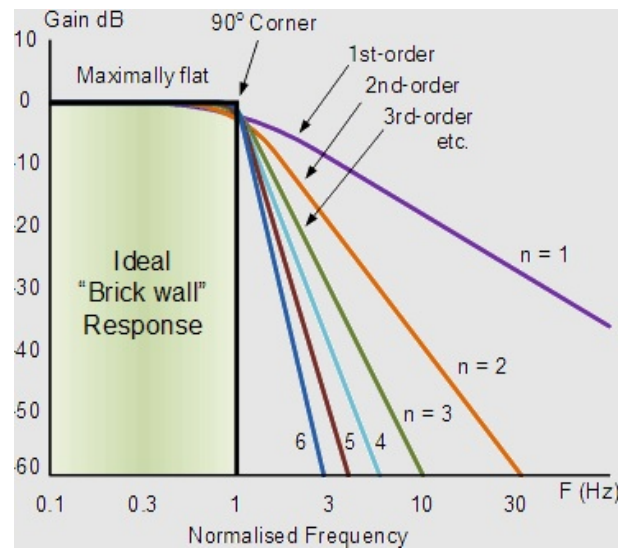


Figure 5.15: Examples of Butterworth filter response (extracted from [147])

One observation about Butterworth filters is that they have a known transfer function:

$$H(j\omega) = \frac{1}{\sqrt{1 + \left(\frac{\omega}{\omega_c}\right)^{2n}}} \quad (5-1)$$

where

ω_c is the cut-off frequency;

n is the order of the filter.

Another type of filtering used was the wavelet transform. This transform was used with the aim to data extraction, with the same purpose of [148] and [149].

According to [150]: "A function $\psi \in L^2(\mathbb{R})$ is called an orthonormal wavelet if it can be used to define a Hilbert basis, that is a complete orthonormal system, for the Hilbert space $L^2(\mathbb{R})$ of square integrable functions."

The Hilbert basis is constructed as the family of functions $\{\psi_{jk} : j, k \in \mathbb{Z}\}$ by means of dyadic translations and dilations of ψ . In this way, using a wavelet transform with the signals altered with the base change done earlier becomes simpler, since it has the format:

$$[W_\psi f](a, b) = \frac{1}{\sqrt{|a|}} \int_{-\infty}^{\infty} \overline{\psi\left(\frac{x-b}{a}\right)} f(x) dx \quad (5-2)$$

where

$[W_\psi f](a, b)$ is a wavelet transform;

a is the dyadic dilation;

b is the dyadic position;

Another transform used in the thesis was the Fast Fourier Transform (FFT) [151], which in an algorithm to computes a discrete Fourier transform of sequence. The Fourier analysis basically converts a signal from its original domain to frequency domain. It is a useful tool to classify and filter a signal. Let x_0, \dots, x_{N-1} be complex numbers. The discrete Fourier transform (DFT) is defined by the formula:

$$X_k = \sum_{n=0}^{N-1} x_n e^{-i2\pi kn/N} \quad k = 0, \dots, N-1, \quad (5-3)$$

where $e^{i2\pi/N}$ is a Primitive Nth root of 1.

The FFT algorithm used in this thesis was the Cooley–Tukey algorithm, presented and descript in [152] and [153].

The last filtering technique used in this thesis is the Pulse Code Modulation (PCM) [154] [155] [156]. PCM is a method to digitally represents sample analog signals. Is commonly used in Compact Discs and digital telephony. Basically PCM is a type of waveform encoder, which tries to reproduce the signal sample by sample. Thus, we can write each waveform as a matrix A $m \times n$, where each row is a sample and each column is a variable.

By performing a simple base change, using a matrix T , it is possible to define the following transformation:

$$\mathbf{Y} = \mathbf{TA} \quad (5-4)$$

where

$$\mathbf{TA} = \begin{bmatrix} T_1A_1 & T_1A_3 & T_1A_3 & \dots & T_1A_n \\ T_2A_1 & T_2A_3 & T_2A_3 & \dots & T_2A_n \\ & & \dots & & \\ T_mA_1 & T_mA_3 & T_mA_3 & \dots & T_mA_n \end{bmatrix}. \quad (5-5)$$

This base change represents a rotation, so that A is projected onto the columns of T . This type of PCA defines independence by taking into account the variance of the data in the original base.

5.4.2 Filters by each bio signals

As discussed in the previous subsection, all signal filtering tools were implemented digitally using *Labview*[®] for the real-time implementation and the *Matlab*[®] Toolbox called *EegLab*[®] for the offline implementation.

In the case of the EEG signals, first a low-pass filter with a cut-off frequency of 90Hz was used within the *EEGLab* tool. This frequency was chosen because, as seen in Table 5.1, the EEG frequencies do not exceed 80Hz. Next, a segmentation using PCM (Pulse Code Modulation) was used, and after that a wavelet transform, was applied. The Figure 5.16 a simplified scheme of the filters implemented in EEG signals:



Figure 5.16: Scheme of EEG signal filtering

This sequence of filtering is very similar to [148], but the constants and tuning parameters of the algorithm have been changed to better adapt to the application of the thesis. The PCM filtering segmentation combined with wavelet transform is commonly used to decoding EEG signals [158] [157]. The same happens with wavelet transform [159] [160] [161].

For the ECG signals, it was sufficient to use a low-pass filter with a cut-off frequency of 110 Hz, since the frequency of ECG signals is in the range 0.5 Hz to 100 Hz [162] [163]. After that, a FFT was applied to the signal, in order to facilitate the identification of the R-R interval component of the signal to identify a possible stress signal, similarly to [165] and [166]. In the thesis, The Figure 5.17 a simplified scheme of the filters implemented in ECG signals:



Figure 5.17: Scheme of ECG signal filtering

For the EMG signals, a sixth-order Butterworth filter was used, in order to make the detection of the trigger signals. This filter is commonly used for ECG signal detection, since this type of signal is usually evaluated by its threshold, as shown in [167],[168], [169] and[170]. However, the filter order was increased in order to be more similar to a switching function, due to the type of controller to be used, and also to better characterize the muscle activation of the biceps brachii (muscle grouping where the electrodes were inserted). The Figure 5.18 a simplified scheme of the filters implemented in EMG signals:



Figure 5.18: Scheme of EMG signal filtering

After characterizing the signals, creating the test procedures, and determining which filtering techniques to perform, the next step was to run the experiments. This way the database was created and the results and evaluation of the signals were analyzed.

5.5

Data Analysis

The first point in the data analysis was that the EEG signals were very good for movement inference (thinking or performing). The EMG signals, on the other hand, were only useful when the volunteers actually moved the limb. Furthermore, the EMG signals was very useful to infer muscular fatigue. In relation to the ECG, it was verified that it was not very useful for inferring movement intention; however, it was an excellent factor for inferring emotional exhaustion and frustration when not being able to execute a movement.

The first point in the data analysis was that the EEG signals were very good for movement inference (thinking or performing). The EMG signals, on the other hand, were only useful when the volunteers actually moved the limb. In relation to the ECG, it was verified that it was not very useful for inferring movement intention; however, it was an excellent factor for inferring emotional exhaustion and frustration when not being able to execute a movement. The Figure 5.19 a simplified scheme of acquisition and actuation system implemented:

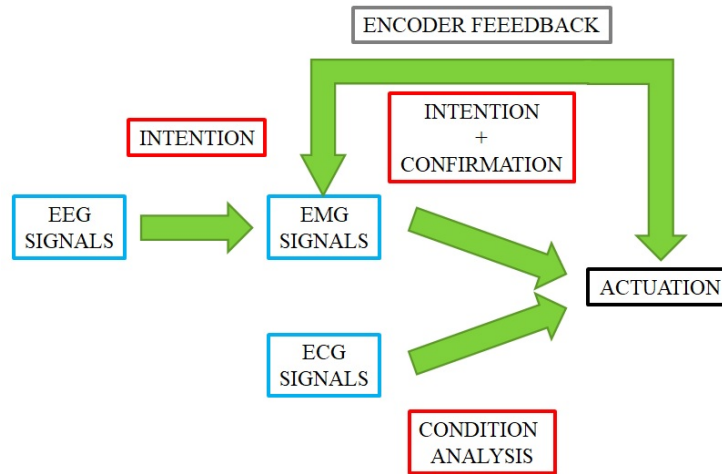


Figure 5.19: Scheme of acquisition and actuation system

After characterizing and filtering the signals, a database analysis was performed to cross-check the signal peaks in order to evaluate the following points:

- Is there a difference between just thinking and thinking and executing?
- Is there a difference when the movements are contralateral or not?
- Are there differences in the signals depending on the origin of the lesion?
- Are there differences in the EMG signals?

Looking at the movements and signals from tests 1, 2 and 3, it was possible to observe a slight difference between the signals from tests 1 and 2 and the signals acquired in test 3 from the EEG channels. In the first two, there was activation of the channels located at T3, C3, T4 and C4, whereas in test 3 there was only activation of the channels T3, CZ and T4. Thus, it can be seen that there is a difference when there is only planning and when there is planning and execution. There was no change in the ECG signals in general in tests 1 and 3, but both were different from test 2.

Observing the movements and signals of tests 1 and 2, it was possible to observe a slight difference between the signals compared to the EEG channels.

In test 1, there was activation of localized channels T3, C3, T4 and C4, whereas in test 2 there was only activation of channels T3 and C3 when the volunteers bent their right arm, and T4 and C4 when they bent their left arm.

Thus, it can be seen that there is a difference when there is only movement of only one arm and when there is a contralateral movement. There was a difference in the ECG signal when contralateral movements were performed from when movements with only one limb were performed. This probably occurred because there was a possible recruitment of some muscle group when performing contralateral movements.

The three volunteers with brachial lesions were tested. It was observed that the volunteer with OBPL had no EMG signals in the injured limb (although the arm had slight spasms when electro-stimulated) and the EEG signals matched the stimuli in the same way as the healthy volunteers.

Regarding the ECG signals, a variation was observed between the signals of tests 1 and 3, denoting fatigue and stress of the volunteer. Another observation for this volunteer was that he had his arm bent involuntarily while thinking about bending his arm and there was no variation in the EEG signals, always having the C4 and T4 channels activated regardless of whether he thinks or executes the movement.

The volunteers with brachial injury caused by a fall also showed EEG and ECG signals the same as the other volunteers, but the EMG signals were erratic, so the performed filtering had low efficiency.

Having completed all the signal processing and characterization steps, the next stage will consist of mathematical modeling, control simulations, and real-time control of the orthosis, as discussed in the next chapter.

6

Robust and Adaptive Control Techniques Applied to the Orthosis

6.1

Types of Controllers

In this section, several control techniques will be presented. According to the control theory, controllers can be divided into three classes:

- Classic Control Techniques;
- Intelligent Control Techniques;
- Modern and Robust Control Techniques;

6.1.1

Classic Control Techniques

Classical control theory provides the foundation for stability. The concepts of gain margin and phase margin have been proposed to evaluate the relative stability of SISO systems under two types of uncertainty in the plant: changes in the gain and changes in the phase rotation.

Among the existing classical control techniques, the most used in the literature is the Proportional, Integral Derivative (PID) control. This is a control technique based on three gains, one proportional, one integral and one derivative, in order to adjust and minimize the error of the system (Figure 6.1). This technique is very common for set-point search [171].

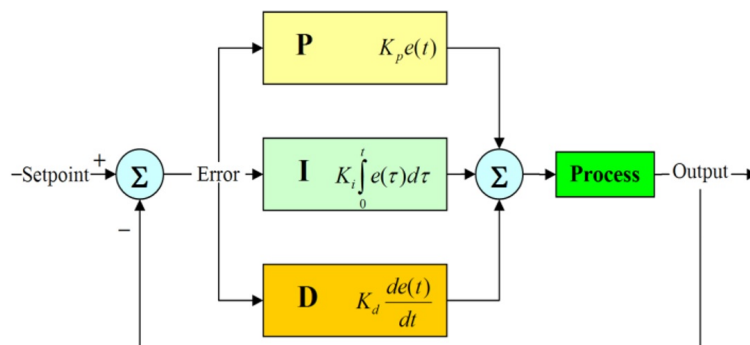


Figure 6.1: Basic scheme of a PID controller.

6.1.2 Intelligent Control Techniques

Intelligent control basically involves three control techniques, called genetic algorithms, neural networks and fuzzy logic. All three techniques mimic certain aspects of nature to motivate their algorithms [172], such as mimicking the behavior of the DNA strand [65], the behavior of a human neuron, or in the inference-generalization mode of the human being (Figure 6.2).

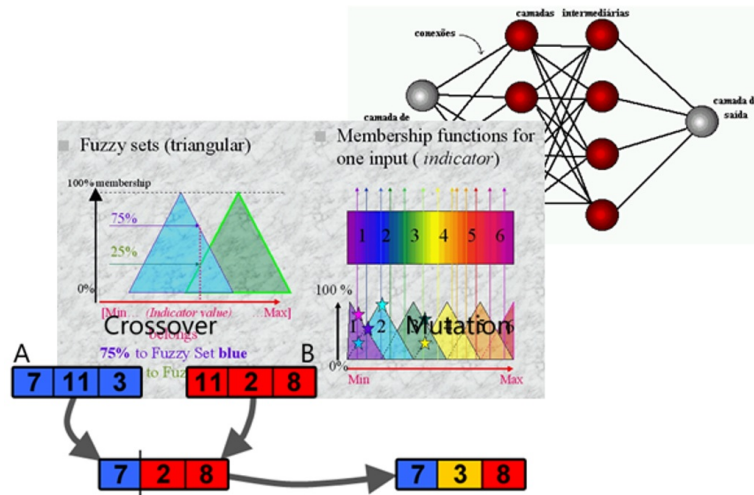


Figure 6.2: Examples of Intelligent Controls.

"Reinforcement learning" and "deep learning" have become a fourth technique in intelligent control. They rely on computational intelligence and optimization of an object or cost function to learn policies which produce the best result, similar to how a human learns what strategy works best for a certain task [173].

6.1.3 Modern and Robust Control Techniques

Robust control theory, an active field of research since the late 1970s, aims for control actions to perform tasks even with uncertainties in the plant model, the dynamics, and the operation of sensors and actuators.

Many control techniques have been added to classic control models, adding elements such as filters, nonlinear treatments, optimization algorithms, search algorithms and others. In the present thesis, three types of control will be mentioned: Adaptive Control, Extremum Seeking Control and Sliding Mode Control.

In each case, the controllers work as "system tuners", either by adjusting the gains of a PID controller or by adapting the model of the plant.

The term “adaptive system” was formally introduced into the control literature in 1957 [174]. Another definition is that of [175] in 1961, which defined that “an adaptive system is a system designed from an adaptive point of view”. Intuitively, an adaptive controller is a controller that can modify its behavior in response to changes in process dynamics and/or disturbances. Adaptive control aims to adjust the desired response so that the system functions by “adapting” this response. In the work [55] the Model Reference Adaptive Control (MRAC) was implemented in FES system.

The Extremum Seeking algorithm [176], on the other hand, works to minimize a cost function (error), causing the system to reach a predetermined objective, by analyzing only its input-output relation (Figure 6.3). Extremum Seeking Control (ESC) is an old technique that is being renewed and widely used for its ease of implementation, its lack of need for more sophisticated modeling, its robustness with respect to changes in the plant, and its wide application as a real-time control algorithm. The model proposed by Krstic [176] of the ESC is based on two sinusoidal excitations, with different amplitudes, passing through a set of filters. In those cases, the Extremum Seeking algorithm is used through a model-free algorithm combined with some stochastic or probabilistic process, as shown in [64].

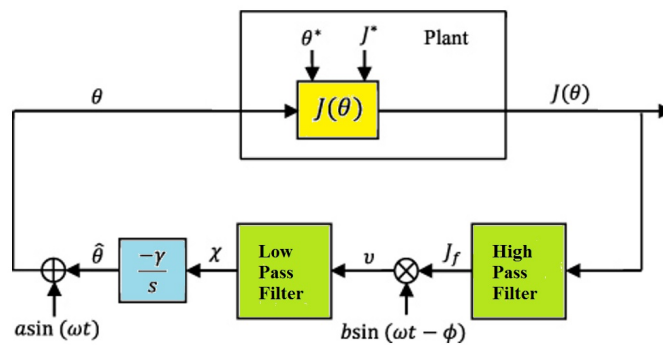


Figure 6.3: Classic ESC Scheme (adapted of [176]).

where, $J(\theta)$ is a given cost function;

θ^* is the unknown input;

f^* is the unknown output;

$\hat{\theta}$ is the estimated unknown input;

$-\gamma/s$ is an integrator;

The goal of the algorithm is to make $\hat{\theta}$ as small as possible, so the output of $f(\theta)$ will be directed to the minimum of f^* . The $a \sin(\omega t)$ disturbance signal is fed into the system to get the gradient information of $f(\theta)$. The theorem of ESC [176] shows that the residual error can be decreased from increasing of

the parameter ω and decreasing the parameter a . That algorithm was applied in [55], [63] and [64], but all in FES.

Within the robust control techniques, there are the so-called Sliding Mode Controls (SMC). This set of techniques is used basically in nonlinear systems or systems with parametric uncertainties, as is the case of musculoskeletal systems [73] [62] [65]. Elements such as arm length, motor threshold, and muscle fatigue are phenomena unique to an individual. As presented in the previous chapters, several recent studies are using sliding mode control for exoskeletons, orthosis, and prosthesis. Figure 6.4 presents the generic scheme of SMC.

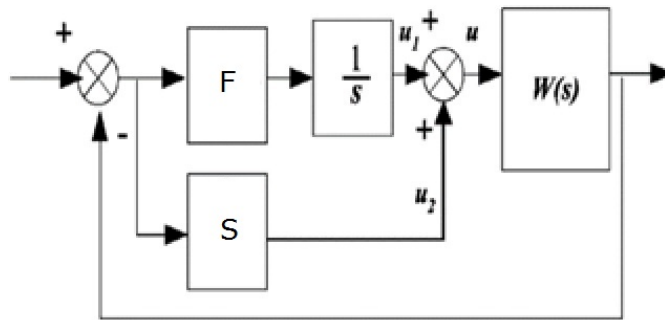


Figure 6.4: Generic SMC Scheme (adapted of [192]).

where F is a switching function;

S is a sliding surface;

$W(s)$ is the plant or cost function.

The next subsection will describe some variants of SMC.

6.1.4 High-Order Sliding Mode Controller

The sliding mode controller is based on a switching function and a sliding surface. The switching function plays the role of changing direction in the control action and the sliding surface is the "best direction" of convergence of the algorithm [177] [178], [179] and [180]. According to [178]: "*The switching function is a function that switches the signal when it crosses a threshold or surface. The sliding surface is an "asymptotically stable surface (S), such that all trajectories of the system converge on these surfaces in finite time and slide along them until they reach the desired destination at their intersection.*". Figure 6.5 presents the convergence with and without the switching function.

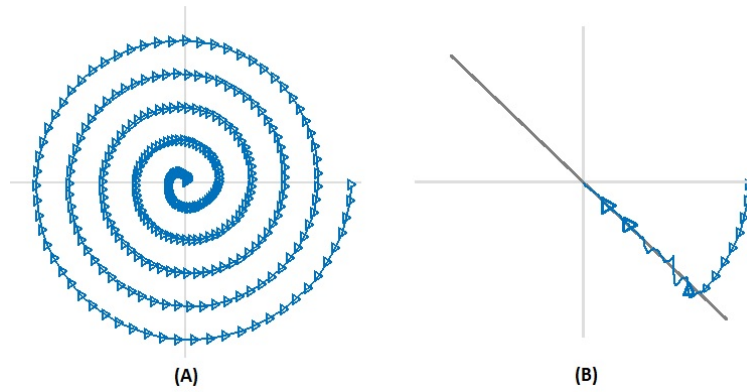


Figure 6.5: (A) Common Convergence (B) SMC Convergence.

According to [181]: "The term "Conventional" sliding mode control (SMC) was introduced in the book *Sliding Mode Control and Observation* [182] by the authors, working in the area of high-order sliding mode (HOSM) control. The term is related to all publications on n -dimensional systems with m -dimensional control and with sliding modes and state trajectories in a manifold of order $n-m$."

The scheme is the same of the conventional SMC, see Figure 6.4, but the key about the HOSM is the switching function [183]. Equations (6-1) to (6-4) present the generic formulation of a plant to be controlled with the Supertwisting Sliding Mode controller. Consider the sliding variable dynamics:

$$\dot{X} = f(X, t) + B(t)u(t) \quad (6-1)$$

$$y = \sigma(X, t) \quad (6-2)$$

$$(6-3)$$

With functions $f(X, t)$ and $B(t)$ are assumed to be sufficiently smooth and $\sigma(X, t)$ is a smooth output function and let it be understood in the Filippov sense [181]. The deviation of the sliding variable can be expressed as:

$$\dot{\sigma}(X, t) = \frac{\partial \sigma}{\partial t} + \frac{\partial \sigma}{\partial x}(f(X, t) + B(t)u(t) + d(t)) \quad (6-4)$$

$$\ddot{\sigma}(X, t) = \frac{\partial \dot{\sigma}}{\partial t} + \frac{\partial \dot{\sigma}}{\partial x}(f(X, t) + B(t)u(t) + d(t)) + \frac{\partial \dot{\sigma}}{\partial u} \dot{u}(t) \quad (6-5)$$

In addition, the following control law can be applied:

$$u(t) = -c_1 \sqrt{\sigma} \text{sign}(\sigma) + \nu \quad (6-6)$$

$$\dot{\nu} = -c_2 \text{sign}(\sigma) \quad (6-7)$$

To ensure convergence in a finite time, it is necessary to have the following sufficient conditions [184]:

$$c_2 > \frac{\phi}{\Gamma_{min}} \quad (6-8)$$

$$c_1 \geq \frac{4\phi\Gamma_{max}(c_2 + \phi)}{\Gamma_{min}^3(c_2 - \phi)} \quad (6-9)$$

where

$$\phi > |\ddot{\sigma}(X, t)| \quad (6-10)$$

$$0 \leq \Gamma_{min} \leq \left| \frac{\partial \ddot{\sigma}}{\partial u} \right| \leq \Gamma_{max} \quad (6-11)$$

with c_1 and c_2 being two positive constants that should be manually tuned to be large enough to ensure a good performance [185]. Furthermore, ϕ , Γ_{min} and Γ_{max} are specified conditions for finite time convergence. The article [186] evaluates several approaches to define ϕ , Γ_{min} and Γ_{max} . Thus, if the plant to be controlled can be modeled in this format, the controller can be implemented efficiently.

6.2 Mathematical Modelling

The first muscular model found is the Hill model. He observed that the elasticity of tendons influences the force generated in the muscles, so that the system could be modeled as a mass-spring system (Figure 6.6), which was known as a Hill's muscular model of four elements (widely used still today, as shown at [187]), with CE being the elastic component (muscle) and VER and PEE are the elastic components of the tendons.

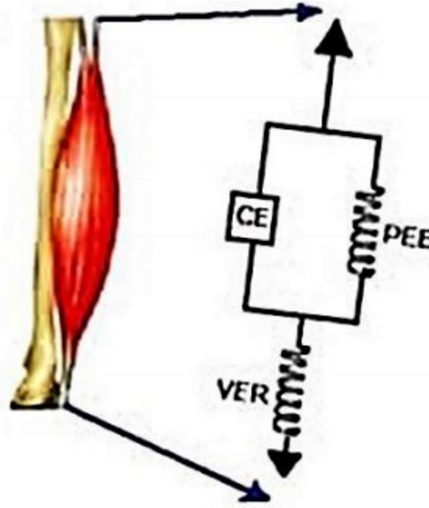


Figure 6.6: Figure showing the dynamics of muscular contraction [47].

Exists several studies for activation of neuromotor receptor, as shown at [188]. As a basis for the muscle model and activation of neuromotor receptors, the model described by Houk and Simon [43] was used:

$$T(s) = \frac{F_m(s)}{u(s)} = K \frac{\left(1 + \frac{s}{0.15}\right) \left(1 + \frac{s}{1.5}\right) \left(1 + \frac{s}{16}\right)}{\left(1 + \frac{s}{0.2}\right) \left(1 + \frac{s}{5}\right) \left(1 + \frac{s}{37}\right)}, \quad (6-12)$$

with $\frac{F_m(s)}{u(s)}$ being a function of transference of the motor force performed F_m and the electro-stimulus $u(s)$, K the static muscle gain. It is important to emphasize that, in the present study, since the orthosis will be placed on the arm of the volunteer, this muscle activation dynamics will be considered as a disturbance, since the bending of the elbow will be done through a servomotor, as described previously. However, the interference of the user and the orthosis (assisting or hindering movement) cannot be ignored.

The complete mathematical modelling of the upper limb has seven degrees of freedom (DoF) [189] [190] [191]. However, because both the testing

system and the orthosis maintain the bending motion in a single plane, the mathematical modeling can be simplified to a set of two bars, as presented in [65].

Associated with this we also have the dynamics of arm movement, as shown in Figure 6.7:

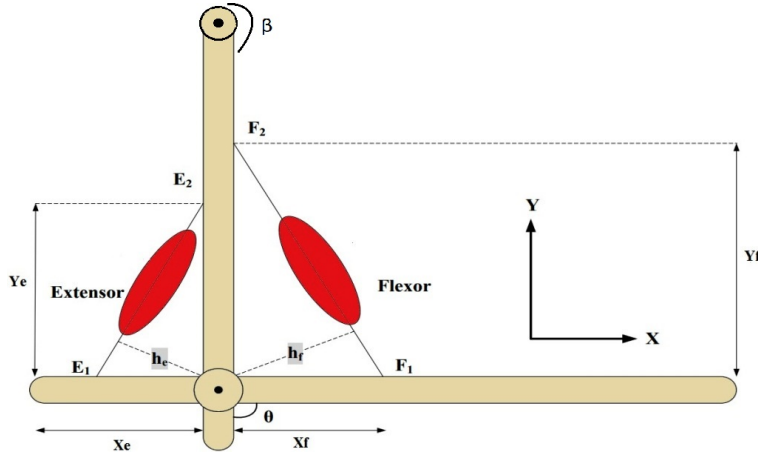


Figure 6.7: Schematic diagram of an arm movement, adapted from [73].

with:

- Y_e the vertical projection of the length of extensor muscle;
- Y_f the vertical projection of the length of flexor muscle;
- X_e the horizontal projection of the length of extensor muscle;
- X_f the horizontal projection of the length of flexor muscle;
- θ is the elbow bending angle;
- β is the shoulder bending angle

Using the Euler-Lagrange method, the following set of equations is obtained:

$$K(\lambda(t), \dot{\lambda}(t)) = \frac{1}{2}m \|V\|^2 + \frac{1}{2}I\dot{\lambda}^2 \quad (6-13)$$

$$L(\lambda(t), \dot{\lambda}(t)) = K(\lambda(t), \dot{\lambda}(t)) - U(\lambda(t)) \quad (6-14)$$

$$\tau = \frac{d}{dt} \left(\frac{\partial L(\lambda, \dot{\lambda})}{\partial \dot{\lambda}} \right) - \frac{\partial L(\lambda, \dot{\lambda})}{\partial \lambda} \quad (6-15)$$

where K is the kinetic energy, U is the potential energy, λ is the angle of the joints, m is the mass of the orthosis, V is the vector of angular velocity, I is the inertia, τ is the torque from the servomotor, and L is the Lagrangian

function. The position vector \mathbf{P} of the mass center of each link can be written as:

$$\mathbf{P} = \begin{bmatrix} x \\ y \end{bmatrix} = \begin{bmatrix} l_1 \sin(\beta) + l_2 \sin(\beta + \theta) \\ -l_1 \cos(\beta) - l_2 \cos(\beta + \theta) \end{bmatrix} \quad (6-16)$$

with l_i as the length of the arm and forearm, θ is the elbow bending angle and β is the planar shoulder bending angle.

Then, the angular velocity \mathbf{V} can be written as:

$$\mathbf{V} = \begin{bmatrix} \dot{x} \\ \dot{y} \end{bmatrix} = \begin{bmatrix} l_2 \cos(\beta + \theta) \dot{\theta} \\ l_2 \sin(\beta + \theta) \dot{\theta} \end{bmatrix} \quad (6-17)$$

In this way, equations (6-13), (6-14) and (6-15) can be written as:

$$K(\lambda(t), \dot{\lambda}(t)) = \frac{1}{2} m_2 l_2^2 \dot{\theta}^2 + \frac{1}{2} I_2 \dot{\theta}^2 \quad (6-18)$$

$$L(\lambda(t), \dot{\lambda}(t)) = \frac{1}{2} m_2 l_2^2 \dot{\theta}^2 + \frac{1}{2} I_2 \dot{\theta}^2 + m_2 l_2 \cos(\beta + \theta) + m_2 l_1 \cos(\beta) \quad (6-19)$$

$$\tau = m_2 l_2^2 \ddot{\theta} + m_2 g I_2 \sin(\beta + \theta) \quad (6-20)$$

Noting that the actuation system of the orthosis is a DC Servo motor, one can use the following standard modeling:

$$\frac{K_a}{R_a} V_a = J \ddot{\theta} + C(\theta) + \frac{K_a K_m}{R_a} \dot{\theta} + \tau \quad (6-21)$$

where K_a is the motor torque constant, R_a is the armature resistance, K_m is the electromotive force constant, V_a is the armature tension, J is the total inertia of the rotor and load relative to the shaft, τ is the motor torque and C is the viscous friction force.

Substituting (6-20) into (6-21), then:

$$\frac{K_a}{R_a} V_a = J \ddot{\theta} + C(\theta) + \frac{K_a K_m}{R_a} \dot{\theta} + m_2 l_2^2 \ddot{\theta} + m_2 g I_2 \sin(\beta + \theta) \quad (6-22)$$

The orthosis system can be rewritten as follows:

$$\mathbf{X} = \begin{bmatrix} \theta \\ \dot{\theta} \end{bmatrix} \quad (6-23)$$

then

$$\dot{\mathbf{X}} = \begin{bmatrix} \dot{\theta} \\ \ddot{\theta} \end{bmatrix} = f(X, t) + B(t)u(t) + d(t) \quad (6-24)$$

$$(6-25)$$

where

$$f(X, t) = \begin{bmatrix} \dot{\theta}^2 \\ (m_2 l_2^2 + J - 1)(-C - (m_2 g l_2 \sin(\beta + \theta))) - (\frac{K_a K_m}{R_a}) \dot{\theta} \end{bmatrix} \quad (6-26)$$

and

$$B(t) = \begin{bmatrix} 0 \\ (m_2 l_2^2 + J - 1)(\frac{K_a}{R_a}) \end{bmatrix} \quad (6-27)$$

and

$$d(t) = \begin{bmatrix} 0 \\ F_{ext} \end{bmatrix} \quad (6-28)$$

where:

$f(X, t) + B(t)u(t)$ is the system dynamics

$d(t)$ is the disturbance the interference of the user and the orthosis (assisting or hindering movement)).

6.3

Control Requirements, Parameters and Objectives

Using the EEG+EMG+ECG signal indicators, it is possible to send a signal that corresponds to a certain elbow bending angle, causing the orthosis' servomotor to rotate to fulfill the given task. Thus, the chosen controller should be robust to the following characteristics:

- Uncertainties in the model;
- Uncertainties in the dynamics;
- Uncertainties in the control;
- Uncertainties in the sensors;

In this way, robust or adaptive controllers are best suited for this task. The first goal, after defining the mathematical modeling, is to define which is the control objective. Since the goal of the orthosis is to assist in the execution of the elbow bending movement, it is then intended to minimize the angular error ($\tilde{\theta}$) in order to ensure the desired movement (θ_d).

$$\tilde{\theta} = \theta_d - \theta_e \quad (6-29)$$

As in [193], [194], [195] and [196], one can define a sliding surface (σ) of the type:

$$\sigma(t) = \dot{\tilde{\theta}} + \xi \tilde{\theta} \quad (6-30)$$

with ξ as an arbitrary positive constant which defines the convergence rate.

Then,

$$\dot{\sigma}(X, t) = \frac{\partial \sigma}{\partial t} + \frac{\partial \sigma}{\partial x} (f(X, t) + B(t)u(t) + d(t)) \quad (6-31)$$

$$\ddot{\sigma}(X, t) = \frac{\partial \dot{\sigma}}{\partial t} + \frac{\partial \dot{\sigma}}{\partial x} (f(X, t) + B(t)u(t) + d(t)) + \frac{\partial \dot{\sigma}}{\partial u} \dot{u}(t) \quad (6-32)$$

Substituting the modelling:

$$\begin{aligned} \dot{\sigma}(X, t) = & \ddot{\theta} + (m_2 l_2^2 + J - 1)(-C - (m_2 g l_2 \sin(\beta + \theta))) \\ & - (m_2 l_2^2 + J - 1) \left(\frac{K_a K_m}{R_a} \right) \dot{\theta} - \\ & \dot{\theta}_d - \ddot{\theta}_d + (m_2 l_2^2 + J - 1) \left(\frac{K_a}{R_a} \right) u(t) - F_{ext} \end{aligned} \quad (6-33)$$

$$\begin{aligned} \ddot{\sigma}(X, t) = & (m_2 l_2^2 + J - 1) \left(\frac{K_a}{R_a} \right) \\ & + (m_2 l_2^2 + J - 1) (-C(m_2 g l_2 \cos(\beta + \theta)) \dot{\theta} \\ & [1 + (m_2 l_2^2 + J - 1) \left(\frac{K_a K_m}{R_a} \right) - F_{ext}] \ddot{\theta} \end{aligned} \quad (6-34)$$

Now, we can apply the control law (6-6)-(6-7)

$$u(t) = -c_1 \sqrt{\sigma} \text{sign}(\sigma) + \nu \quad (6-35)$$

$$\dot{\nu} = -c_2 \text{sign}(\sigma) \quad (6-36)$$

with

$$c_2 > \frac{\phi}{\Gamma_{min}} \quad (6-37)$$

$$c_1^2 \geq \frac{4\phi\Gamma_{max}(c_2 + \phi)}{\Gamma_{min}^3(c_2 - \phi)} \quad (6-38)$$

The standard switching function $\text{sign}(\sigma)$ can be replaced by a function that is more tenuous with respect to the slope in order to reduce the chattering effect that is common when using an SMC, similar to that suggested in [197]. Figure 6.8 presents the behavior of some switching functions.

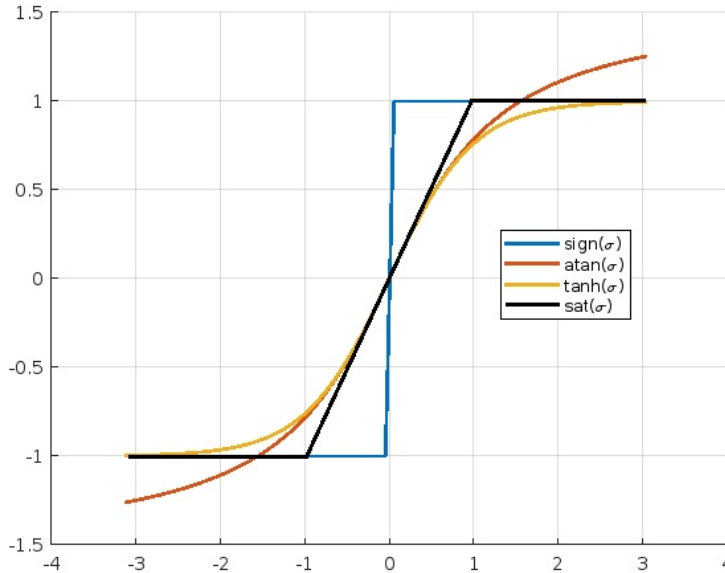


Figure 6.8: Behavior of some switching functions.

Thus, the control law becomes:

$$u(t) = -c_1\sqrt{\sigma}F + \nu \quad (6-39)$$

$$\dot{\nu} = -c_2F \quad (6-40)$$

With F as a generic switching function. In the present study, the \tanh was chosen as the switching function, to be compared with the standard function (sign), because it is a smoother function. In this way, the control law becomes:

$$u(t) = -c_1\sqrt{\sigma}\tanh(\sigma) + \nu \quad (6-41)$$

$$\dot{\nu} = -c_2\tanh(\sigma) \quad (6-42)$$

6.3.1 Stability Proof

To ensure that the controller works properly, the stability of the system as a whole must be proven, including the introduction of the controller. So, as described in [193], [194], [195], [197] and [196], it is sufficient to find a Lyapunov function that can show the stability of the controller. From [198], [199] and [200] we can write:

$$\mathbf{V}(\mathbf{s}) = \zeta^T \mathbf{P} \zeta \quad (6-43)$$

then

$$\dot{\zeta} = \begin{bmatrix} \tanh'(s) & -c_1\sqrt{\sigma}\tanh(s) + 1 \\ -c_2 & c_2\tanh(s) \end{bmatrix} \quad (6-44)$$

and then

$$\dot{\zeta} = \tanh'(s) \begin{bmatrix} -c_1 & 1 \\ -c_2 & 0 \end{bmatrix} \zeta \quad (6-45)$$

Since \mathbf{P} is a symmetric positive-definite matrix, by Zubov's Theorem [201], it is correct to affirm that \mathbf{V} is monotonically decreasing and the origin is asymptotically stable.

6.3.2

Real Parameters

As described in the previous chapters, the orthosis was entirely made through digital manufacturing. All parts of the orthosis were sized to support a maximum weight of 50kg. The standard dimensions of the arm and forearm were defined according to Figure 6.7 and Table 6.1.

Table 6.1: Ergonomic Measurements(extracted by[65])

Dimension	<i>Adopted Values</i>
X_f (m)	$7.0 * 10^{-2}$
X_e (m)	$5.5 * 10^{-2}$
Y_f (m)	$14.0 * 10^{-2}$
Y_e (m)	$11.0 * 10^{-2}$
I ($\text{Kg} * \text{m}^2$)	$1.6 * 10^{-3}$
m_1 (Kg)	0.3
m_2 (Kg)	0.3
g (m/s^2)	9.81

Furthermore, the following specifications were taken from the servomotor datasheet (Table 6.2):

Table 6.2: Servomotor Parameters

Parameter	<i>Adopted Values</i>
R_a (Ω)	0.87
J ($\text{Nm}/(\text{Rad}/\text{s}^2)$)	0.12
K_a ($\text{V}/(\text{Rad}/\text{s})$)	0.56
K_m ($\text{V}/(\text{Rad}/\text{s})$)	0.56

The HOSM constants were adjusted empirically to decrease chattering without affecting convergence time, leaving $c_1 = 400$, $c_2 = 40$ and $\xi = 0.3$.

The PID constants were adjusted empirically to decrease the angular error, leaving $k_p = 2.62$, $k_i = 0.15$ and $k_d = 10$.

6.3.3

Embedded Electronics

All the simulations made in *Matlab*[®] needed to be adapted for real implementation, so the first challenge was to specify the electronics. For this, a servo motor capable of moving up to 50kg, an *Arduino nano*[®], an ECG sensor for the *Arduino nano*[®] with I2C communication, a *MyoWare*[®] EMG sensor,

also with I2C communication for the *Arduino nano*[®], and the *Emotiv Epoc*[®] Neuroheadset were specified.

However, as explained in the previous section, due to the pandemic of COVID-19, the prices and import of the sensors have become unfeasible. In this way, the original idea was modified to use a multiparameter monitor, as explained in the previous section. This monitor sends signals via RS232 protocol. These signals are received by *Labview*[®] (Figure 5.14) and, after all the filtering already presented in the previous section, the intention of movement is sent to the *Arduino nano*[®], which moves the orthosis servomotor to the desired position.

Although the system lost mobility because of the sensors (all the standard system are wired), the rest of the orthosis was built with low power consumption, so that only one 12v 3A source was enough to drive the system.

6.3.4 Simulations and Real-Time Actuation

The objective of this section is to show the robustness of the chosen controller (HOSM) in comparison to other controllers, which main advantage is the set-point search. A classic and simple-to-tune controller was chosen, the PID controller, designed to control a linear or linearized system. Similar propositions were made as in [65]:

$$P(s) = \frac{15,7(s^2 + 33.1s + 1180)}{(s + 83.5)(s + 61.7)(s + 56)(s^2 + 4.2s + 12)} e^{-0.012s} \quad (6-46)$$

and

$$u(t) = -c_1 \sqrt{\sigma} \tanh(\sigma) + \nu \quad (6-47)$$

$$\dot{\nu} = -c_2 \tanh(\sigma) \quad (6-48)$$

where the function $\tanh(\tau s)$ can be expressed as [202]:

$$\tanh(\tau s) = \frac{e^{\tau s} - e^{-\tau s}}{e^{\tau s} + e^{-\tau s}} \quad (6-49)$$

For systems with very small delays, the following trivial approximation may be performed [203]

$$e^{-\tau s} \cong \frac{1}{1 + \tau s}. \quad (6-50)$$

Thus, after the proper approximations and linearizations, it was possible to compare the PID controller with three robust nonlinear controllers. The controllers chosen were the conventional Sliding Mode, the standard High Order Sliding Mode, and the High Order Sliding Mode using a more tenuous switching function, as seen in the previous subsection. The tuned gains of each controller are shown in Section 6.3.2.

Using the *Matlab*[®] environment, a sine wave and a pulse were simulated as inputs in order to check the robustness of each controller.

Figures 6.9 and 6.10 present the behavior of the PID controller, Traditional HOSM controller, Tanh HOSM controller and Conventional Sliding Mode controller for predefined reference inputs (step and sine, respectively).

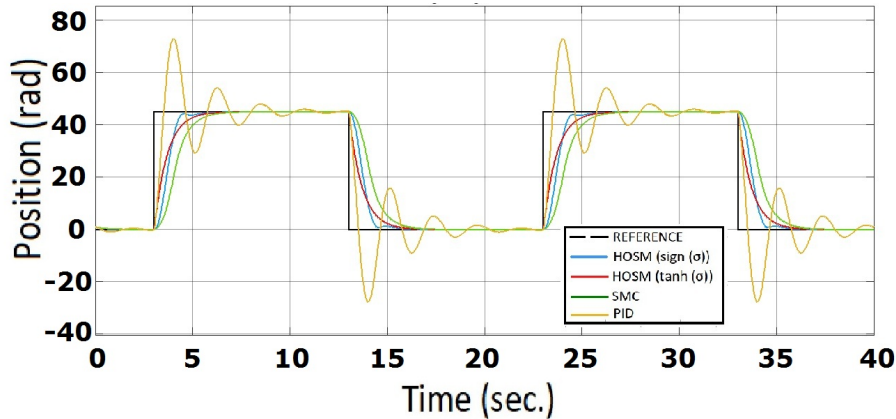


Figure 6.9: Behavior of the controllers for step inputs.

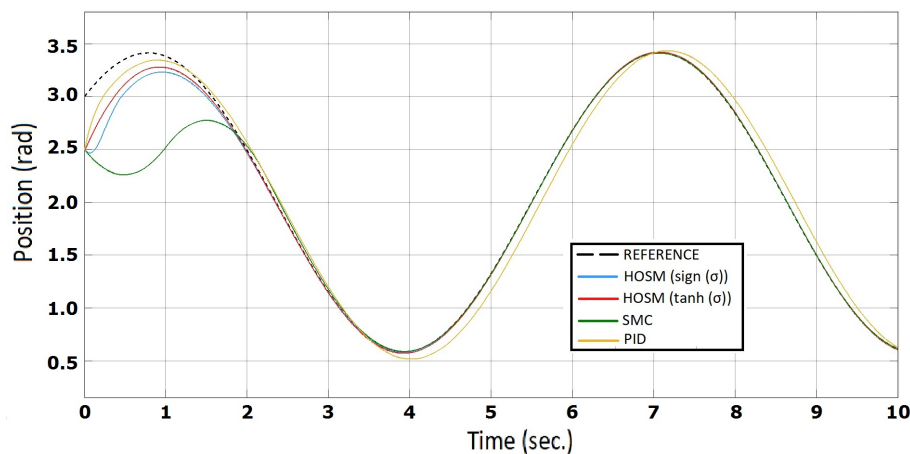


Figure 6.10: Behavior of the controllers for sinusoidal inputs.

Figure 6.11 presents the angular error of the PID controller, Traditional HOSM controller, tanh HOSM controller and Conventional Sliding Mode controller for a sinusoidal reference.

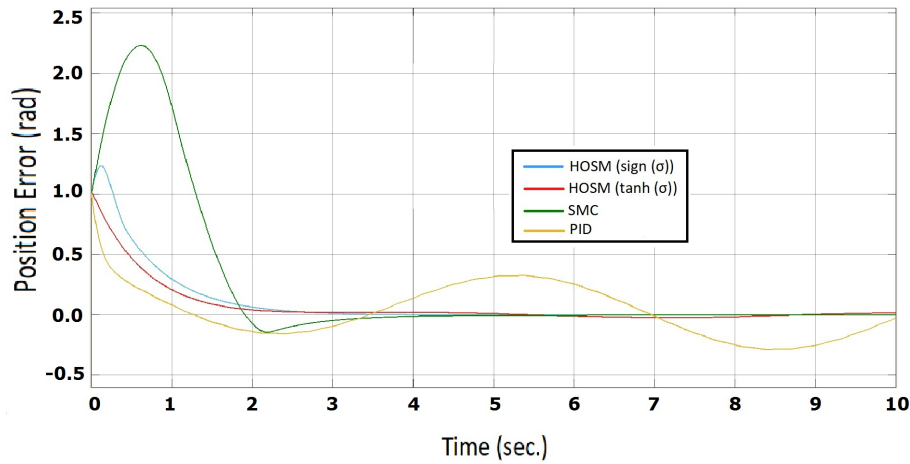


Figure 6.11: Angular error of the controllers for sinusoidal inputs.

For the real-time implementation, the elbow bending orthosis was used, given an input excitation via EEG and adjusted given the angle value of the encoder and the EMG signals. For the request to bend the elbow to a specific angle (45 degrees), the control algorithm worked effectively, as shown in Figure 6.12 and Figure 6.13.

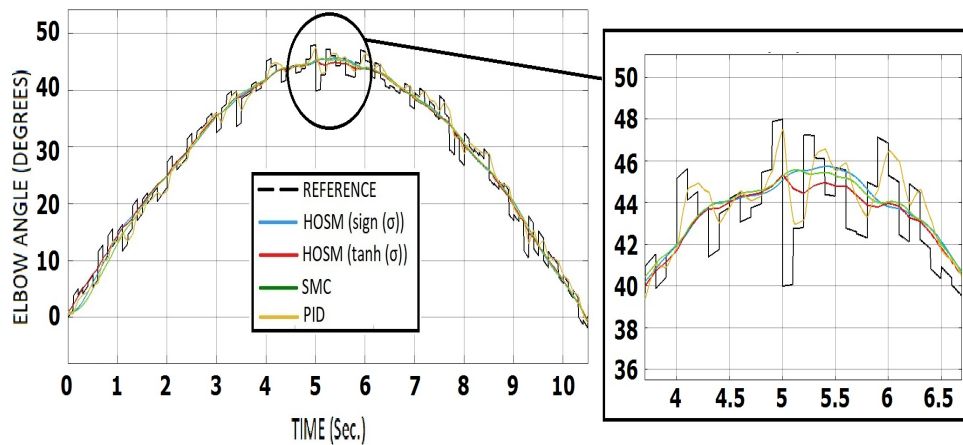


Figure 6.12: Real-time example 1.

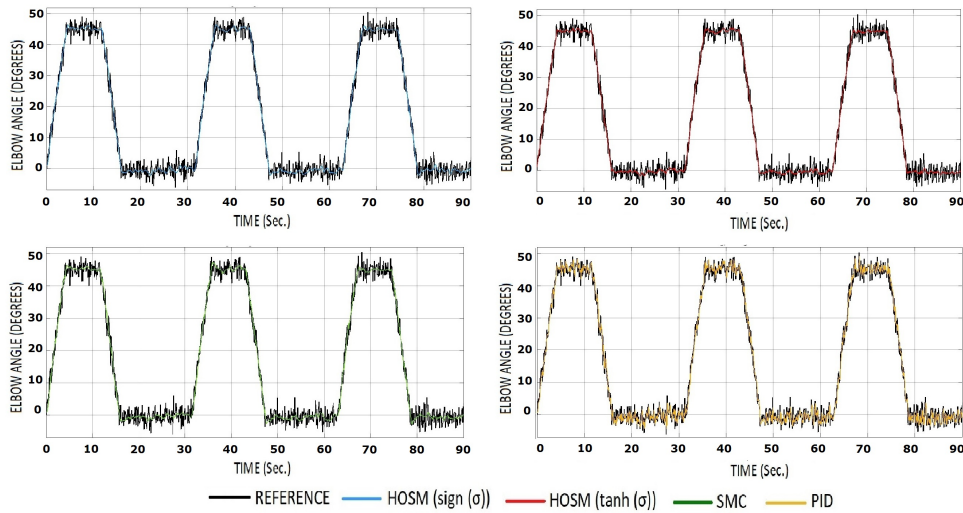


Figure 6.13: Real-time example 2.

As observed in the pictures, the encoder reference signal was quite noisy. This happened because the volunteer moved the arm slowly to reach the target angle (in the case of the pictures it was the 45 degree angle). However, when asked for an action, such as "putting your hand in your mouth", the action was not as satisfactory, probably because it involved another region of the brain, as seen in the previous chapter.

7

Conclusions

This thesis has addressed the several challenges involved in building an orthosis to be activated through the decoding of the movement intention, while controlled by a servomotor. Some important aspects of the study should be pointed out in order to consolidate the acquired knowledge, highlight the advances, and point to future directions and new studies to come.

7.1

Advances and Outcomes

The entire study was able to evolve the knowledge in several areas, each interconnected with the other to obtain the final result: the creation of a general functional orthosis.

Under the aspect of Industry 4.0, the presented contribution was the creation of procedures to facilitate the digitization of upper limbs, besides demonstrating that it is possible to use these techniques for this purpose. Furthermore, the use of simulation tools such as *X sens*[®] and *SolidWorks*[®] allowed a better understanding of the body movement dynamics and the impact of orthosis insertion on the natural dynamics of the body already adapted to the injury. Another interesting point achieved by this thesis, within the Industry 4.0 context, was the use of open-programmed and low-cost electronics, compared to the electronics currently adopted in commercial orthoses. This allows a greater popularization of the orthosis and access for low-income people.

Under the aspect of optimization, this thesis was able to propose an orthosis that is lighter for the user than the existing alternatives, which decreases the chances of giving up its use, as it increases the ease of adaptation. In addition, there was a considerable increase in mechanical strength, which increased the life span of the orthosis and ensured it was more robust to daily use.

In addition, the use of Industry 4.0 concepts allied to multi-lattice optimization allowed the orthosis to use FDM technology, whose characteristic of low and medium mechanical strength is widely known, to be used efficiently, which considerably lowered the production cost.

With respect to biological signal processing, there were three contributions achieved by the thesis. The first was the combination of the characterization of the three signals (EEG, EMG and ECG), so that the inference of movement could be made, allowing the orthosis to be activated in an assertive way regardless of the user who was operating it. The second was the creation of a database of defined movements, so that it can be used for future works, in addition to serving as a comparison of bio-type and motor aspects related to a given profession or activity. Finally, an efficient filtering of the signals was achieved, precise enough to distinguish which electrodes capture what types of movements, as well as the differences between planning, executing, and executing and planning, as well as the differences between a defined target and an activity associated with a specific movement.

Furthermore, the combination of additive manufacturing techniques with the capture of signals through the developed apparatus facilitated the creation of test execution procedures, ensuring that all volunteers performed the same movements.

Under the aspect of control, the advance was in the use of nonlinear and robust control techniques for the performance of the orthosis, together with a modeling that treats the parametric uncertainties and the disturbances in a more realistic way, without the need for approximations or linearizations. Classic controllers were also implemented in the experimental system, however with larger errors.

The comparison between the simulation and the real application showed satisfactory results, since the system managed to reach the predefined angles even under the presence of disturbances inherent to human physiology, not to mention the imprecision of the sensors and the involuntary interference of the individuals studied. Notice that the system may fail when asked for an associative task instead of a defined target since, for this type of movement, the brain uses not only the motor cortex and somatosensory cortex, but also other regions that associate events and activities, such as vision and touch, to execute a movement.

Still related to control, this thesis adopted a smoother switching function compared to the usual choices for HOSM. The chosen function has interesting practical applications, giving the controller greater robustness to uncertainties and less chattering effects.

7.2

Future Works

Future works related to the proposed orthosis design can be summarized as:

- Standardization of technical procedures developed to create a common chain of processes;
- Enabling medium-scale production;
- Implementation of other optimization techniques to make the orthosis even lighter without losing the desired mechanical characteristics;
- Implementation of more electrodes in other regions, such as somatosensory association and visual association, to improve movement inference;
- Performing associative tasks, to improve the quality of life of the users;
- Improving the quality of acquired signals to minimize system noise, through additional filtering procedures;
- Implementation of a fully wearable system to ensure user autonomy;
- Implementation of ergonomic modifications, to make the orthosis more attractive to its daily use.

Bibliography

- [1] JEFFERSON, G.. The mind of mechanical man. BMJ, 1(4616):1105–1110, Jun 1949.
- [2] RZYMAN, G.; SZKOPEK, J.; REDLARSKI, G. ; PALKOWSKI, A.. Upper limb bionic orthoses: General overview and forecasting changes. Applied Sciences, 10(15):5323, Jul 2020.
- [3] HISKEY, D.. “first robot created in 400 bc was a steam-powered pigeon”. <http://mentalfloss.com/article/13083/first-robot-created-400-bce-was-steam-powered-pigeon>, 2012. last access in 27/01/2021.
- [4] PARÉ, A.. La Méthode de traiter lês plaies faites par les arquebuses et autres bastons à feu. A Lyon, 1545.
- [5] LOVETT, R. W.. The history of scoliosis. JBJS, 2(1):54–62, 1913.
- [6] PÉDRON, F.. Histoire d’Ambroise chirurgien du roi. O. Orban, 1980.
- [7] GOLDBERG, J.. On paré and prosthetics. <https://nyamcenterforhistory.org/2014/12/19/on-pare-and-prosthetics/>, 2014. last access in 23/09/2020.
- [8] PARÉ, A.. Prosthesis, 16th century. <https://commons.wikimedia.org>, 2010. last access in 27/09/2020.
- [9] FUENTES, L.. The most common 3d printed prosthetics in 2021. <https://all3dp.com/2/the-most-common-3d-printed-prosthetics/>, 2021. last access in 27/01/2021.
- [10] DÍAZ, I.; GIL, J. J. ; SÁNCHEZ, E.. Lower-limb robotic rehabilitation: Literature review and challenges. Journal of Robotics, 2011:1–11, 2011.
- [11] BIDDISS, E. A.; CHAU, T. T.. Upper limb prosthesis use and abandonment: A survey of the last 25 years. Prosthetics and Orthotics International, 31(3):236–257, Sep 2007.

- [12] MCCABE, J. P.; HENNIGER, D.; PERKINS, J.; SKELLY, M.; TATSUOKA, C. ; PUNDIK, S.. **Feasibility and clinical experience of implementing a myoelectric upper limb orthosis in the rehabilitation of chronic stroke patients: A clinical case series report.** PLOS ONE, 14(4):e0215311, Apr 2019.
- [13] PUNDIK, S.; MCCABE, J.; KESNER, S.; SKELLY, M. ; FATONE, S.. **Use of a myoelectric upper limb orthosis for rehabilitation of the upper limb in traumatic brain injury: A case report.** Journal of Rehabilitation and Assistive Technologies Engineering, 7:205566832092106, Jan 2020.
- [14] GARBELLINI, S.; ROBERT, Y.; RANDALL, M.; ELLIOTT, C. ; IMMS, C.. **Rationale for prescription, and effectiveness of, upper limb orthotic intervention for children with cerebral palsy: a systematic review.** Disability and Rehabilitation, 40(12):1361–1371, Mar 2017.
- [15] BARBOSA, W. S.; WANDERLEY, R. F. F.; GIOIA, M. M.; GOUVEA, F. C. ; GONÇALVES, F. M.. **Additive or subtractive manufacturing: Analysis and comparison of automotive spare-parts.** Journal of Remanufacturing, Oct 2021.
- [16] BARBOSA, W. S.; GIOIA, M. M.; NATIVIDADE, V. G.; WANDERLEY, R. F. F.; CHAVES, M. R.; GOUVEA, F. C. ; GONÇALVES, F. M.. **Industry 4.0: examples of the use of the robotic arm for digital manufacturing processes.** International Journal on Interactive Design and Manufacturing (IJIDeM), Sep 2020.
- [17] COALITION, T. A.. **3d printed prosthetics | where we are today.** <https://www.amputee-coalition.org/3d-printed-prosthetics/>, 2019. last access in 27/01/2021.
- [18] FURTADO, F.. **A serviÇO do corpo.** <https://cienciahoje.org.br/a-servico-do-corpo/>, 2021. last access in 27/01/2021.
- [19] VUJAKLIJA, I.; FARINA, D.. **3d printed upper limb prosthetics.** Expert Review of Medical Devices, 15(7):505–512, Jul 2018.
- [20] TEN KATE, J.; SMIT, G. ; BREEDVELD, P.. **3d-printed upper limb prostheses: a review.** Disability and Rehabilitation: Assistive Technology, 12(3):300–314, Feb 2017.

- [21] XU, G.; GAO, L.; TAO, K.; WAN, S.; LIN, Y.; XIONG, A.; KANG, B.; ZENG, H.. **Three-dimensional-printed upper limb prosthesis for a child with traumatic amputation of right wrist**. *Medicine*, 96(52):e9426, Dec 2017.
- [22] KOPRNICKY, J.; NAJMAN, P.; SAFKA, J.. **3d printed bionic prosthetic hands**. In: 2017 IEEE INTERNATIONAL WORKSHOP OF ELECTRONICS, CONTROL, MEASUREMENT, SIGNALS AND THEIR APPLICATION TO MECHATRONICS (ECMSM). IEEE, May 2017.
- [23] GARAVAGLIA, L.; PAGLIANO, E.; ARNOLDI, M. T.; LOMAURO, A.; ZANIN, R.; BARANELLO, G.; ALIVERTI, A.; PITTACCIO, S.. **Two single cases treated by a new pseudoelastic upper-limb orthosis for secondary dystonia of the young**. In: 2017 INTERNATIONAL CONFERENCE ON REHABILITATION ROBOTICS (ICORR), p. 1260–1265, 2017.
- [24] CABRERA, A.. **Myorthotics: Digital manufacturing in the development of a diy interactive rehabilitation orthosis**. Paper presented at Fab13, 1, 2017.
- [25] RADIŠA, R.; GULIŠIJA, Z.; MANASIJEVIĆ, S.. **Optimization of casting process design**. ISSN, 1259:111–114, 1821.
- [26] HARZHEIM, L.; GRAF, G.. **A review of optimization of cast parts using topology optimization**. *Structural and multidisciplinary optimization*, 31(5):388–399, 2006.
- [27] WANG, Y.; KANG, Z.. **Structural shape and topology optimization of cast parts using level set method**. *International Journal for Numerical Methods in Engineering*, 111(13):1252–1273, 2017.
- [28] ALLAIRE, G.; JOUVE, F.; MICHAILIDIS, G.. **Casting constraints in structural optimization via a level-set method**. In: 10TH WORLD CONGRESS ON STRUCTURAL AND MULTIDISCIPLINARY OPTIMIZATION, 2013.
- [29] SOUZA, R. P. D.. **Otimização de parâmetros mecânicos e microestruturais dos moldes em areia de sílica ligados quimicamente pelo processo de cura a frio em fundição de aço**. PhD thesis, Universidade Federal do Rio Grande do Norte, 2015.

- [30] VASSOLER, J.. **Otimização do projeto de polias fabricadas em ferro fundido cinzento gg-15 utilizadas no setor de ordenhadeiras.** Elementos finitos, 2018.
- [31] CARREIRA, J. A. A.. **Design e otimização de peças estruturais metálicas para processos de fabricação aditiva.** PhD thesis, Instituto Politécnico do Porto, 2017.
- [32] INÁCIO, S. A. C.. **Otimização de Topologia de Estruturas Construídas com Material Ortotrópico.** PhD thesis, Faculdade de Ciências e Tecnologia (FCT), 2019.
- [33] PANASENKO, G. P.. **Multi-scale modelling for structures and composites,** volumen 615. Springer, 2005.
- [34] KANG, D.; PARK, S.; SON, Y.; YEON, S.; KIM, S. H. ; KIM, I.. **Multi-lattice inner structures for high-strength and light-weight in metal selective laser melting process.** Materials & Design, 175:107786, 2019.
- [35] HELOU, M.; KARA, S.. **Design, analysis and manufacturing of lattice structures: an overview.** International Journal of Computer Integrated Manufacturing, 31(3):243–261, 2018.
- [36] LI, C.; LEI, H.; LIU, Y.; ZHANG, X.; XIONG, J.; ZHOU, H. ; FANG, D.. **Crushing behavior of multi-layer metal lattice panel fabricated by selective laser melting.** International Journal of Mechanical Sciences, 145:389–399, 2018.
- [37] HABIB, F.; IOVENITTI, P.; MASOOD, S. ; NIKZAD, M.. **Fabrication of polymeric lattice structures for optimum energy absorption using multi jet fusion technology.** Materials & Design, 155:86–98, 2018.
- [38] LEI, H.; LI, C.; MENG, J.; ZHOU, H.; LIU, Y.; ZHANG, X.; WANG, P. ; FANG, D.. **Evaluation of compressive properties of slm-fabricated multi-layer lattice structures by experimental test and μ -ct-based finite element analysis.** Materials & Design, 169:107685, 2019.
- [39] USHIJIMA, K.; CANTWELL, W. ; CHEN, D.. **Prediction of the mechanical properties of micro-lattice structures subjected to multi-axial loading.** International Journal of Mechanical Sciences, 68:47–55, 2013.

- [40] BERTOLINO, G.; MONTEMURRO, M. ; DE PASQUALE, G.. **Multi-scale shape optimisation of lattice structures: an evolutionary-based approach**. *International Journal on Interactive Design and Manufacturing (IJIDeM)*, 13(4):1565–1578, 2019.
- [41] KAZEMI, H.; VAZIRI, A. ; NORATO, J. A.. **Multi-material topology optimization of lattice structures using geometry projection**. *Computer Methods in Applied Mechanics and Engineering*, 363:112895, 2020.
- [42] DOLHEM, R.. **Histoire de l'électrostimulation en médecine et en rééducation**. *Annales de Réadaptation et de Médecine Physique*, 51:427–431, 07 2008.
- [43] HOUK, J. C.; SIMON, W.. **Responses of golgi tendon organs to forces applied to muscle tendon**. In: *IN J. NEUROPHYSIOL.*, volumen 30, p. 1466–1481, 1967.
- [44] HAFEZ, D.; BEVAN, A. ; RAY, W. Z.. **Nerve transfers for spinal cord injury**. *Peripheral Nerve Neurosurgery*, p. 297, 2018.
- [45] BAZAREK, S.; BROWN, J. M.. **The evolution of nerve transfers for spinal cord injury**. *Experimental Neurology*, p. 113–426, 2020.
- [46] WRIGHT, P. A.; GRANAT, M. H.. **Therapeutic effects of functional electrical stimulation of the upper limb of eight children with cerebral palsy**. *Developmental Medicine & Child Neurology*, 42(11):724–727, 2000.
- [47] ZAJAC, F.. **Muscle and tendon: Properties, models, scaling, and application to biomechanics and motor control**. In: *CRC CRIT REV. BIOMED. ENG.*, volumen 17, p. 359–411, 1989.
- [48] NIU, C. M.; BAO, Y.; ZHUANG, C.; LI, S.; WANG, T.; CUI, L.; XIE, Q. ; LAN, N.. **Synergy-based fes for post-stroke rehabilitation of upper-limb motor functions**. *IEEE Transactions on Neural Systems and Rehabilitation Engineering*, 27(2):256–264, 2019.
- [49] NIGG, B.; HERZOG, W.. **Biomechanics of musculo-skeletal system**. John Wiley Sons, September 1994.
- [50] PIYUS, C. K.; CHERIAN, V. A. ; NAGESWARAN, S.. **EMG based FES for post-stroke rehabilitation**. *IOP Conference Series: Materials Science and Engineering*, 263:052025, nov 2017.

- [51] SANTANA, J.; SANTANA FILHO, V.; CANDIDO, E. A. ; FREIRE, R. D. F.. **Eletroestimulação funcional no controle da espasticidade em paciente hemiparetico.** revista fafibe online, 9(1), 2010.
- [52] BEAR, M.; CONNORS, B. ; PARADISO, M. A.. **Neuroscience: Exploring the Brain, Enhanced Edition: Exploring the Brain.** Jones & Bartlett Learning, 2020.
- [53] PERES, A.; SOUZA, V. H.; CATUNDA, J.; MAZZETO-BETTI, K.; SANTOS, T.; D. VARGAS, C.; BAFFA, O.; DE ARAUJO, D.; PONTES-NETO, O.; LEITE, J. ; CAVALCANTI GARCIA, M. A.. **Can somatosensory electrical stimulation relieve spasticity in post-stroke patients? a tms pilot study.** Biomedizinische Technik. Biomedical engineering, 63, 05 2017.
- [54] BARBOSA, W. S.; TEMPORÃO, G. P. ; MEGGIOLARO, M. A.. **Control techniques for neuromuscular electrical stimulation: a brief survey.** In: 2021 IEEE INTERNATIONAL CONFERENCE ON BIOINFORMATICS AND BIOMEDICINE (BIBM), p. 2998–3005. IEEE, 2021.
- [55] DE SOUZA BARBOSA, W.. **Controle de um sistema de eletroestimulação funcional.** Master's thesis, Universidade do Estado do Rio de Janeiro, 2014.
- [56] MICERA, S.; SABATINI, A. ; P., D.. **Adaptive fuzzy control of electrically stimulated muscles for arm movements.** In: MEDICAL AND BIOLOGICAL ENGINEERING AND COMPUTING, volumen 37, 1999.
- [57] GOLLEE, H.; HUNT, K.. **Nonlinear modelling and control of electrically stimulated muscle: A local model network approach.** International Journal of Control, 68:1259–1288, 11 2010.
- [58] YU-LUEN CHEN; WEOI-LUEN CHEN; CHIN-CHIH HSIAO; TE-SON KUO ; JIN-SHIN LAI. **Development of the fes system with neural network + pid controller for the stroke.** In: 2005 IEEE INTERNATIONAL SYMPOSIUM ON CIRCUITS AND SYSTEMS, p. 5119–5121 Vol. 5, May 2005.
- [59] LYNCH, C.; POPOVIC, M.. **Closed-loop control for fes: Past work and future directions.** In: 10TH ANNUAL CONFERENCE OF THE INTERNATIONAL FES SOCIETY, p. 2–4. Citeseer, 2005.

- [60] MOHAMMADZAHERI, M.; CHEN, L. ; GRAINGER, S.. **A critical review of the most popular types of neuro control**. Asian Journal of Control, 14:1 – 11, 01 2012.
- [61] KIRSCH, N.; ALIBEJI, N. ; SHARMA, N.. **Nonlinear model predictive control of functional electrical stimulation**. Control Engineering Practice, 58:319–331, 2017.
- [62] OLIVEIRA, T. R.; COSTA, L. R.; CATUNDA, J. M. Y.; PINO, A. V.; BARBOSA, W. ; DE SOUZA, M. N.. **Time-scaling based sliding mode control for neuromuscular electrical stimulation under uncertain relative degrees**. Medical Engineering & Physics, 44:53–62, 2017.
- [63] ROUX OLIVEIRA, T.; R. COSTA, L.; V. PINO, A. ; PAZ, P.. **Extremum seeking-based adaptive pid control applied to neuromuscular electrical stimulation**. Anais da Academia Brasileira de Ciências, 91, 02 2019.
- [64] PAZ, P.; ROUX OLIVEIRA, T.; VISINTAINER PINO, A. ; PAULA FONTANA, A.. **Model-free neuromuscular electrical stimulation by stochastic extremum seeking**. IEEE Transactions on Control Systems Technology, PP:1–16, 02 2019.
- [65] BARBOSA, W. S.; TEMPORAO, G. P. ; MEGGIOLARO, M. A.. **Human arm stabilization and rehabilitation using intelligent control techniques**. In: 2020 IEEE INTERNATIONAL CONFERENCE ON BIOINFORMATICS AND BIOMEDICINE (BIBM), p. 2692–2697, Los Alamitos, CA, USA, dec 2020. IEEE Computer Society.
- [66] AKIN, M.; KURT, M. B.; SEZGIN, N. ; BAYRAM, M.. **Estimating vigilance level by using eeg and emg signals**. Neural Computing and Applications, 17(3):227–236, May 2007.
- [67] FERREIRA, A.; CELESTE, W. C.; CHEEIN, F. A.; BASTOS-FILHO, T. F.; SARCINELLI-FILHO, M. ; CARELLI, R.. **Human-machine interfaces based on emg and eeg applied to robotic systems**. Journal of NeuroEngineering and Rehabilitation, 5(1):10, 2008.
- [68] KIGUCHI, K.; HAYASHI, Y.. **Motion estimation based on emg and eeg signals to control wearable robots**. In: 2013 IEEE INTERNATIONAL CONFERENCE ON SYSTEMS, MAN, AND CYBERNETICS, p. 4213–4218, 2013.

- [69] LIANG, H.; ZHU, C.; IWATA, Y.; MAEDONO, S.; MOCHIDA, M.; YU, H.; YAN, Y. ; DUAN, F.. **Motion estimation for the control of upper limb wearable exoskeleton robot with electroencephalography signals.** In: 2018 IEEE INTERNATIONAL CONFERENCE ON CYBORG AND BIONIC SYSTEMS (CBS), p. 228–233, 2018.
- [70] SZU-YU LIN; CHIH-I HUNG; HSIN-I WANG; WU, Y. ; PO-SHAN WANG. **Extraction of physically fatigue feature in exercise using electromyography, electroencephalography and electrocardiography.** In: 2015 11TH INTERNATIONAL CONFERENCE ON NATURAL COMPUTATION (ICNC), p. 561–566, 2015.
- [71] HOODA, N.; DAS, R. ; KUMAR, N.. **Fusion of eeg and emg signals for classification of unilateral foot movements.** Biomedical Signal Processing and Control, 60:101990, Jul 2020.
- [72] KIM, B.; KIM, L.; KIM, Y.-H. ; YOO, S. K.. **Cross-association analysis of eeg and emg signals according to movement intention state.** Cognitive Systems Research, 44:1–9, Aug 2017.
- [73] DE BRITO NUNES, G. N. N. V.. **Modelação e controlo não-linear do sistema motor humano.** Master's thesis, Universidade Nova de Lisboa, 2009.
- [74] DIAS, N. S. M.. **Interface Cérebro-Máquina Baseada em Biotelemetria e Eléctrodos Secos.** PhD thesis, Universidade do Minho (Portugal), 2009.
- [75] BERMUDEZ, R. M. J.. **Proposta de um sistema baseado em redes neurais e wavelets para caracterização de movimentos do segmento mão-braço.** Master's thesis, Universidade Federal do Rio Grande do Sul, 2018.
- [76] BABAIASL, M.; GOLDAR, S. N.; BARHAGHTALAB, M. H. ; MEIGOLI, V.. **Sliding mode control of an exoskeleton robot for use in upper-limb rehabilitation.** In: 2015 3RD RSI INTERNATIONAL CONFERENCE ON ROBOTICS AND MECHATRONICS (ICROM), p. 694–701. IEEE, 2015.
- [77] FELLAG, R.; BENYAHIA, T.; DRIAS, M.; GUIATNI, M. ; HAMERLAIN, M.. **Sliding mode control of a 5 dofs upper limb exoskeleton robot.** In: 2017 5TH INTERNATIONAL CONFERENCE ON ELECTRICAL ENGINEERING-BOUMERDES (ICEE-B), p. 1–6. IEEE, 2017.

- [78] MEFOUED, S.; BELKHIAT, D. E. C.. **A robust control scheme based on sliding mode observer to drive a knee-exoskeleton.** Asian Journal of Control, 21(1):439–455, 2019.
- [79] MOKHTARI, M.; TAGHIZADEH, M. ; MAZARE, M.. **Impedance control based on optimal adaptive high order super twisting sliding mode for a 7-dof lower limb exoskeleton.** Meccanica, 56(3):535–548, 2021.
- [80] FAZLI, E.; RAKHTALA, S. M.; MIRRASHID, N. ; KARIMI, H. R.. **Real-time implementation of a super twisting control algorithm for an upper limb wearable robot.** Mechatronics, 84:102808, 2022.
- [81] HEGELE, R.. **Congresso brasileiro sobre acidentes e medicina do tráfego em gramado/rs, 2006.** last access in 13/02/2021.
- [82] GUIZONE, M.. **Lesão do plexo braquial (lpb), suas causas e a possibilidade de cura, 2006.** last access in 13/02/2021.
- [83] UNKNWON. **Brachial plexus.** <https://commons.wikimedia.org/w/index.php?curid=8401004>, 2010. last access in 13/02/2021.
- [84] NETTER, F. H.. **Atlas of human anatomy, Professional Edition E-Book: including NetterReference. com Access with full downloadable image Bank.** Elsevier health sciences, 2014.
- [85] UNKNWON. **Brachial plexus.** <https://anatomyinfo.com/arm-muscles/>, 2021. last access in 23/09/2022.
- [86] SOBOTTA, J.. **Sobotta: atlas de anatomía humana, volumen 1.** Ed. Médica Panamericana, 2006.
- [87] ROBERT TEASELL, M.; HUSSEIN, N.. **Clinical consequences of stroke.** Evidence-Based Review of Stroke Rehabilitation. Ontario: Heart and Stroke Foundation and Canadian Stroke Network, p. 1–30, 2016.
- [88] ROBINSON, MD, R. G.. **Neuropsychiatric consequences of stroke.** Annual review of medicine, 48(1):217–229, 1997.
- [89] PATTEN, C.; LEXELL, J. ; BROWN, H. E.. **Weakness and strength training in persons with poststroke hemiplegia: rationale, method, and efficacy.** Journal of Rehabilitation Research & Development, 41, 2004.
- [90] BRITO, R. G. D.. **Males do AVC.** Revista Neurociencias, 18, 2010.

- [91] TSUCHIMOTO, S.; SHINDO, K.; HOTTA, F.; HANAKAWA, T.; LIU, M.; USHIBA, J.. **Sensorimotor connectivity after motor exercise with neurofeedback in post-stroke patients with hemiplegia.** *Neuroscience*, 416:109–125, Sep 2019.
- [92] MONTE-SILVA, K.; PISCITELLI, D.; NOROUZI-GHEIDARI, N.; BATALLA, M. A. P.; ARCHAMBAULT, P.; LEVIN, M. F.. **Electromyogram-related neuromuscular electrical stimulation for restoring wrist and hand movement in poststroke hemiplegia: A systematic review and meta-analysis.** *Neurorehabilitation and Neural Repair*, 33(2):96–111, Feb 2019.
- [93] UNKNWON. **Brachial plexus.** <https://www.ortoponto.com.br/produto/imobilizador-de-cotovelo-tipo-brace-x-act-rom-endurance-totalmente-aj> 2021. last access in 23/09/2022.
- [94] FLORES, L. P.. **Estudo epidemiológico das lesões traumáticas de plexo braquial em adultos.** *Arquivos de Neuro-Psiquiatria*, 64(1):88–94, Mar 2006.
- [95] MORAN, S. L.; STEINMANN, S. P.; SHIN, A. Y.. **Adult brachial plexus injuries: mechanism, patterns of injury, and physical diagnosis.** *Hand clinics*, 21(1):13–24, 2005.
- [96] MALESSY, M. J.; PONDAAG, W.; VAN DIJK, J. G.. **Electromyography, nerve action potential, and compound motor action potentials in obstetric brachial plexus lesions.** *Neurosurgery*, 65, Oct 2009.
- [97] BINTI HJ DOLLAH, P.. **Obstetric brachial plexus palsy.** <http://www.myhealth.gov.my/en/obstetric-brachial-plexus-palsy/>, 2019. last access in 16/02/2021.
- [98] SHAKOR, P.; NEJADI, S.; PAUL, G.; MALEK, S.. **Review of emerging additive manufacturing technologies in 3d printing of cementitious materials in the construction industry.** *Frontiers in Built Environment*, p. 85, January 2019.
- [99] BARBOSA, W. S.; GOUVEA, F. C.; MARTINS, A. R. F.; BELMONTE, S. L.; WANDERLEY, R. F. F.. **Development of spare-parts process chain in oil & gas industry using industry 4.0 concepts.** *International Journal of Engineering and Technology (IJET)*, dec 2021.

- [100] BARBOSA, W. S.; GONÇALVES, F. M.; HENRIQUES, F. R.; GOUVEA, F. C. ; WANDERLEY, R. F. F.. **Development and validation of a biosignal measurement device to assist in teleoperated diagnosis.** In: ASIA-PACIFIC CONFERENCE ON COMPUTER SCIENCE AND DATA ENGINEERING 2021 (IEEE CSDE 2021), Dec. 2021.
- [101] BARBOSA, W. S.; GONÇALVES, F. M.; HENRIQUES, F. R.; GOUVEA, F. C. ; GIOIA, M. M.. **Industry 4.0: Construction of a waterproof wearable biosignal device to assist in submerged offshore work.** In: IEEE 8TH 2022 INTERNATIONAL CONFERENCE ON CONTROL, DECISION AND INFORMATION TECHNOLOGIES (IEEE CODIT 2022), May 2022.
- [102] GUBÁN, M.; KOVÁCS, G.. **Industry 4.0 conception.** Acta Technica Corviniensis-Bulletin of Engineering, 10(1), 2017.
- [103] ROJKO, A.. **Industry 4.0 concept: Background and overview.** International Journal of Interactive Mobile Technologies, 11(5), 2017.
- [104] MAKSIMCHUK, OLGA; PERSHINA, TATYANA. **A new paradigm of industrial system optimization based on the conception "industry 4.0".** MATEC Web Conf., 129:04006, 2017.
- [105] THUEMMLER, C.; BAI, C.. **Health 4.0: How virtualization and big data are revolutionizing healthcare.** Springer, 2017.
- [106] HERMANN, M.; PENTEK, T. ; OTTO, B.. **Design principles for industrie 4.0 scenarios.** In: 2016 49TH HAWAII INTERNATIONAL CONFERENCE ON SYSTEM SCIENCES (HICSS), p. 3928–3937. IEEE, 2016.
- [107] ALDEA, A.; IACOB, M.-E.; WOMBACHER, A.; HIRALAL, M. ; FRANCK, T.. **Enterprise architecture 4.0—a vision, an approach and software tool support.** In: 2018 IEEE 22ND INTERNATIONAL ENTERPRISE DISTRIBUTED OBJECT COMPUTING CONFERENCE (EDOC), p. 1–10. IEEE, 2018.
- [108] OKANO, M. T.. **Iot and industry 4.0: the industrial new revolution.** In: INTERNATIONAL CONFERENCE ON MANAGEMENT AND INFORMATION SYSTEMS, volumen 25, p. 26, 2017.
- [109] KENSEK, K.. **Building information modeling.** Routledge, 2014.

- [110] BARBOSA, W. S.; BELMONTE, S. L. R.; GONCALVES, F. M.; HENRIQUES, F. R.; GOUVEA, F. C.; GRIPPA, A. L. A. A. ; LIMA, T. H. G.. **Use of industry 4.0 techniques for anatomical reproduction of human heart comparing with traditional imaging methods.** Progress in Addictive Manufacturing, Oct 2022.
- [111] MUHOVIČ, J.; BOVCON, B.; KRISTAN, M.; PERŠ, J. ; OTHERS. **Obstacle tracking for unmanned surface vessels using 3-d point cloud.** IEEE Journal of Oceanic Engineering, 45(3):786–798, 2019.
- [112] GUERRERO, J.; SALCUDEAN, S. E.; MCEWEN, J. A.; MASRI, B. A. ; NICOLAOU, S.. **Real-time vessel segmentation and tracking for ultrasound imaging applications.** IEEE transactions on medical imaging, 26(8):1079–1090, 2007.
- [113] DU, Y.-C.; SHIH, C.-B.; FAN, S.-C.; LIN, H.-T. ; CHEN, P.-J.. **An imu-compensated skeletal tracking system using kinect for the upper limb.** Microsystem Technologies, 24(10):4317–4327, 2018.
- [114] NGUYEN, D. S.; VIGNAT, F.. **A method to generate lattice structure for additive manufacturing.** In: 2016 IEEE INTERNATIONAL CONFERENCE ON INDUSTRIAL ENGINEERING AND ENGINEERING MANAGEMENT (IEEM), p. 966–970, 2016.
- [115] NAGESHA, B.; DHINAKARAN, V.; VARSHA SHREE, M.; MANOJ KUMAR, K.; CHALAWADI, D. ; SATHISH, T.. **Review on characterization and impacts of the lattice structure in additive manufacturing.** Materials Today: Proceedings, 21:916–919, 2020. International Conference on Recent Trends in Nanomaterials for Energy, Environmental and Engineering Applications.
- [116] AL-KETAN, O.; ROWSHAN, R. ; AL-RUB, R. K. A.. **Topology-mechanical property relationship of 3d printed strut, skeletal, and sheet based periodic metallic cellular materials.** Additive Manufacturing, 19:167–183, 2018.
- [117] BEYER, C.; FIGUEROA, D.. **Design and Analysis of Lattice Structures for Additive Manufacturing.** Journal of Manufacturing Science and Engineering, 138(12), 09 2016.
- [118] SAVIO, G.; MENEGHELLO, R. ; CONCHERI, G.. **Geometric modeling of lattice structures for additive manufacturing.** Rapid Prototyping Journal, 2018.

- [119] SEHARING, A.; AZMAN, A. H. ; ABDULLAH, S.. **A review on integration of lightweight gradient lattice structures in additive manufacturing parts.** *Advances in Mechanical Engineering*, 12(6):1687814020916951, 2020.
- [120] BAI, L.; ZHANG, J.; CHEN, X.; YI, C.; CHEN, R. ; ZHANG, Z.. **Configuration optimization design of ti6al4v lattice structure formed by slm.** *Materials*, 11(10):1856, 2018.
- [121] FENG, Q.; TANG, Q.; LIU, Z.; LIU, Y. ; SETCHI, R.. **An investigation of the mechanical properties of metallic lattice structures fabricated using selective laser melting.** *Proceedings of the Institution of Mechanical Engineers, Part B: Journal of Engineering Manufacture*, 232(10):1719–1730, 2018.
- [122] MASKERY, I.; HUSSEY, A.; PANESAR, A.; AREMU, A.; TUCK, C.; ASHCROFT, I. ; HAGUE, R.. **An investigation into reinforced and functionally graded lattice structures.** *Journal of Cellular Plastics*, 53(2):151–165, 2017.
- [123] ONAL, E.; FRITH, J. E.; JURG, M.; WU, X. ; MOLOTNIKOV, A.. **Mechanical properties and in vitro behavior of additively manufactured and functionally graded ti6al4v porous scaffolds.** *Metals*, 8(4):200, 2018.
- [124] LEARY, M.; MAZUR, M.; WILLIAMS, H.; YANG, E.; ALGHAMDI, A.; LOZANOVSKI, B.; ZHANG, X.; SHIDID, D.; FARAHBOD-STERNAHL, L.; WITT, G. ; OTHERS. **Inconel 625 lattice structures manufactured by selective laser melting (slm): Mechanical properties, deformation and failure modes.** *Materials & Design*, 157:179–199, 2018.
- [125] XIAO, Z.; YANG, Y.; XIAO, R.; BAI, Y.; SONG, C. ; WANG, D.. **Evaluation of topology-optimized lattice structures manufactured via selective laser melting.** *Materials & Design*, 143:27–37, 2018.
- [126] LEARY, M.; MAZUR, M.; ELAMBASSERIL, J.; MCMILLAN, M.; CHIRENT, T.; SUN, Y.; QIAN, M.; EASTON, M. ; BRANDT, M.. **Selective laser melting (slm) of als12mg lattice structures.** *Materials & Design*, 98:344–357, 2016.
- [127] AREMU, A.; MASKERY, I.; TUCK, C.; ASHCROFT, I.; WILDMAN, R. ; HAGUE, R.. **A comparative finite element study of cubic unit cells for selective laser melting.** In: 2014 INTERNATIONAL SOLID

- FREEFORM FABRICATION SYMPOSIUM. University of Texas at Austin, 2014.
- [128] AL-SAEDI, D. S.; MASOOD, S.; FAIZAN-UR-RAB, M.; ALOMARAH, A. ; PONNUSAMY, P.. **Mechanical properties and energy absorption capability of functionally graded f2bcc lattice fabricated by slm.** *Materials & Design*, 144:32–44, 2018.
- [129] ULLAH, I.; BRANDT, M. ; FEIH, S.. **Failure and energy absorption characteristics of advanced 3d truss core structures.** *Materials & Design*, 92:937–948, 2016.
- [130] BERGONZI, L.; VETTORI, M.; STEFANINI, L. ; ALCAMO, L.. **Different infill geometry influence on mechanical properties of fdm produced pla different infill geometry influence on mechanical properties of fdm produced pla.** *IOP Conference Series Materials Science and Engineering*, 1038, 03 2021.
- [131] KRONR. **infill.** last access in 15/10/2022.
- [132] SANTOS, P. H. B. N. D.. **Estudo de técnicas de processamento de sinais de eletroencefalograma (eeg) com enfoque em sinais convulsivos,** 2014.
- [133] SANEI, S.; CHAMBERS, J. A.. **EEG signal processing.** John Wiley & Sons, 2013.
- [134] DA COSTA FLORISBAL, G.. **Análise e classificacao de sinais de eeg a partir de movimentacao passiva em pacientes sedados,** 2021.
- [135] SILVA, G. M. D.; OTHERS. **Caracterização e filtragem de eletroencefalograma contaminado por eletromiografia dos músculos faciais.** PhD thesis, Universidade Federal de Uberlândia, 2020.
- [136] TORTORA, G. J.; DERRICKSON, B.. **Corpo Humano: Fundamentos de Anatomia e Fisiologia.** Artmed Editora, 2016.
- [137] SALGUEIRO, A. T. F.. **Detecção de problemas cardíacos usando sinais de electrocardiograma (ECG).** PhD thesis, Universidade de Coimbra, 2020.
- [138] LOPES, F. R.; MEGGIOLARO, M. A.. **Classification of eeg signals using genetic programming.** In: COBEM-2017, 2017.

- [139] CHAVES DE MELO, G.; MEGGIOLARO, M.. **Selection of subject-specific eeg channels and features for online performance with a bci.** In: CONEM2018, 01 2018.
- [140] ACHANCCARAY, D. R.; MEGGIOLARO, M. A.. **Detection of artifacts from eeg data using wavelet transform, high-order statistics and neural networks.** In: XVII BRAZILIAN CONFERENCE ON AUTOMATICA, volumen 23, p. 1–1, 2008.
- [141] BALTAZAR, R. F.. **Basic and bedside electrocardiography.** Lippincott Williams & Wilkins, 2009.
- [142] TAHA, T. E.; EL-SAYED, A. ; EL-SOUDY, S. R.. **A survey on classification of ecg signal study.** Communications on Applied Electronics (CAE), 6(11):10–5120, 2016.
- [143] JAMBUKIA, S. H.; DABHI, V. K. ; PRAJAPATI, H. B.. **Classification of ecg signals using machine learning techniques: A survey.** In: 2015 INTERNATIONAL CONFERENCE ON ADVANCES IN COMPUTER ENGINEERING AND APPLICATIONS, p. 714–721. IEEE, 2015.
- [144] HARGROVE, L.; ZHOU, P.; ENGLEHART, K. ; KUIKEN, T. A.. **The effect of ecg interference on pattern-recognition-based myoelectric control for targeted muscle reinnervated patients.** IEEE Transactions on Biomedical Engineering, 56(9):2197–2201, 2009.
- [145] FAUST, F. G.; OTHERS. **Uso da variabilidade da frequência cardíaca na avaliação da interação homem-computador.** PhD thesis, Universidade Federal de Santa Catarina, 2022.
- [146] WIKIPEDIA. **Butterworth filter.** last access in 15/07/2019.
- [147] ELETRONIC TUTORIALS. **Butterworth filter.** last access in 15/07/2019.
- [148] PANDA, R.; KHOBRADE, P. S.; JAMBHULE, P. D.; JENGTHE, S. N.; PAL, P. ; GANDHI, T. K.. **Classification of eeg signal using wavelet transform and support vector machine for epileptic seizure diction.** In: 2010 INTERNATIONAL CONFERENCE ON SYSTEMS IN MEDICINE AND BIOLOGY, p. 405–408, 2010.
- [149] KUMAR, N.; ALAM, K. ; SIDDIQI, A. H.. **Wavelet transform for classification of eeg signal using svm and ann.** Biomedical and Pharmacology Journal, 10(4):2061–2069, 2017.

- [150] CHUI, C. K.. **An introduction to wavelets**, volumen 1. Academic press, 1992.
- [151] BURRUS, S.; SELESNICK, I.; PUESCHEL, M.; FRIGO, M. ; JOHNSON, S. G.. **Fast Fourier Transforms**. Connexions online book, 2008.
- [152] BRIGHAM, E. O.. **The fast Fourier transform and its applications**. Prentice-Hall, Inc., 1988.
- [153] SINGLETON, R. C.. **On computing the fast fourier transform**. Communications of the ACM, 10(10):647–654, 1967.
- [154] GIBSON, J. D.. **The communications handbook**. CRC press, 2018.
- [155] NAKATE, A.; BAHIRGONDE, P.. **Feature extraction of eeg signal using wavelet transform**. International Journal of Computer Applications, 124(2), 2015.
- [156] GAFFAR, A. F. O.; MALANI, R.; WAJIANSYAH, A.; PUTRA, A. B. W. ; OTHERS. **A multi-frame blocking for signal segmentation in voice command recognition**. In: 2020 INTERNATIONAL SEMINAR ON INTELLIGENT TECHNOLOGY AND ITS APPLICATIONS (ISITIA), p. 299–304. IEEE, 2020.
- [157] FRYER, T.. **A multichannel eeg telemetry system utilizing a pcm subcarrier**. Biotelemetry, 1(4):202–218, 1974.
- [158] GURRALA, V. K.; YARLAGADDA, P.; KOPPIREDDI, P. ; SREENIVASULA, V. H. P.. **A review on analysis of sleep eeg signals**. In: 2020 4TH INTERNATIONAL CONFERENCE ON ELECTRONICS, COMMUNICATION AND AEROSPACE TECHNOLOGY (ICECA), p. 289–294. IEEE, 2020.
- [159] BARBOSA, A. O.; ACHANCCARAY, D. R. ; MEGGIOLARO, M. A.. **Activation of a mobile robot through a brain computer interface**. In: 2010 IEEE INTERNATIONAL CONFERENCE ON ROBOTICS AND AUTOMATION, p. 4815–4821. IEEE, 2010.
- [160] ACHANCCARAY, D. R.; MEGGIOLARO, M. A.. **Brain computer interface based on electroencephalographic signal processing**. In: XVI IEEE INTERNATIONAL CONGRESS OF ELECTRICAL, ELECTRONIC AND SYSTEMS ENGINEERING-INTERCON, 2009.

- [161] AL-CANAAN, A.; AL, A. ; CHAKIB, H.. **Performance evaluation of scalograms and 1-d wavelet eeg classifiers for prosthetic control system optimisation.** Multi-Knowledge Electronic Comprehensive Journal For Education And Science Publications (MECSJ), 50, 2022.
- [162] VILELA, L. M. D.. **Sistema eletrônico de aquisição de sinais de um eletrocardiograma,** 2020.
- [163] ZONTONE, P.; AFFANNI, A.; BERNARDINI, R.; PIRAS, A. ; RINALDO, R.. **Stress detection through electrodermal activity (eda) and electrocardiogram (ecg) analysis in car drivers.** In: 2019 27TH EUROPEAN SIGNAL PROCESSING CONFERENCE (EUSIPCO), p. 1–5. IEEE, 2019.
- [165] KUMAR M, A.; CHAKRAPANI, A.. **Classification of ecg signal using fft based improved alexnet classifier.** PloS one, 17(9):e0274225, 2022.
- [166] DAVE, T.; PANDYA, U.. **Simultaneous monitoring of motion ecg of two subjects using bluetooth piconet and baseline drift.** Biomedical Engineering Letters, 8(4):365–371, 2018.
- [167] INAM, S.; AL HARMAN, S.; SHAFIQUE, S.; AFZAL, M.; RABAIL, A.; AMIN, F. ; WAQAR, M.. **A brief review of strategies used for emg signal classification.** In: 2021 INTERNATIONAL CONFERENCE ON ARTIFICIAL INTELLIGENCE (ICAI), p. 140–145. IEEE, 2021.
- [168] KHAIRUDDIN, I. M.; NA’IM SIDEK, S.; MAJEED, A. P. A. ; PUZI, A. A.. **Classifying motion intention from emg signal: a k-nn approach.** In: 2019 7TH INTERNATIONAL CONFERENCE ON MECHATRONICS ENGINEERING (ICOM), p. 1–4. IEEE, 2019.
- [169] POURMOHAMMADI, S.; MALEKI, A.. **Stress detection using ecg and emg signals: A comprehensive study.** Computer methods and programs in biomedicine, 193:105482, 2020.
- [170] SAEEDI, H.; POURHOSEINGHOLI, E.. **Comparison the effect of kinetic parameters of innovative storing-restoring hybrid passive (comfort gait) ankle-foot orthosis (afo) with posterior leaf spring afo in drop-foot patients: A prospective cohort study.** Current Orthopaedic Practice, 31(5):437–441, 2020.
- [171] SHAW, J. A.. **The PID ControlAlgorithm-How it works, how to tune it, and how to use it.** Process control solutions, 2003.

- [172] SICSU, B.. **Algoritmos Genéticos**. Ed. Ciência Moderna, 2012.
- [173] GOODFELLOW, I.; BENGIO, Y. ; COURVILLE, A.. **Deep Learning**. MIT Press, 2016. <http://www.deeplearningbook.org>.
- [174] DRENICK, R.; SHAHBENDER, R.. **Adaptive servomechanisms**. Transactions of the American Institute of Electrical Engineers, Part II: Applications and Industry, 76(5):286–292, 1957.
- [175] TRUXAL, J. G.. **The concept of adaptive control**. by Eli Miskin and Ludwig Braun, Jr., New York: McGraw-Hill, 1961.
- [176] ARIYUR, K. B.; KRSTIC, M.. **Extremum Seeking Feedback Tools for Real-Time Optimization**. John Wiley & Sons, Inc., New York, NY, USA, 2005.
- [177] FRIDMAN, L.; LEVANT, A.. **Higher-Order Sliding Modes**, volumen 11, p. 53–101. Marcel Dekker, 01 2002.
- [178] BARTOLINI, G.; PISANO, A.; PUNTA, E. ; USAI, E.. **A survey of applications of second-order sliding mode control to mechanical systems**. International Journal of Control - INT J CONTR, 76:875–892, 06 2003.
- [179] LI, Z.; SUN, J. ; OH, S.. **Path following for marine surface vessels with rudder and roll constraints: an mpc approach**. In: PROCEEDINGS OF THE AMERICAN CONTROL CONFERENCE, p. 3611 – 3616, 07 2009.
- [180] ASHRAFIUON, H.; ERWIN, R. S.. **Sliding mode control of underactuated multibody systems and its application to shape change control**. International Journal of Control, 81(12):1849–1858, 2008.
- [181] UTKIN, V.; POZNYAK, A.; ORLOV, Y. ; POLYAKOV, A.. **Conventional and high order sliding mode control**. Journal of the Franklin Institute, 357(15):10244–10261, 2020.
- [182] SHTESSEL, Y.; EDWARDS, C.; FRIDMAN, L.; LEVANT, A. ; OTHERS. **Sliding mode control and observation**, volumen 10. Springer, 2014.
- [183] ELYOUSSEF, E. S.; DE PIERI, E. R.; MORENO, U. F. ; JUNGERS, M.. **Super-twisting sliding modes tracking control of a nonholonomic wheeled mobile robot**. IFAC Proceedings Volumes, 45(22):429–434, 2012.

- [184] LEVANT, A.. **Sliding order and sliding accuracy in sliding mode control**. International journal of control, 58(6):1247–1263, 1993.
- [185] KRUSE, O.; MUKHAMEJANOVA, A. ; MERCORELLI, P.. **Super-twisting sliding mode control for differential steering systems in vehicular yaw tracking motion**. Electronics, 11(9):1330, 2022.
- [186] MORENO, J.; SÁNCHEZ, T. ; CRUZ-ZAVALA, E.. **Una función de lyapunov suave para el algoritmo super-twisting**. 16th CLCA, p. 182–187, 2014.
- [187] ROCKENFELLER, R.; GÜNTHER, M.. **Hill equation and hatze’s muscle activation dynamics complement each other: enhanced pharmacological and physiological interpretability of modelled activity-pca curves**. Journal of Theoretical Biology, 431, 07 2017.
- [188] SANTUZ, A.; BRÜLL, L.; EKIZOS, A.; SCHROLL, A.; ECKARDT, N.; KIBELE, A.; SCHWENK, M. ; ARAMPATZIS, A.. **Neuromotor dynamics of human locomotion in challenging settings**. iScience, 23(1):100796, Jan 2020.
- [189] ROSALES, Y.; LOPEZ, R.; ROSALES, I.; SALAZAR, S. ; LOZANO, R.. **Design and modeling of an upper limb exoskeleton**. In: 2015 19TH INTERNATIONAL CONFERENCE ON SYSTEM THEORY, CONTROL AND COMPUTING (ICSTCC), p. 266–272. IEEE, 2015.
- [190] GOPURA, R.; BANDARA, D.; KIGUCHI, K. ; MANN, G. K.. **Developments in hardware systems of active upper-limb exoskeleton robots: A review**. Robotics and Autonomous Systems, 75:203–220, 2016.
- [191] GULL, M. A.; BAI, S. ; BAK, T.. **A review on design of upper limb exoskeletons**. Robotics, 9(1), 2020.
- [192] ZHOU, K.; DOYLE, J. C.. **Essentials of robust control**, volumen 104. Prentice hall Upper Saddle River, NJ, 1998.
- [193] HOLLWEG, G. V.; EVALD, P. J.; KOCH, G. G.; MATTOS, E.; TAMBARA, R. V. ; GRÜNDLING, H. A.. **Controlador robusto adaptativo super-twisting sliding mode por modelo de referência para regulação das correntes injetadas em redes fracas por inversores trifásicos com filtro lcl**. Revista Eletrônica de Potência, 26(2):1–12, 2021.
- [194] LEE, S.-D.; LEE, B.-K. ; YOU, S.-S.. **Sliding mode control with super-twisting algorithm for surge oscillation of mooring vessel**

- system. *Journal of the Korean Society of Marine Environment & Safety*, 24(7):953–959, 2018.
- [195] RAFIQ, M.; REHMAN, S.-U.; REHMAN, F.-U.; BUTT, Q. R. ; AWAN, I.. **A second order sliding mode control design of a switched reluctance motor using super twisting algorithm.** *Simulation Modelling Practice and Theory*, 25:106–117, 2012.
- [196] FENG, Z.; FEI, J.. **Design and analysis of adaptive super-twisting sliding mode control for a microgyroscope.** *PloS one*, 13(1):e0189457, 2018.
- [197] TAHOUMI, E.. **New robust control schemes linking linear and sliding mode approaches.** PhD thesis, École centrale de Nantes, 2019.
- [198] MORENO, J. A.. **Lyapunov approach for analysis and design of second order sliding mode algorithms.** In: *SLIDING MODES AFTER THE FIRST DECADE OF THE 21ST CENTURY*, p. 113–149. Springer, 2011.
- [199] MORENO, J. A.; OSORIO, M.. **Strict lyapunov functions for the super-twisting algorithm.** *IEEE transactions on automatic control*, 57(4):1035–1040, 2012.
- [200] DÁVILA, A.; MORENO, J. A. ; FRIDMAN, L.. **Optimal lyapunov function selection for reaching time estimation of super twisting algorithm.** In: *PROCEEDINGS OF THE 48H IEEE CONFERENCE ON DECISION AND CONTROL (CDC) HELD JOINTLY WITH 2009 28TH CHINESE CONTROL CONFERENCE*, p. 8405–8410. IEEE, 2009.
- [201] POZNYAK, A. S.. **Advanced mathematical tools for automatic control engineers: Stochastic techniques.** Elsevier, 2009.
- [202] SHI, Z.; DENG, C.; ZHANG, S.; XIE, Y.; CUI, H. ; HAO, Y.. **Hyperbolic tangent function-based finite-time sliding mode control for spacecraft rendezvous maneuver without chattering.** *IEEE Access*, 8:60838–60849, 2020.
- [203] FRANKLIN, G. F.; POWELL, J. D. ; EMAMI-NAEINI, A.. **Feedback Control of Dynamic Systems.** Prentice Hall Press, Upper Saddle River, NJ, USA, 7th edition, 2014.